

## Supporting Information for

# Ruthenium complexes with triazenide ligands bearing an *N*-heterocyclic moiety, and their catalytic properties in the reduction nitroarenes

Christian Romero-Soto,<sup>a‡</sup> Ana L. Iglesias,<sup>b‡</sup> Amor Velázquez-Ham,<sup>a</sup> Juan P. Camarena-Díaz,<sup>a</sup> Erick Correa-Ayala,<sup>a</sup> Jessica L. Gomez-Lopez,<sup>a</sup> Daniel Chávez,<sup>a</sup> Adrián Ochoa-Terán,<sup>a</sup> Gerardo Aguirre,<sup>a</sup> Arnold L. Rheingold,<sup>c</sup> Douglas B. Grotjahn,<sup>d#</sup> Miguel Parra-Hake,<sup>a</sup> and Valentín Miranda-Soto<sup>\*a</sup>

<sup>a</sup>Tecnológico Nacional de México/Instituto Tecnológico de Tijuana, Centro de Graduados e Investigación en Química. Blvd. Alberto Limón Padilla S/N, Otay Mesa, 22454 Tijuana, B. C. México.

<sup>b</sup>Facultad de Ciencias de la Ingeniería y Tecnología, Universidad Autónoma de Baja California, Blvd. Universitario No. 1000. Valle de las Palmas, 21500 Tijuana, B. C. México.

<sup>c</sup>Department of Chemistry and Biochemistry, University of California at San Diego. La Jolla, CA 92093-0385, USA.

<sup>d</sup>Department of Chemistry and Biochemistry, San Diego State University. 5500 Campanile Drive San Diego, CA 92182-1030, USA.

<sup>‡</sup>These authors contributed equally to the work.

<sup>†</sup>Deceased.

### TABLE OF CONTENTS

NMR, FTIR and HRMS spectra of triazenes <b>1</b> , <b>2</b> , <b>3</b> , <b>4</b> , and <b>9</b> .	S2
NMR and HRMS spectra of complexes <b>5</b> , <b>6</b> , <b>7</b> , and <b>8</b> .	S19
NMR, EIMS and HRMS spectra of complex <b>11</b> , <b>12</b> , and <b>13</b> .	S46
<b>Table S1</b> . Crystallographic data for complex <b>5</b> .	S54
<b>Table S2</b> . Crystallographic data for complex <b>6</b> .	S55
<b>Table S3</b> . Crystallographic data for complex <b>7</b> .	S56
<b>Table S4</b> . Crystallographic data for complex <b>12</b> .	S57
<b>Figure S98</b> . X-ray structure of complex <b>13</b> .	S58
<b>Table S5</b> . Crystallographic data for complex <b>13</b> .	S59
<b>Table S6</b> . Screening of complexes <b>5-10</b> in the reduction of 4-aminonitrobenzene.	S60
GC-MS data of the catalytic hydrogenation of nitrobenzene (Table 1).	S61
GC-MS data of the catalytic hydrogenation of 4-aminonitrobenzene (Table S6).	S68
GC-MS data of the catalytic hydrogenation of nitroarenes (Table 2).	S75
<b>Figure S155</b> . <sup>1</sup> H NMR data of hydrogenation product of entry 9, Table 2 in DMSO- <i>d</i> <sub>6</sub> .	S83
<b>Figure S156</b> . <sup>1</sup> H NMR data of hydrogenation product of entry 10, Table 2 in DMSO- <i>d</i> <sub>6</sub> .	S83
<b>Table S7</b> . Reduction of <i>p</i> -nitrotoluene without NaBH <sub>4</sub> .	S89
GC-MS Data of the Oxyazo intermediate in the reduction of <i>p</i> -nitrotoluene	S89
GC-MS Data of the Azo intermediate in the reduction of <i>p</i> -nitrotoluene	S91
<b>Figures S177-S179</b> . <sup>1</sup> H NMR of Ru-hydride intermediates.	S92
<b>Chart 1</b> . Reutilization of the catalytic system.	S94

NMR, FTIR and HRMS spectra of triazenes 1, 2, 3, 4, and 9

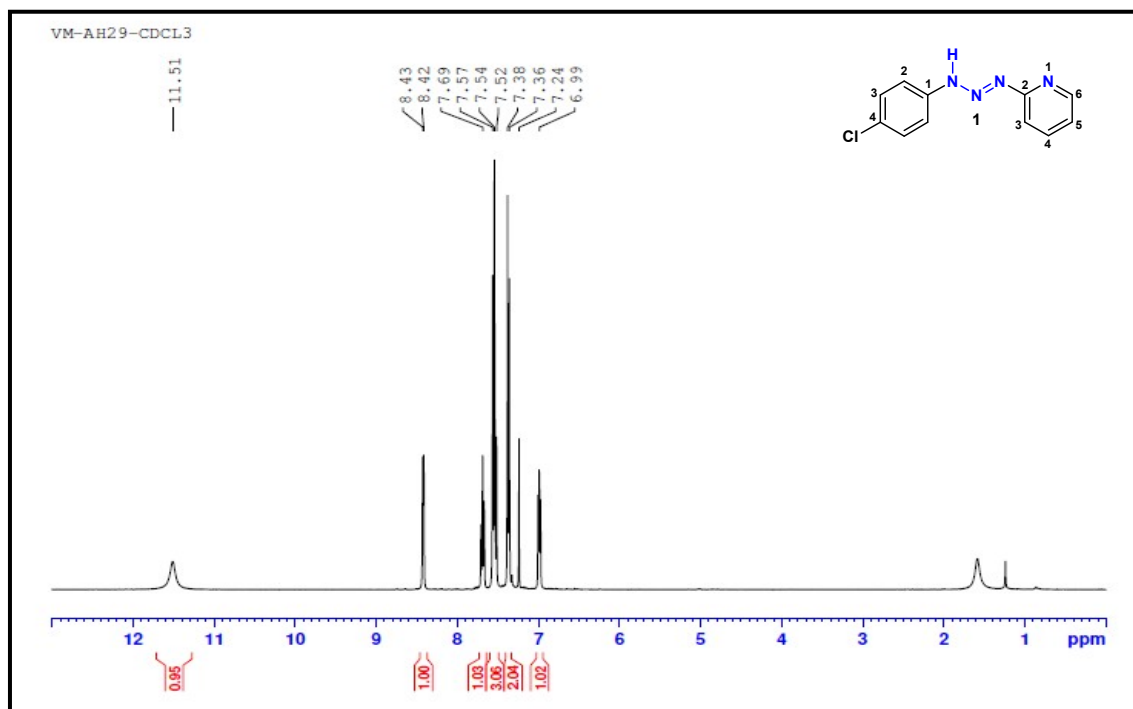


Figure S1.  $^1\text{H}$  NMR spectrum of 1 in  $\text{CDCl}_3$  (400 MHz).

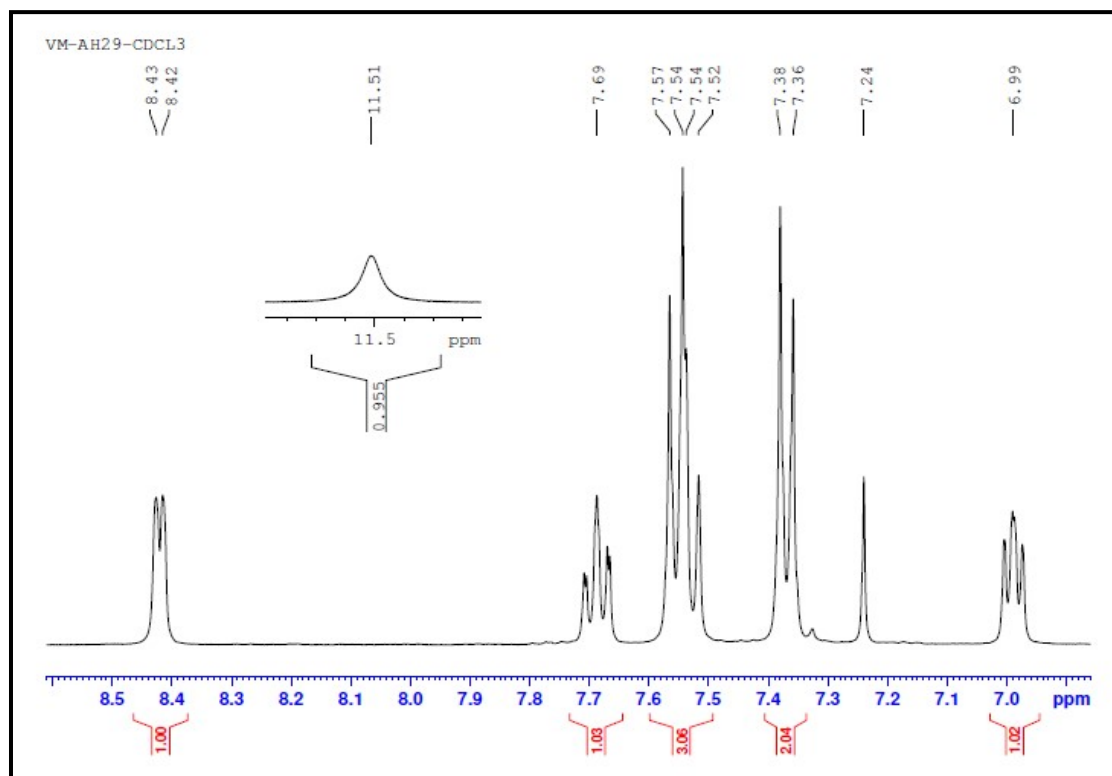
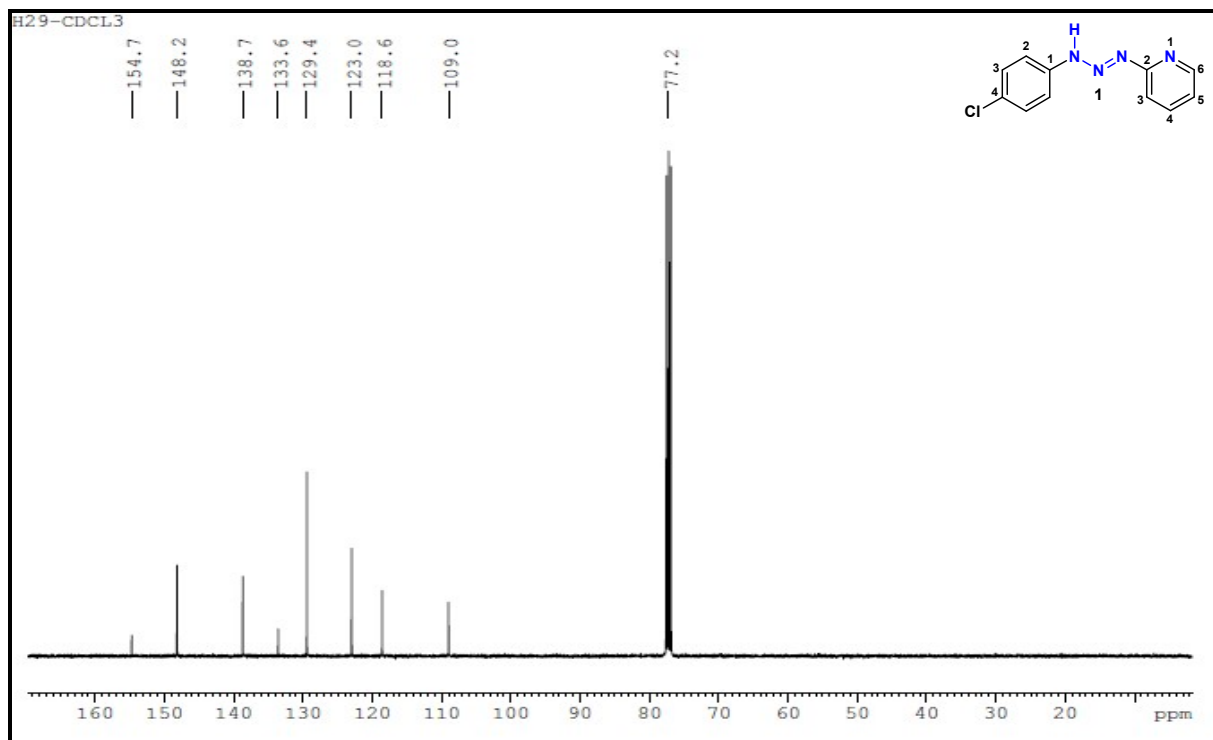
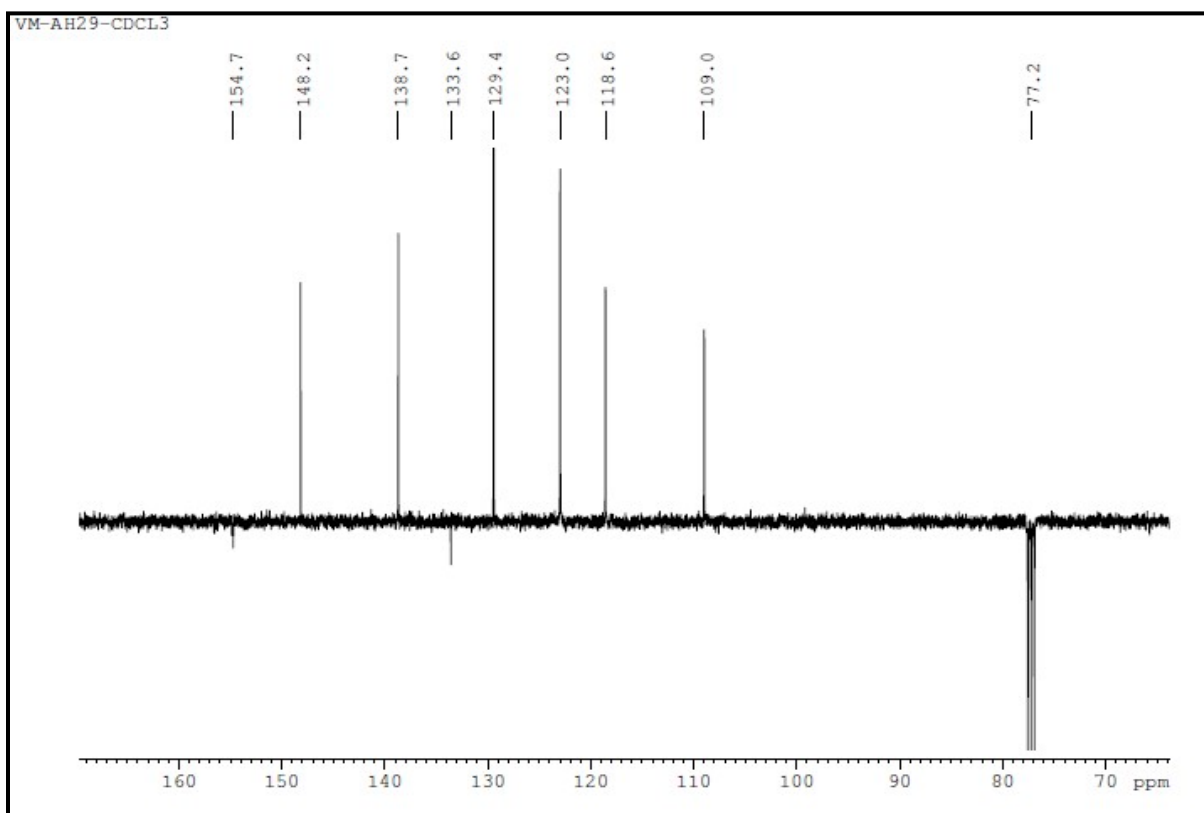


Figure S2. Partial  $^1\text{H}$  NMR spectrum of 1 in  $\text{CDCl}_3$  (400 MHz).



**Figure S3.**  $^{13}\text{C}$   $\{^1\text{H}\}$  NMR spectrum of **1** in  $\text{CDCl}_3$  (100 MHz).



**Figure S4.**  $^{13}\text{C}$   $\{^1\text{H}\}$  NMR-APT spectrum of **1** in  $\text{CDCl}_3$  (100 MHz).

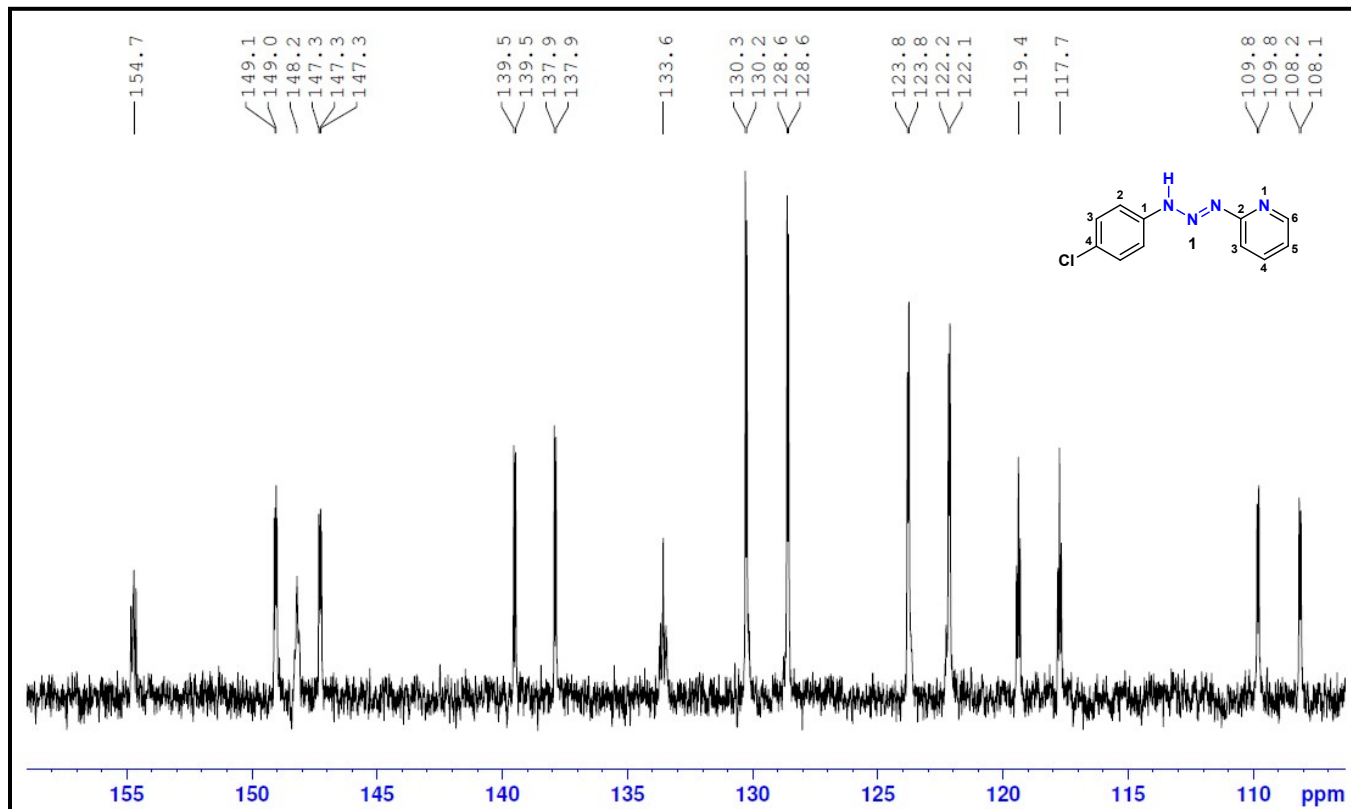


**Figure S5.**  $^{13}\text{C}$  NMR  $^1\text{H}$ -coupled spectrum of **1** in  $\text{CDCl}_3$  (100 MHz).

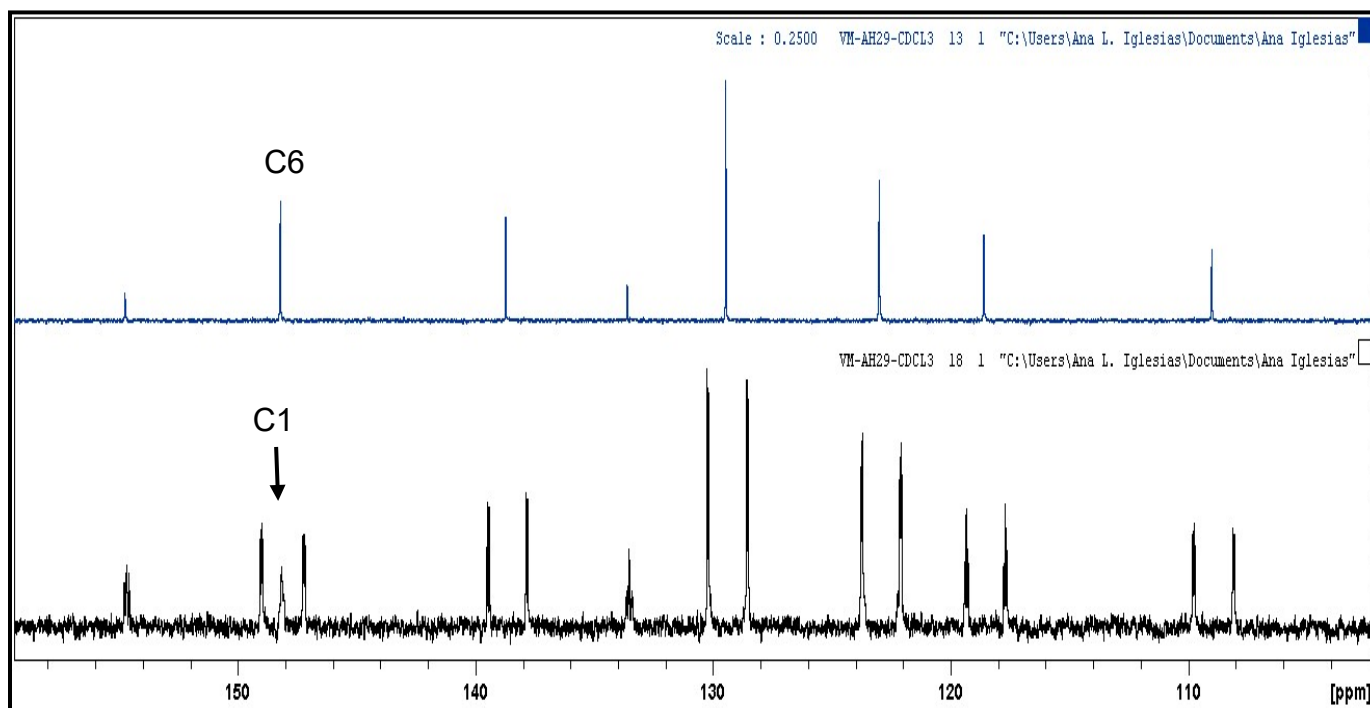


**Figure S6.** Comparison of  $^1\text{H}$ -decoupled and  $^1\text{H}$ -coupled  $^{13}\text{C}$  NMR spectra of **1** in  $\text{CDCl}_3$ .

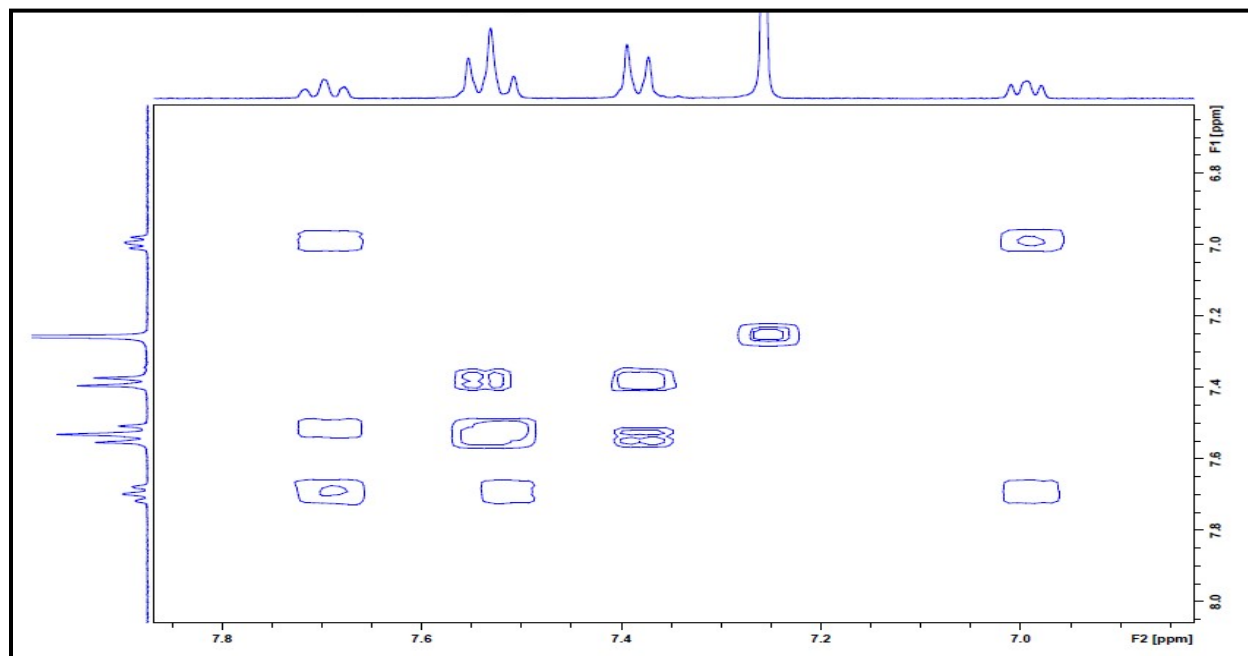


**Figure S7.** Partial  $^1\text{H}$ - $^1\text{H}$  gCOSY spectrum of **1** in  $\text{CDCl}_3$ .

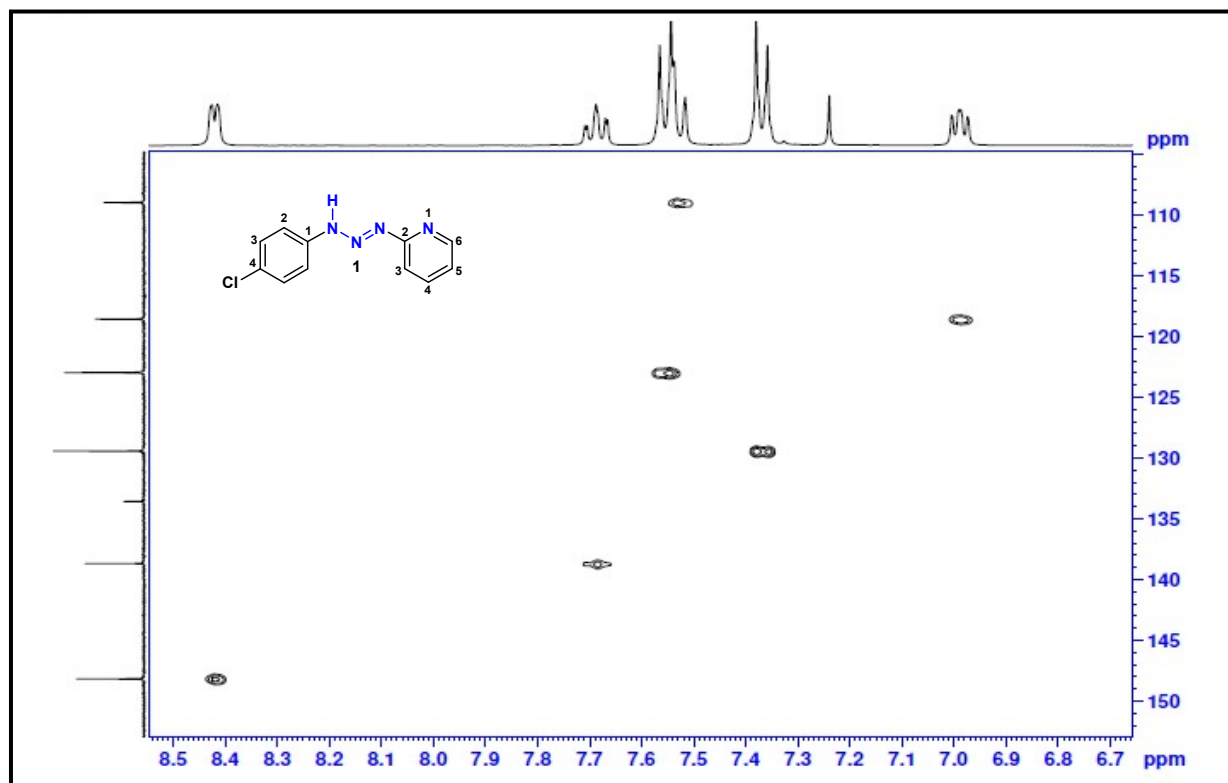


**Figure S8.**  $^1\text{H}$ - $^{13}\text{C}$  HSQC spectrum of **1** in  $\text{CDCl}_3$  (400 MHz).

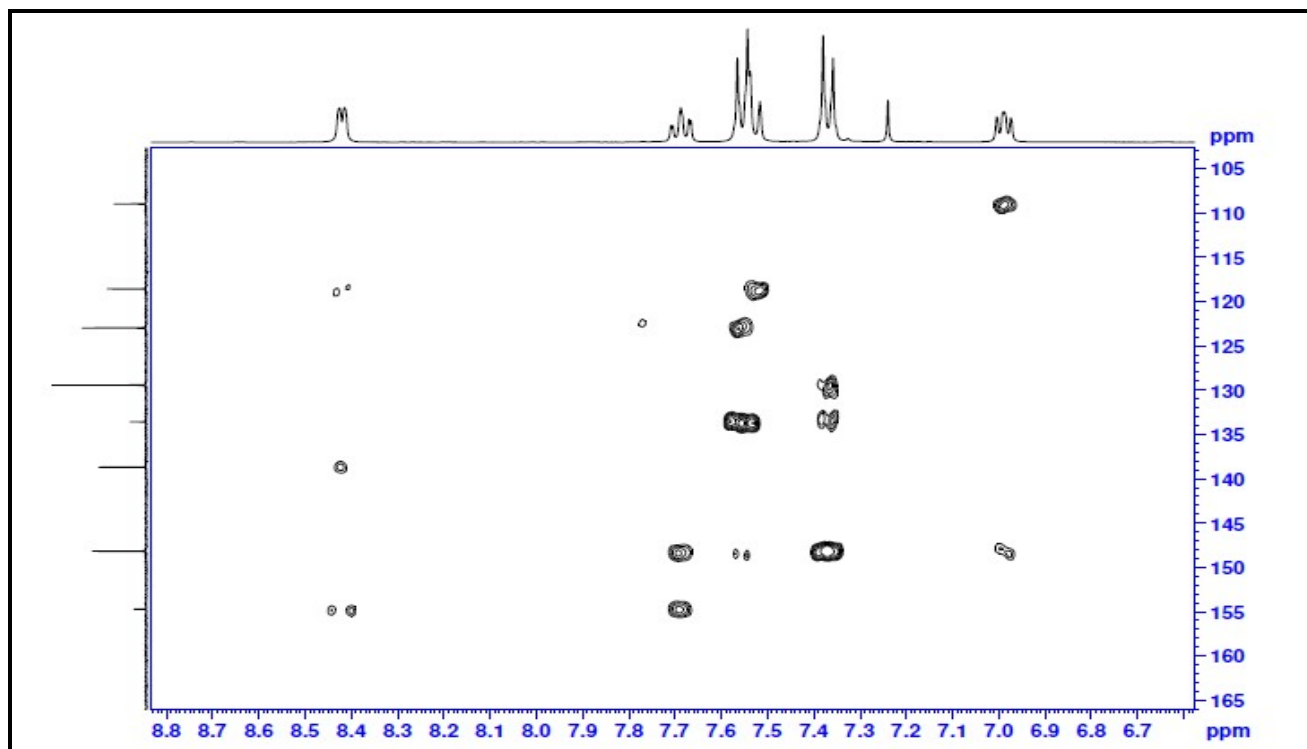


**Figure S9.**  $^1\text{H}$ - $^{13}\text{C}$  HMBC of **1** in  $\text{CDCl}_3$  (400 MHz).

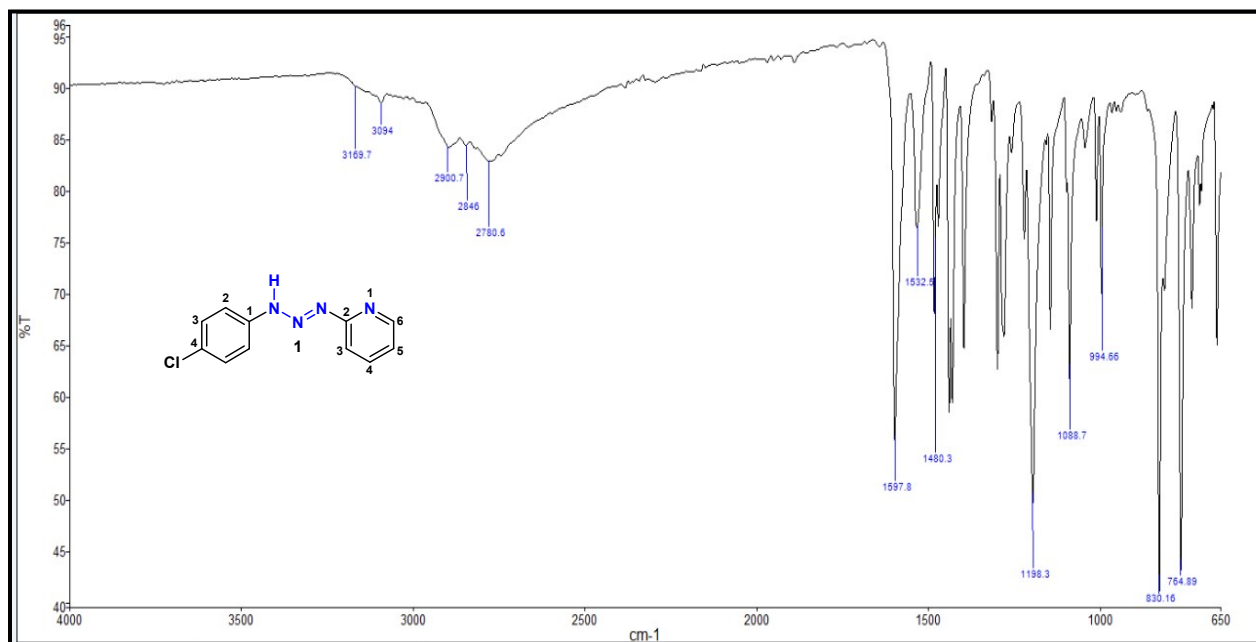


**Figure S10.** FTIR Spectrum of **1** in KBr.

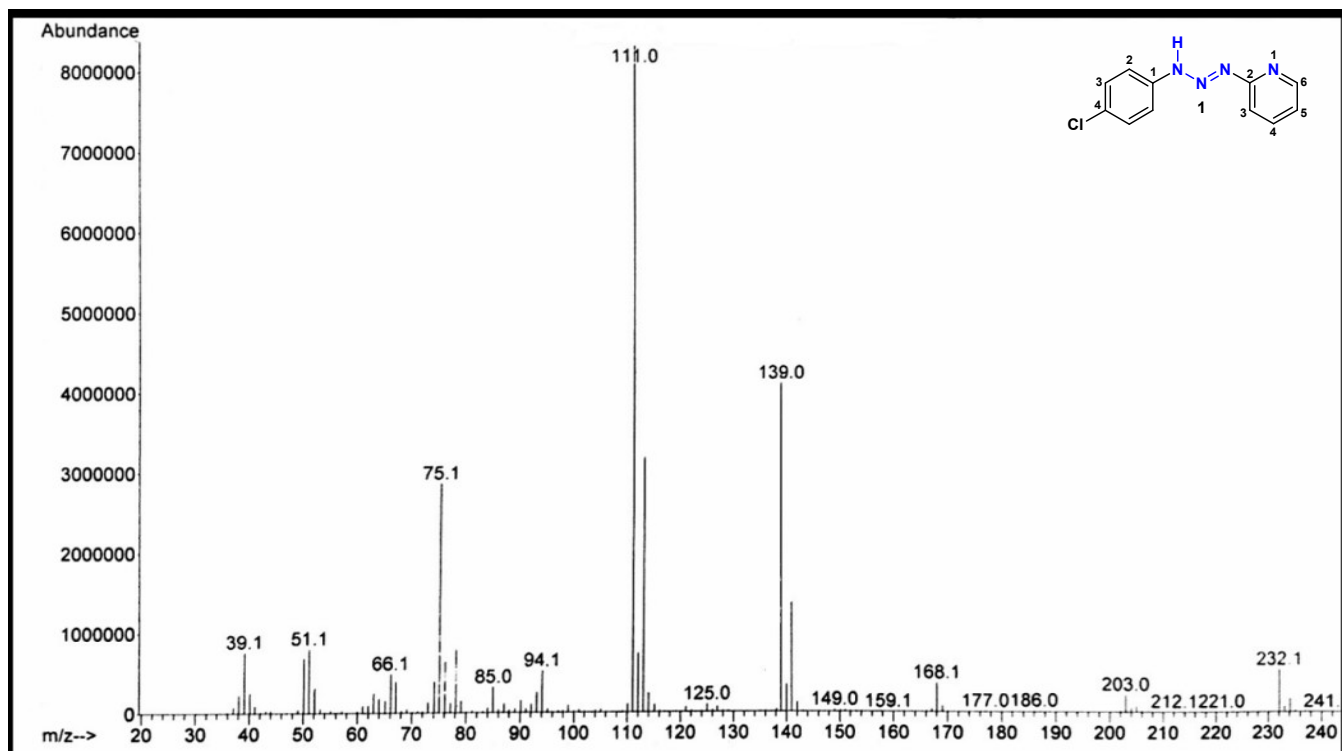


Figure S11. Electron Ionization Mass Spectrum of 1.

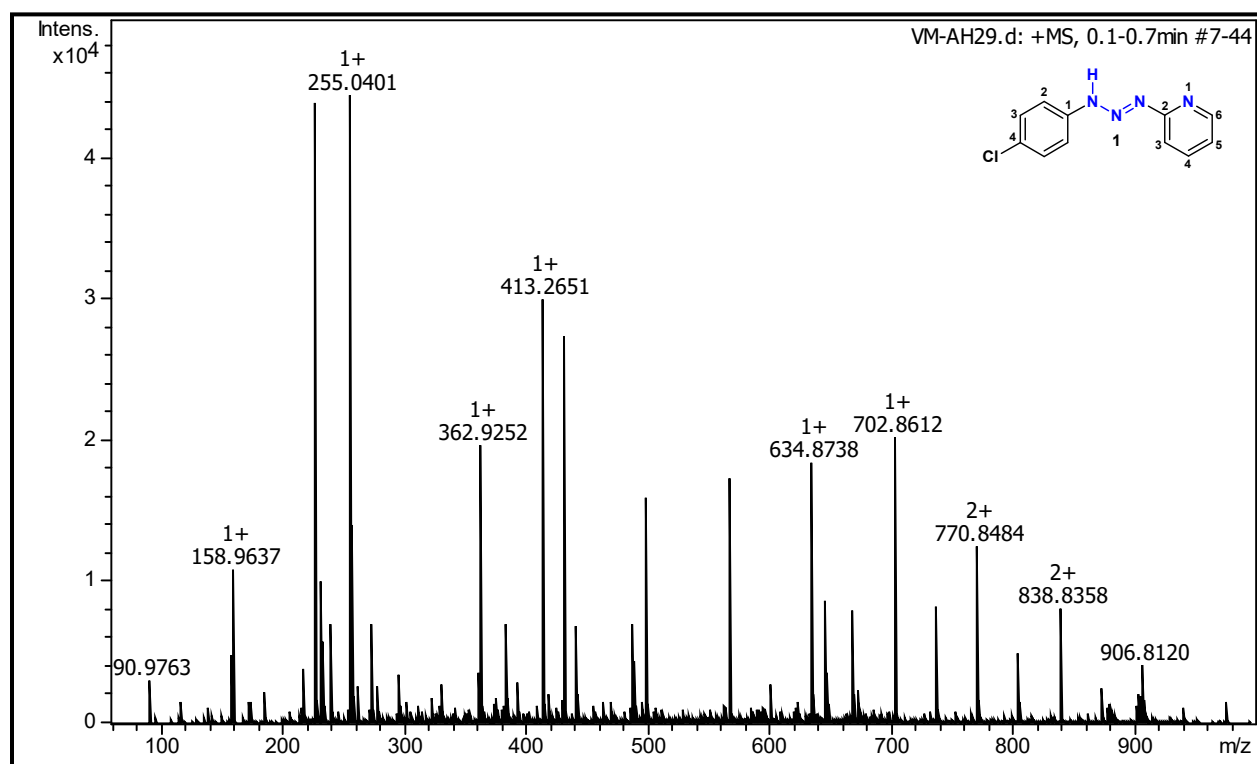
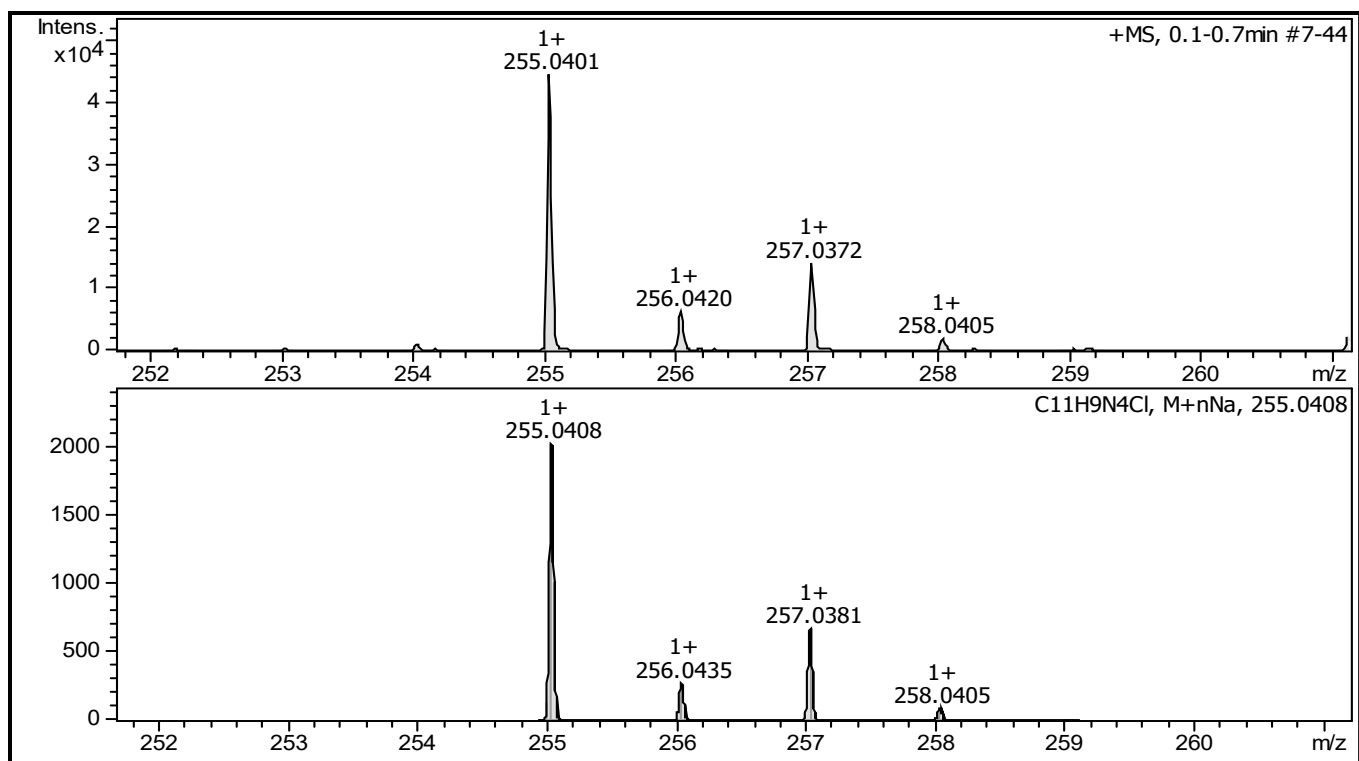
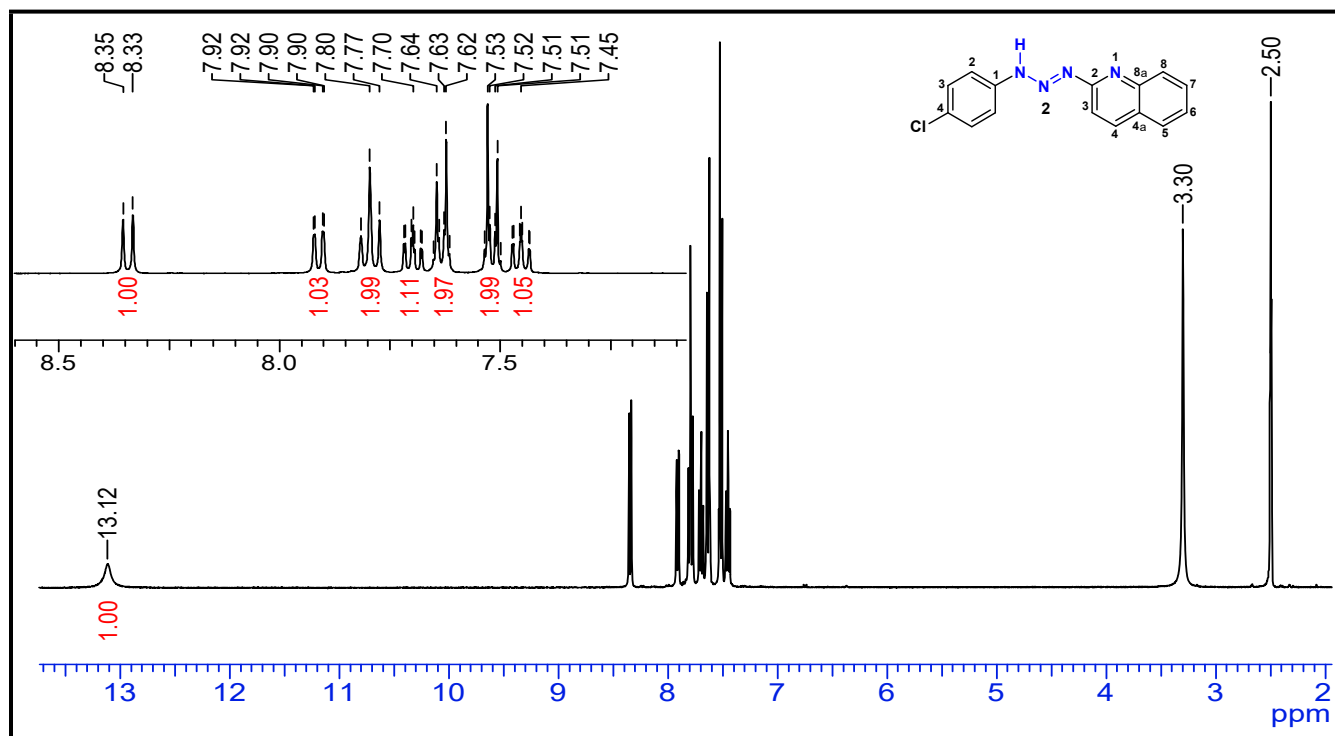


Figure S12. High Resolution Mass Spectrum (HRMS) of 1.



**Figure S13.** HRMS of triazene **1** (above) and calculated spectrum (below) with [M+Na]<sup>+</sup> adduct.



**Figure S14.** <sup>1</sup>H NMR spectrum of **2** in DMSO-*d*<sub>6</sub> (400 MHz).



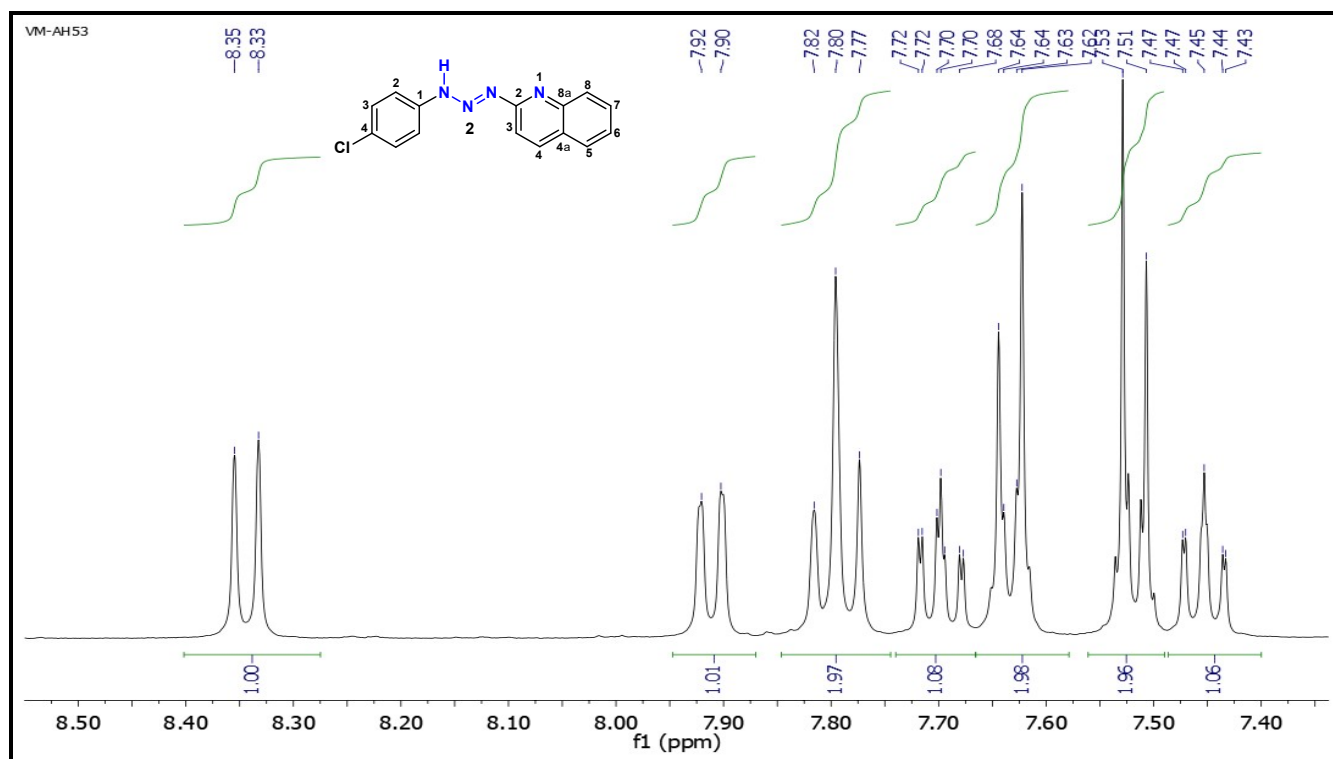


**Figure S15.** Partial  $^1\text{H}$  NMR spectrum of **2** in  $\text{DMSO-}d_6$  (400 MHz).

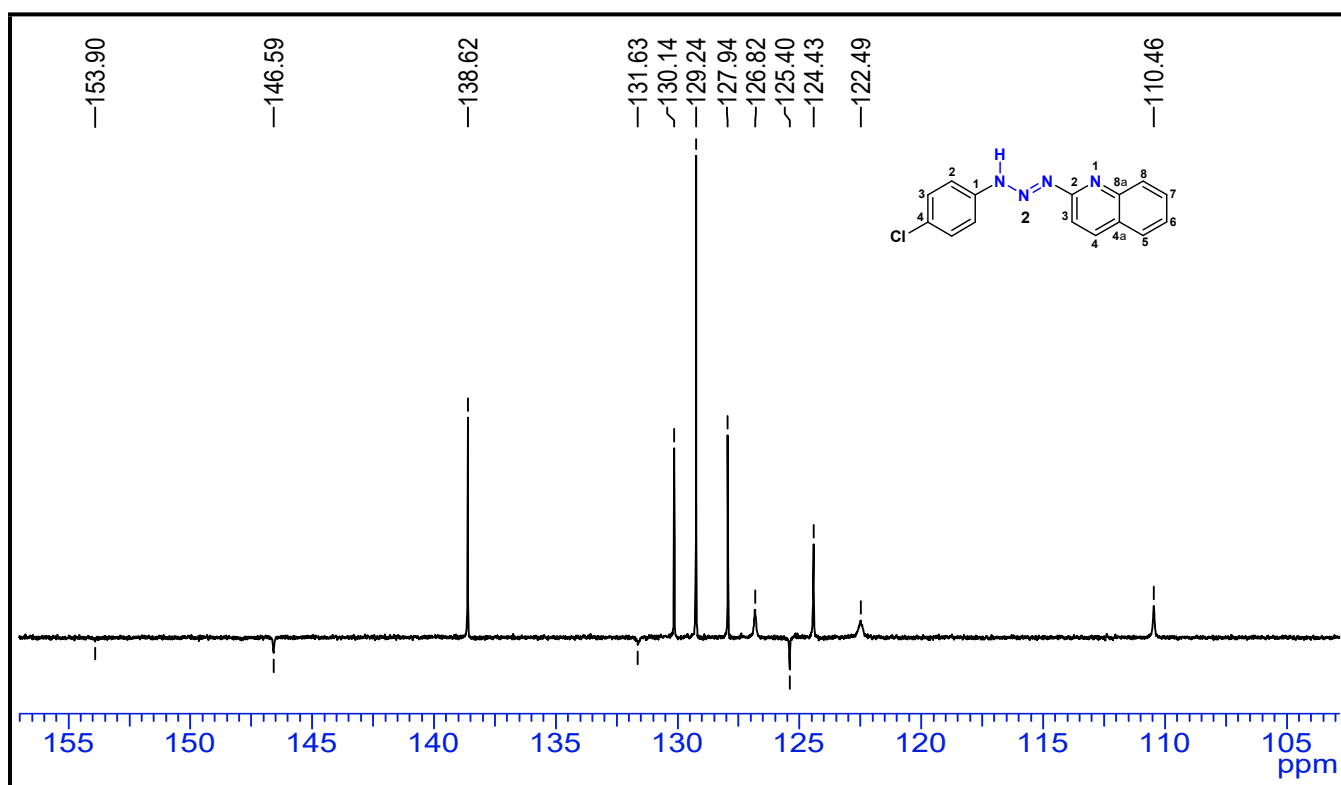


**Figure S16.** Partial  $^{13}\text{C}$   $\{^1\text{H}\}$  NMR-APT spectrum of **2** in  $\text{DMSO-}d_6$  (100 MHz).

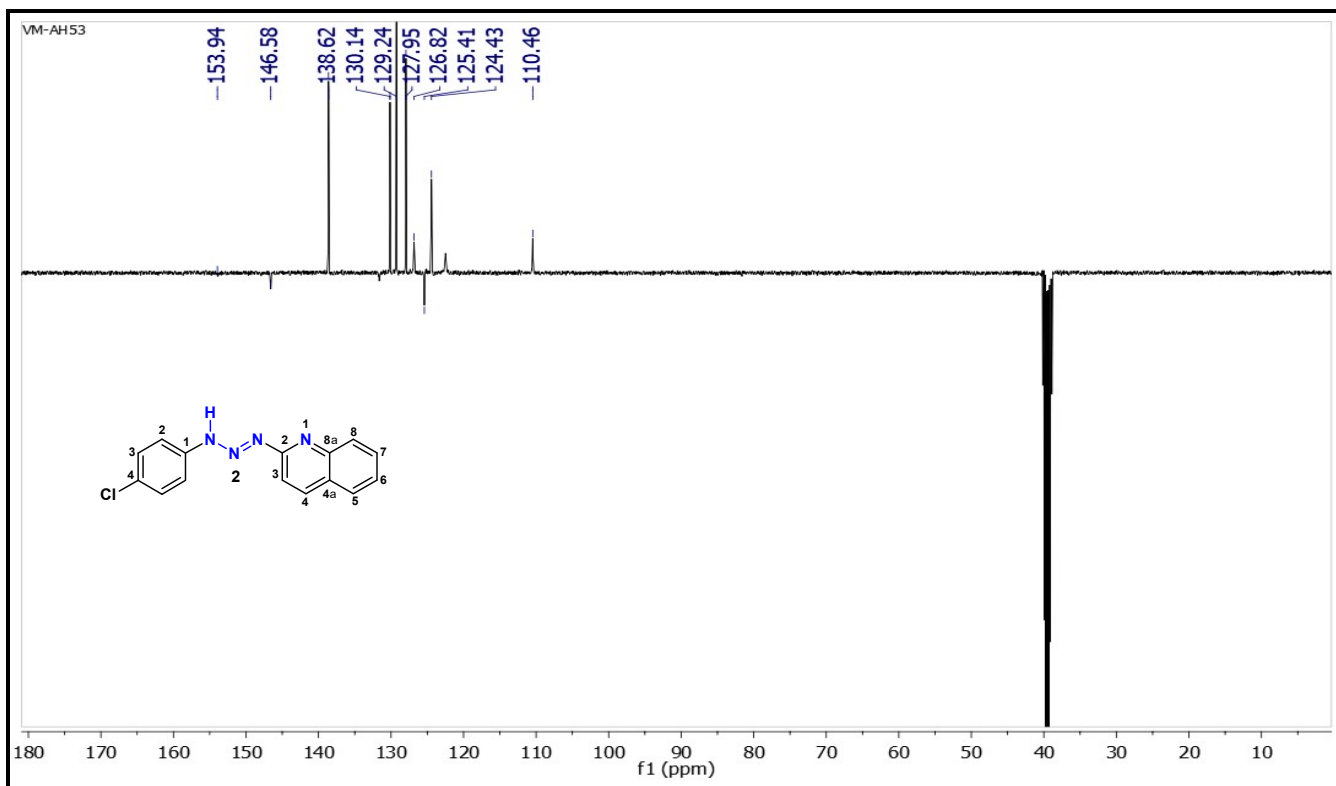


**Figure S17.**  $^{13}\text{C}$   $\{^1\text{H}\}$  NMR-APT spectrum of **2** in  $\text{DMSO-}d_6$  (100 MHz).

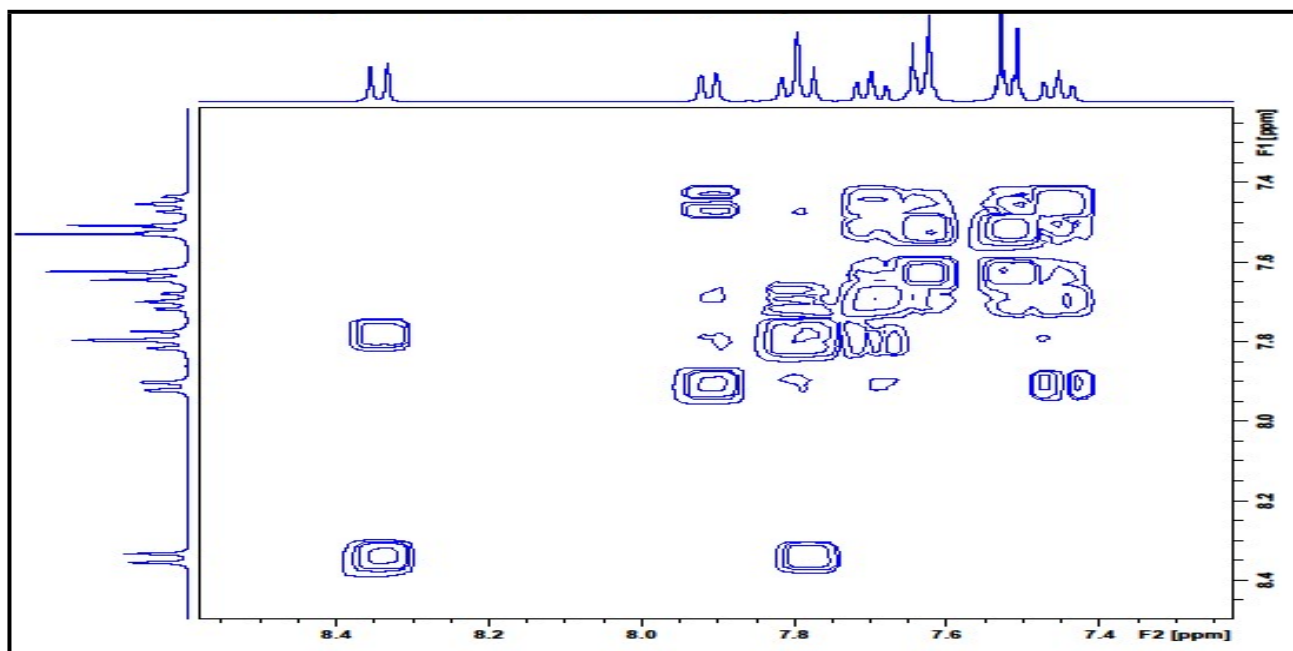


**Figure S18.** Partial  $^1\text{H-}^1\text{H}$  gCOSY NMR spectrum of **2** in  $\text{DMSO-}d_6$  (400 MHz).

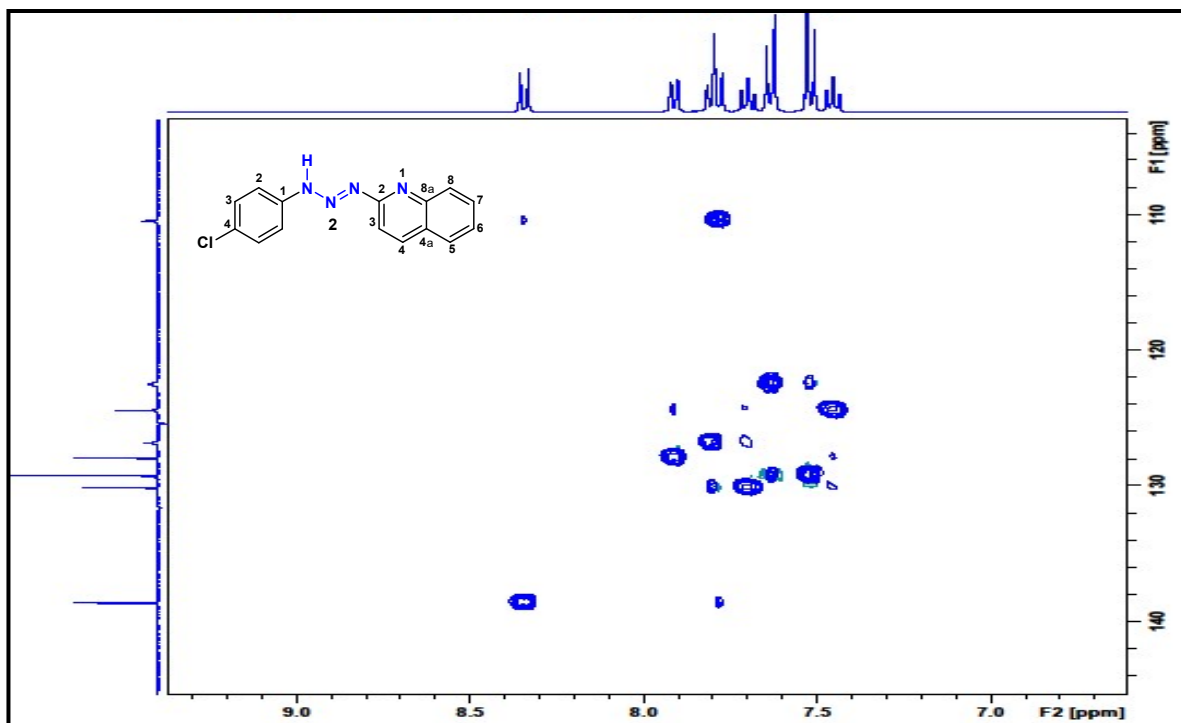


Figure S19. Partial  $^1\text{H}$ - $^{13}\text{C}$  gHSQC NMR spectrum of **2** in  $\text{DMSO-}d_6$ .

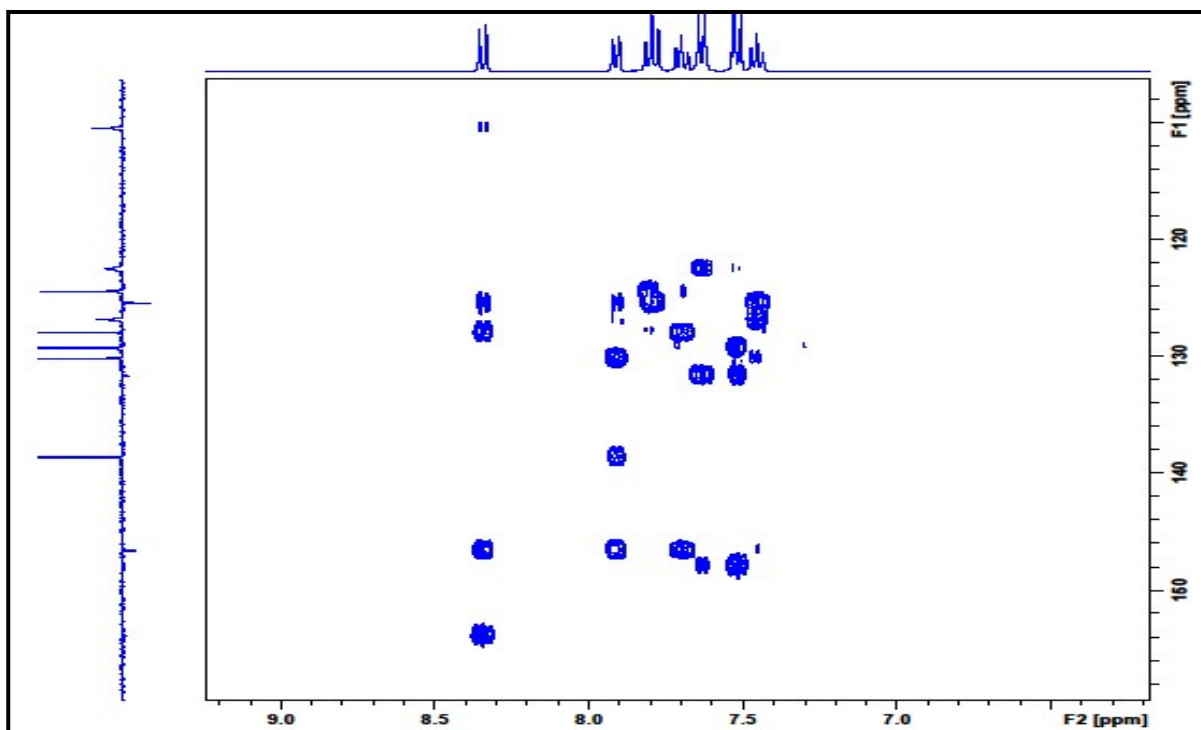


Figure S20. Partial  $^1\text{H}$ - $^{13}\text{C}$  gHMBC NMR spectrum of **2** in  $\text{DMSO-}d_6$ .

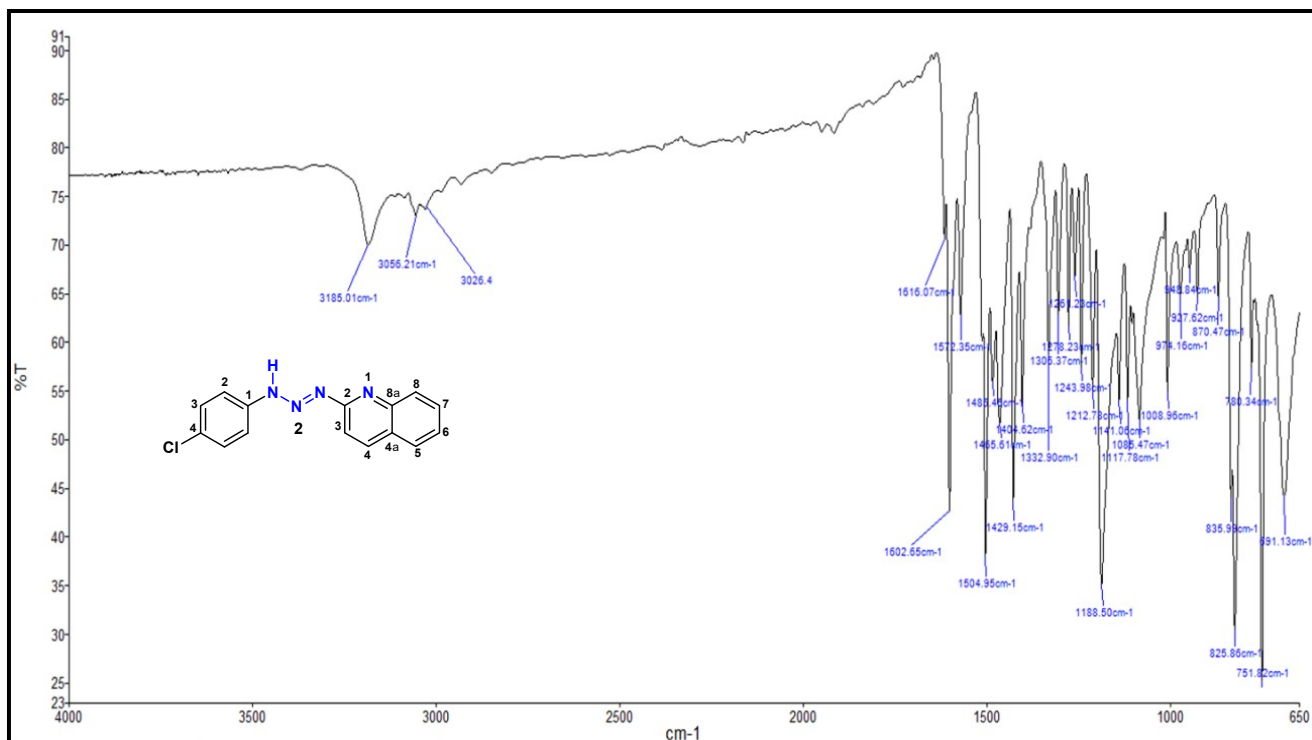


Figure S21. FTIR spectrum of 2 in KBr.

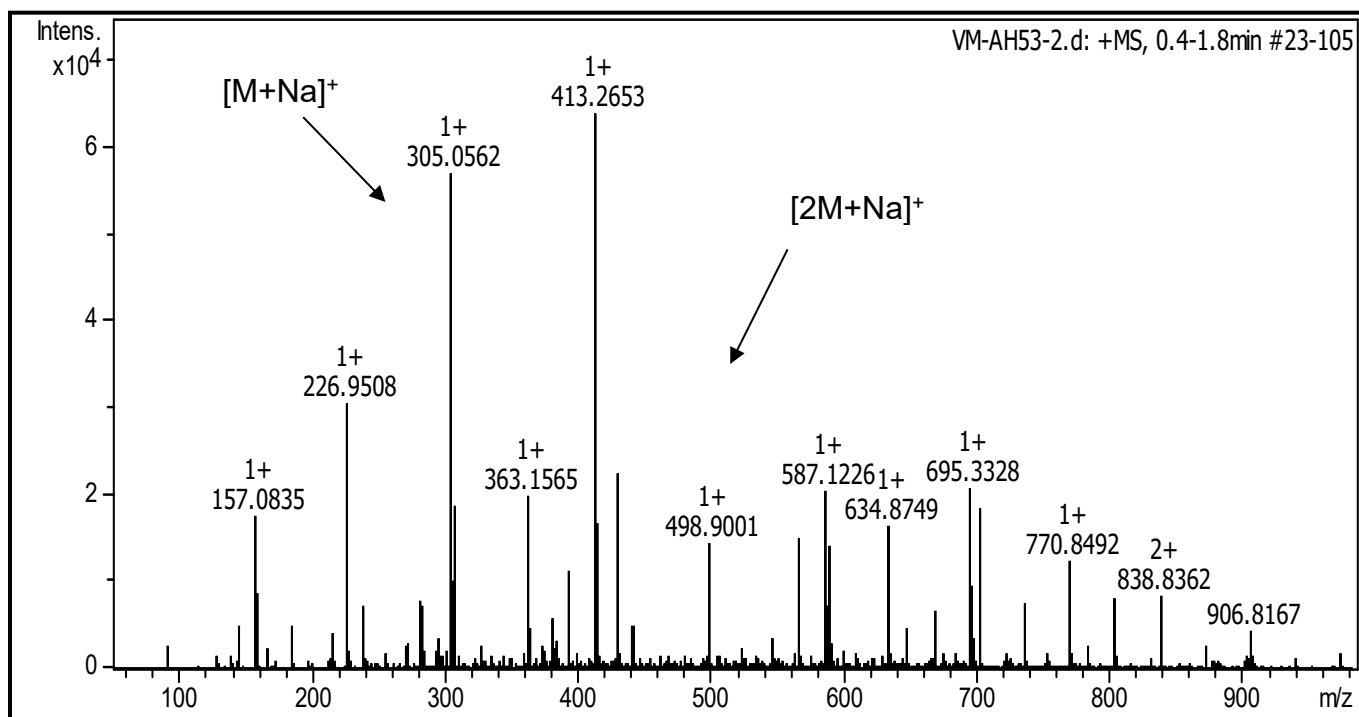


Figure S22. HRMS of 2.

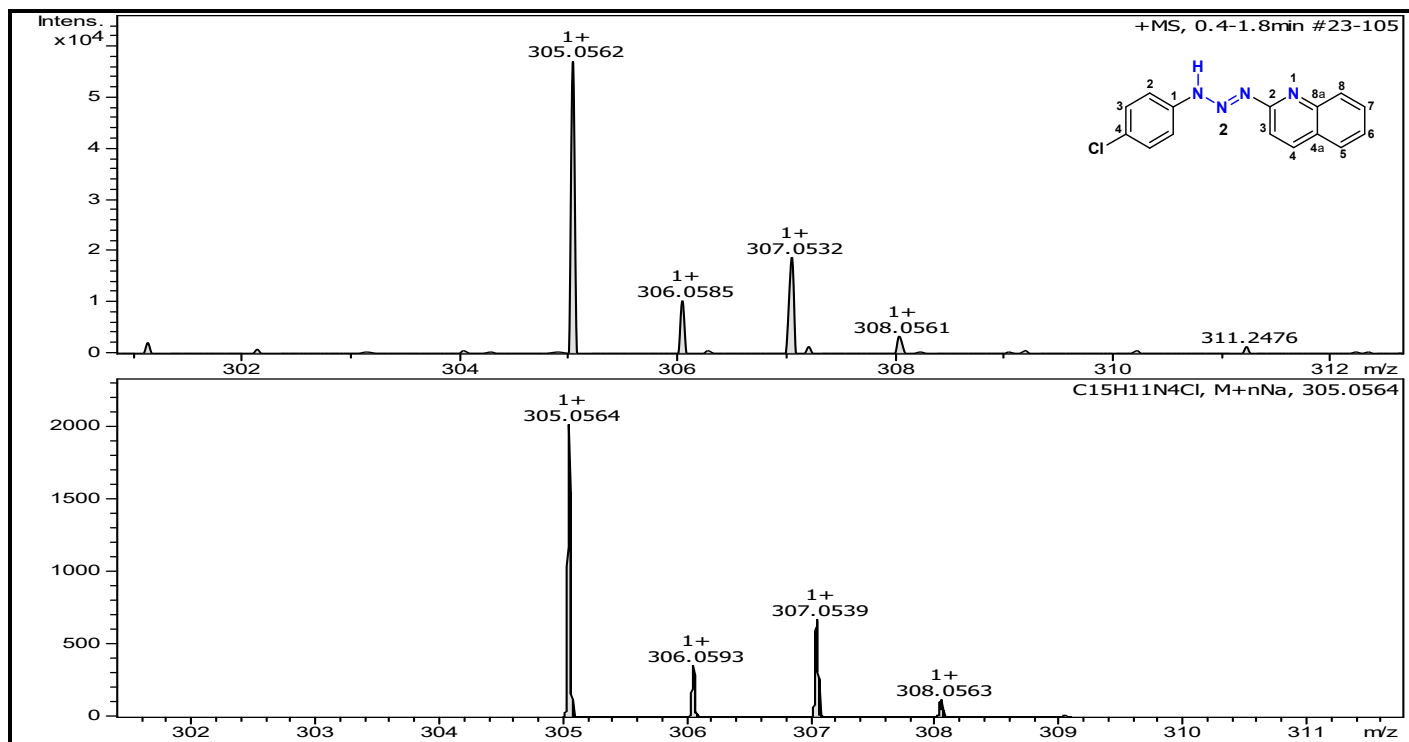
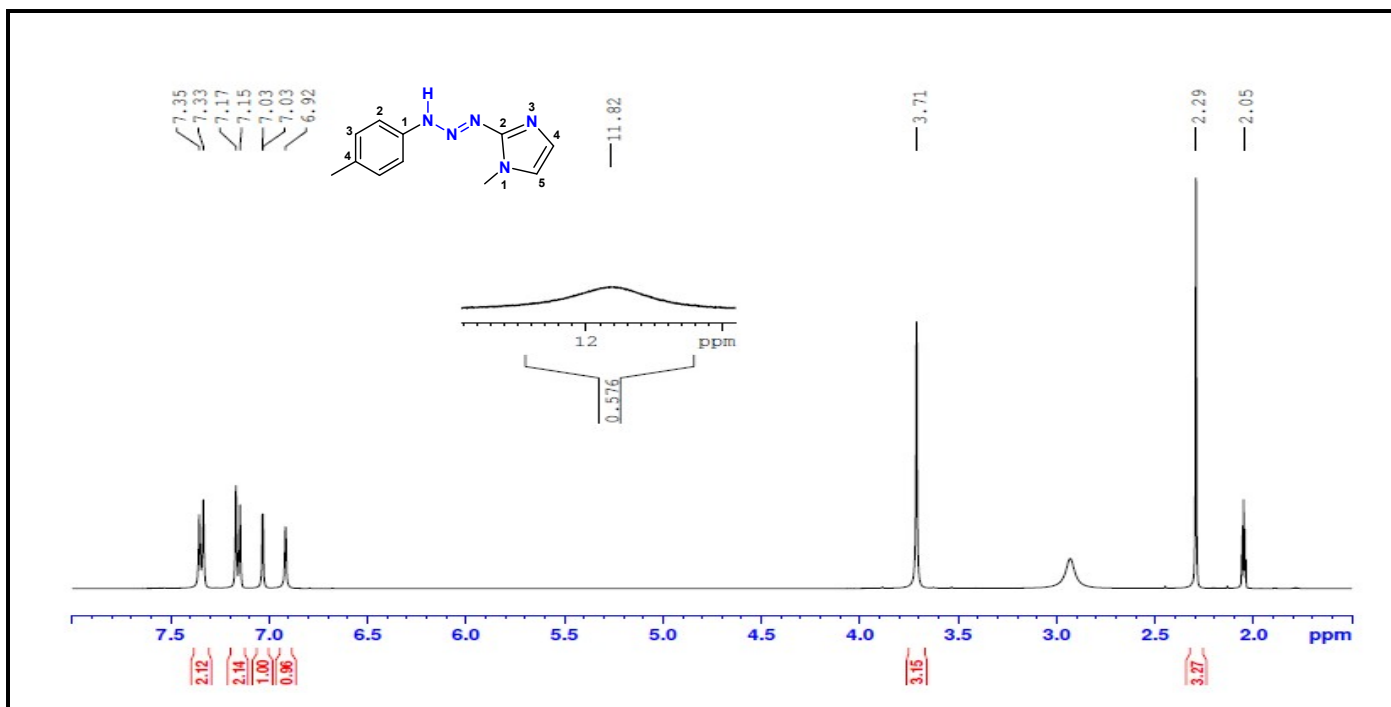
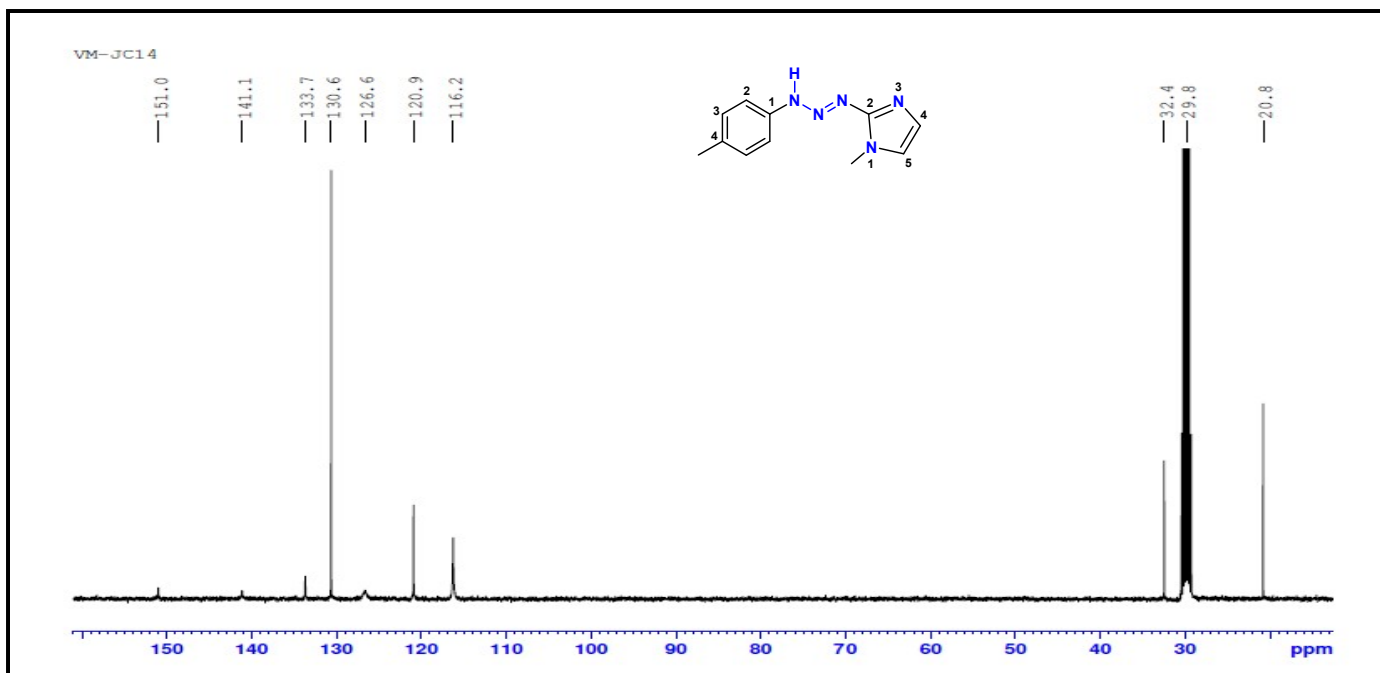


Figure S23. HRMS of triazene 2 (above) and calculated spectrum (below) with [M+Na]<sup>+</sup> adduct.



**Figure S24.**  $^1\text{H}$  NMR spectrum of **3** in  $\text{Acetone-}d_6$  (400 MHz).



**Figure S25.**  $^{13}\text{C}$   $\{^1\text{H}\}$  NMR spectrum of **3** in  $\text{Acetone-}d_6$  (100 MHz).

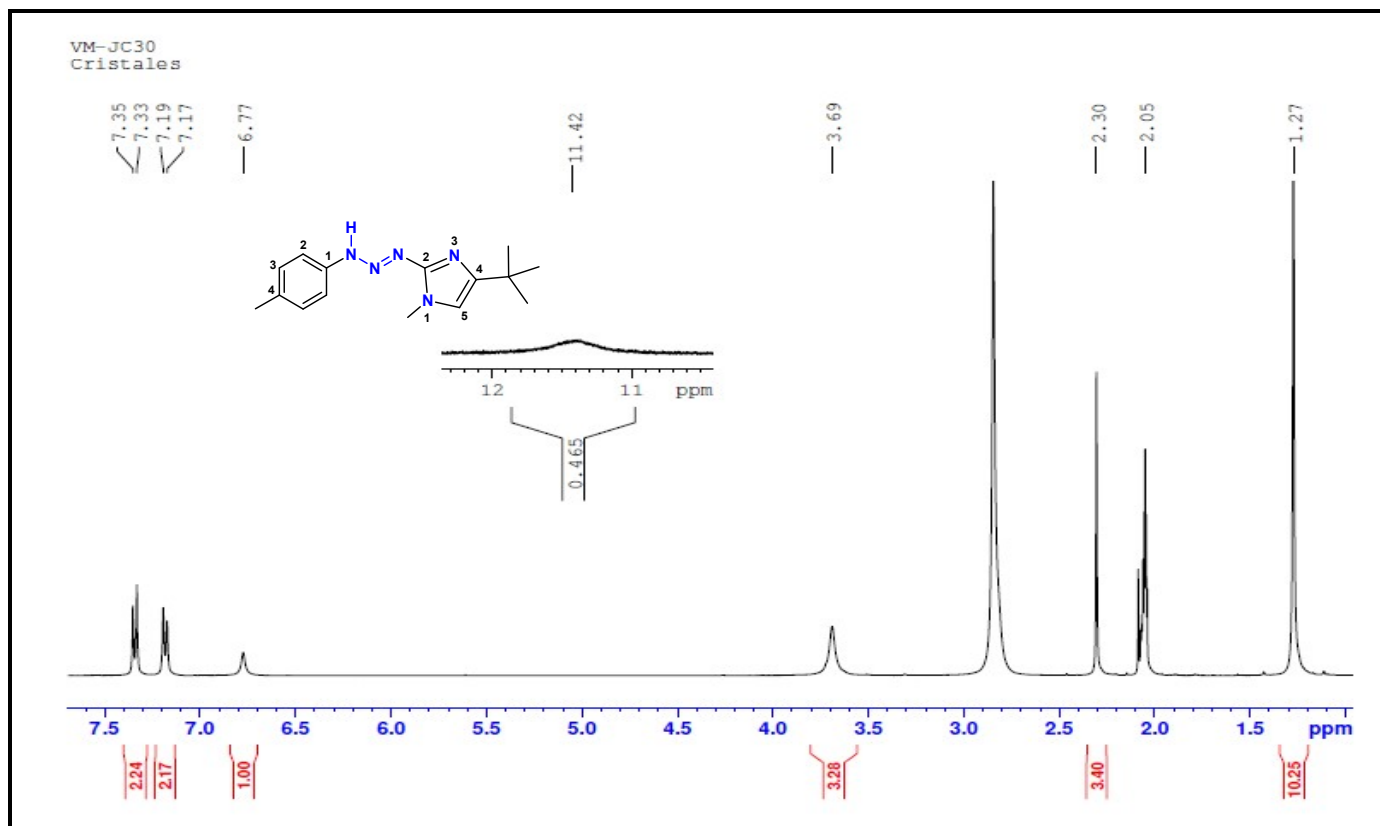


**Figure S26.**  $^1\text{H}$  NMR spectrum of **4** in acetone- $d_6$  (400 MHz).

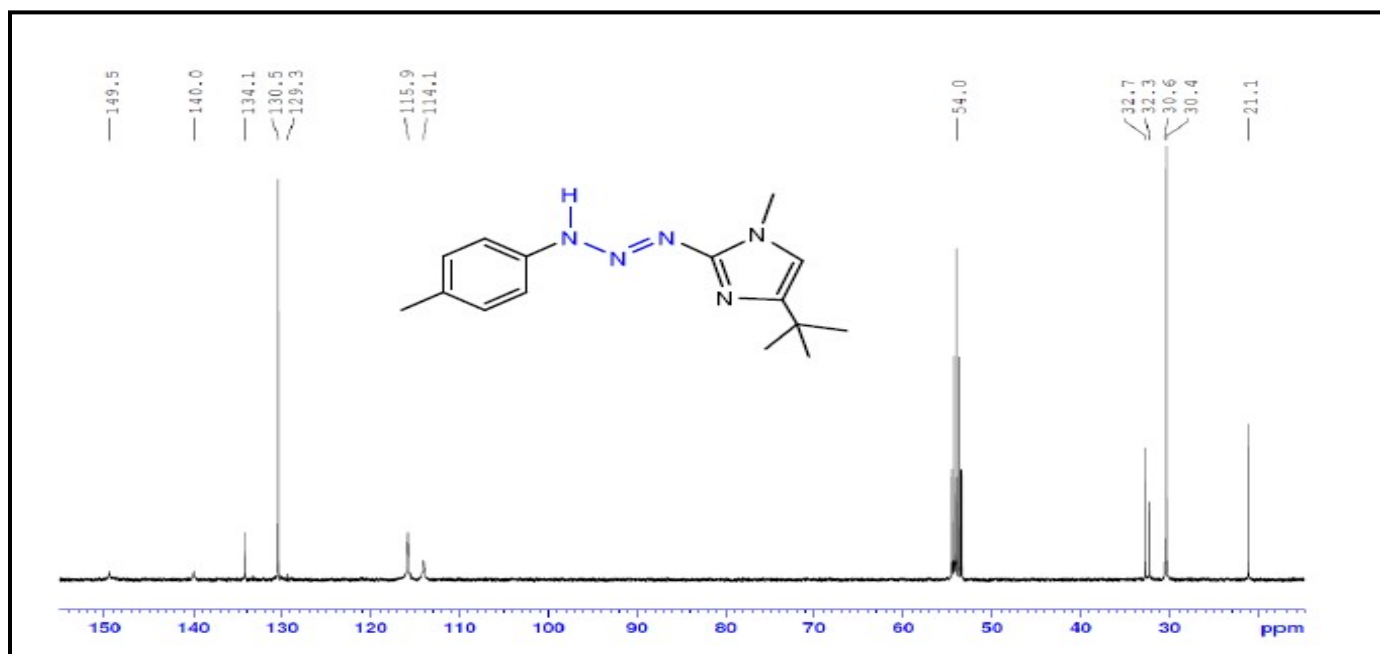


**Figure S27.**  $^{13}\text{C}$  { $^1\text{H}$ } NMR spectrum of **4** in  $\text{CD}_2\text{Cl}_2$  (100 MHz).

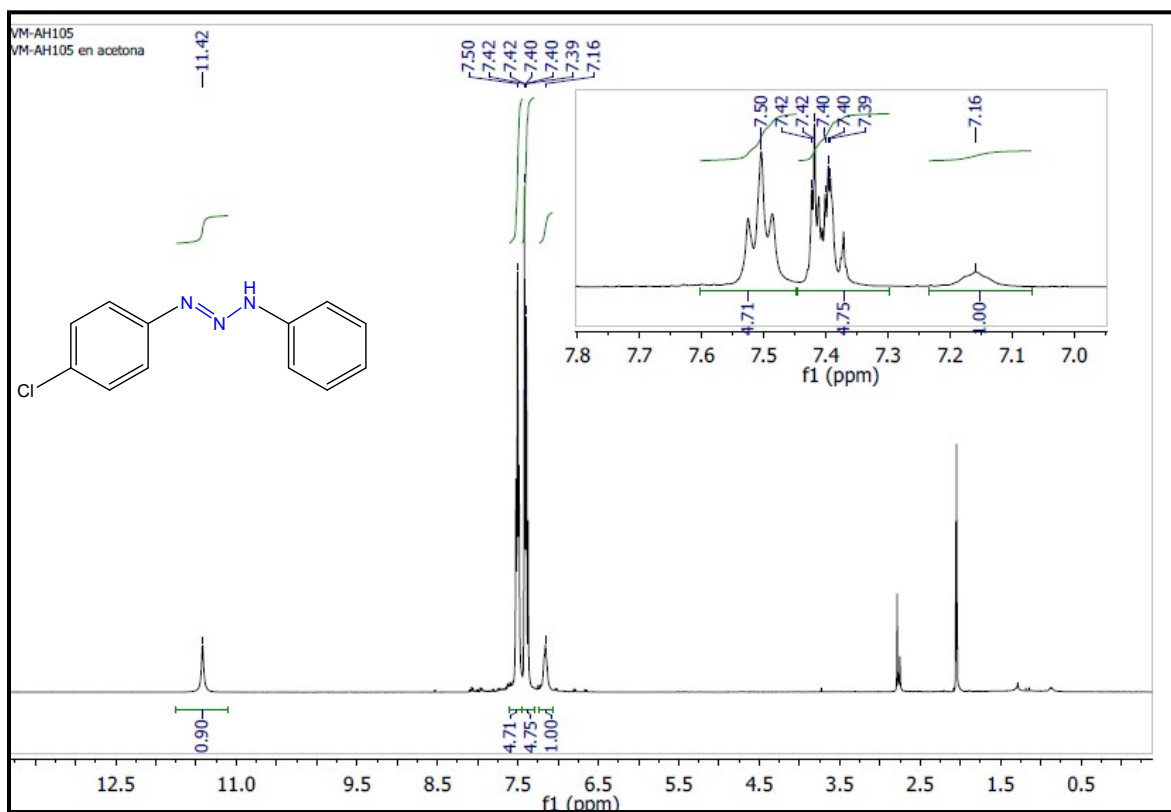


**Figure S28.**  $^1\text{H}$  NMR spectrum of triazene **9** in Acetone- $d_6$  (400 MHz).

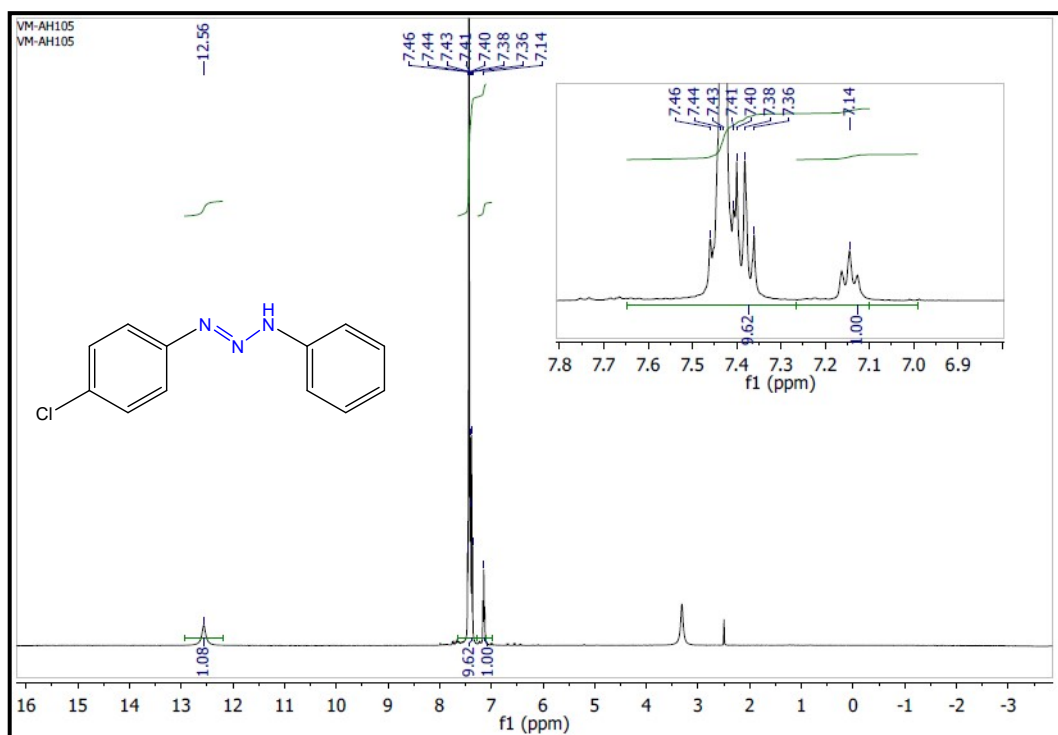


**Figure S29.**  $^1\text{H}$  NMR spectrum of triazene **9** in DMSO- $d_6$  (400 MHz).



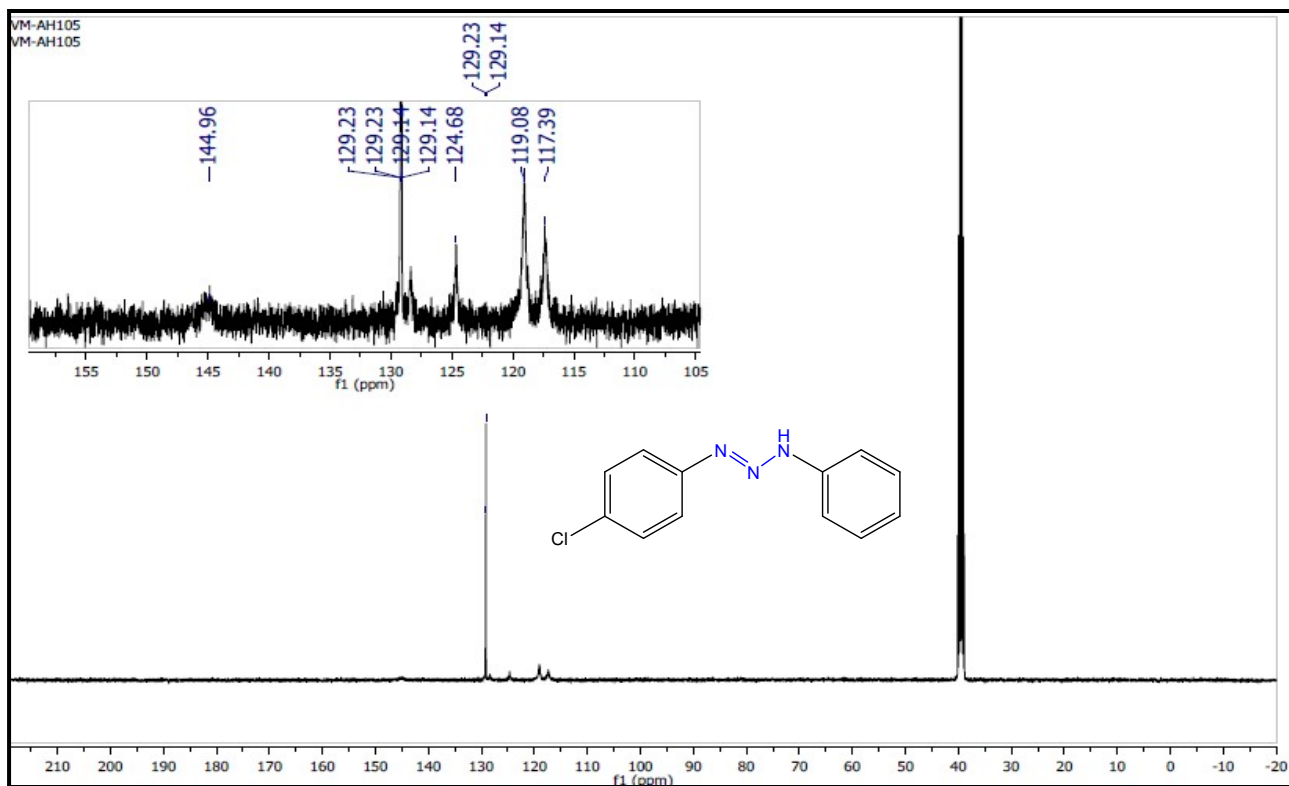


**Figure S30.**  $^{13}\text{C}$   $\{^1\text{H}\}$  NMR spectrum of triazene **9** in in  $\text{DMSO-}d_6$  (100 MHz).

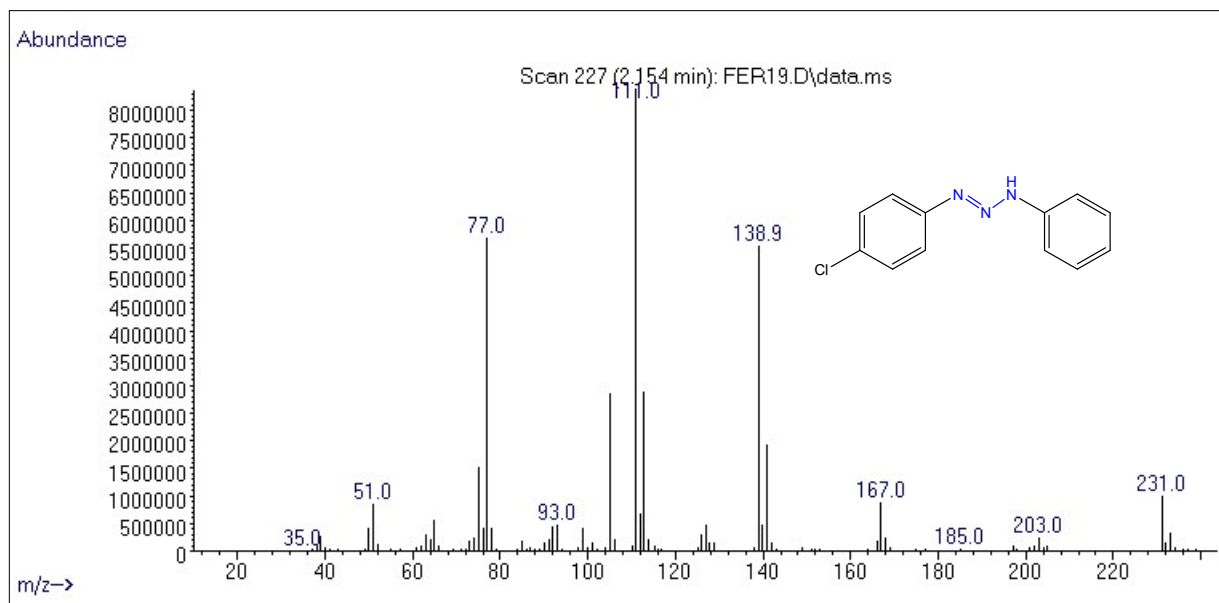


**Figure S31.** Electron-Ionization Mass Spectrum of **9**.

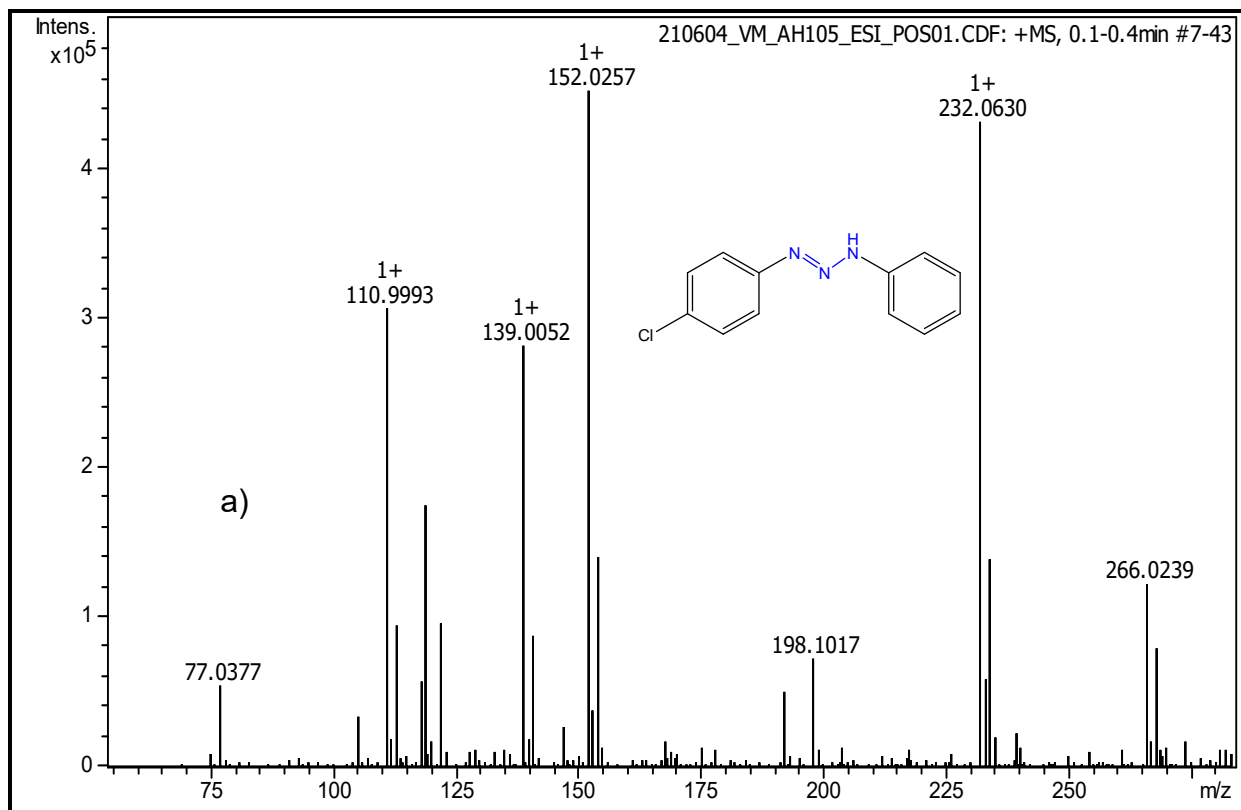


**Figure S32.** High Resolution Mass Spectrum of **9**.

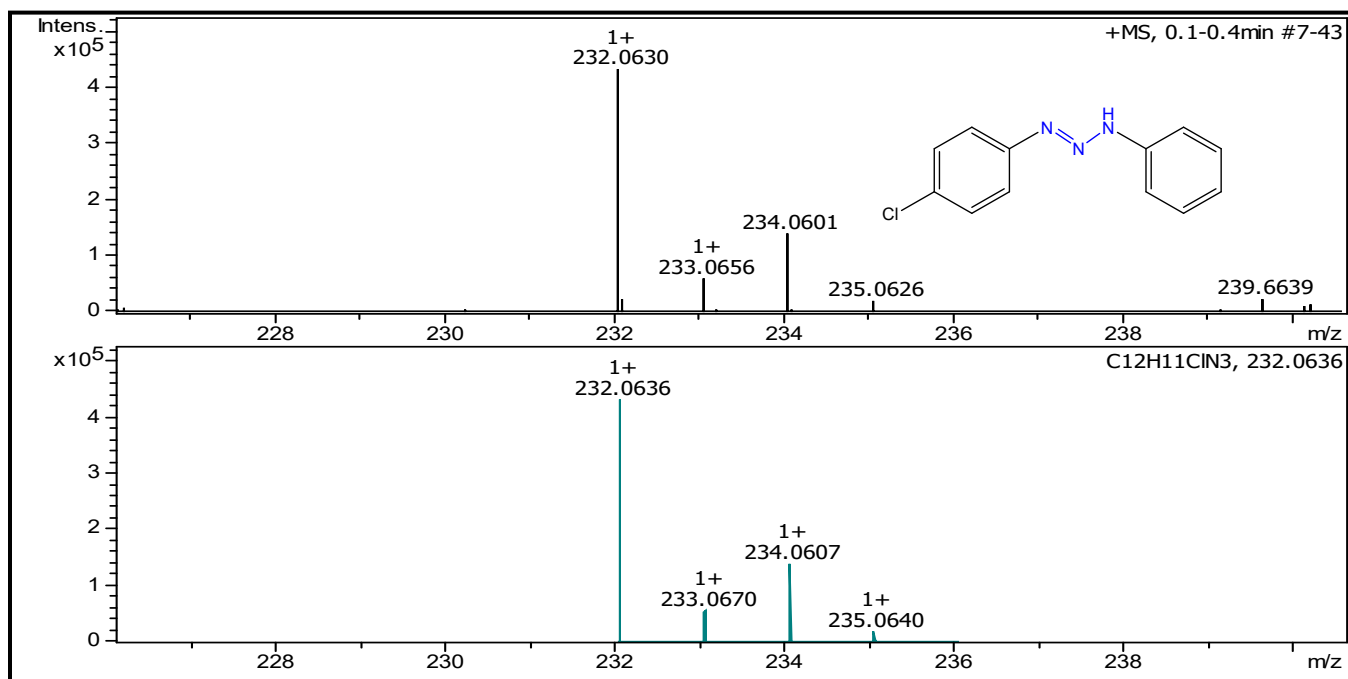


**Figure S33.** HRMS of triazene **9** (above) and calculated spectrum (below) with  $[M+H]^+$ .

NMR and HRMS spectra of complexes 5, 6, 7, and 8

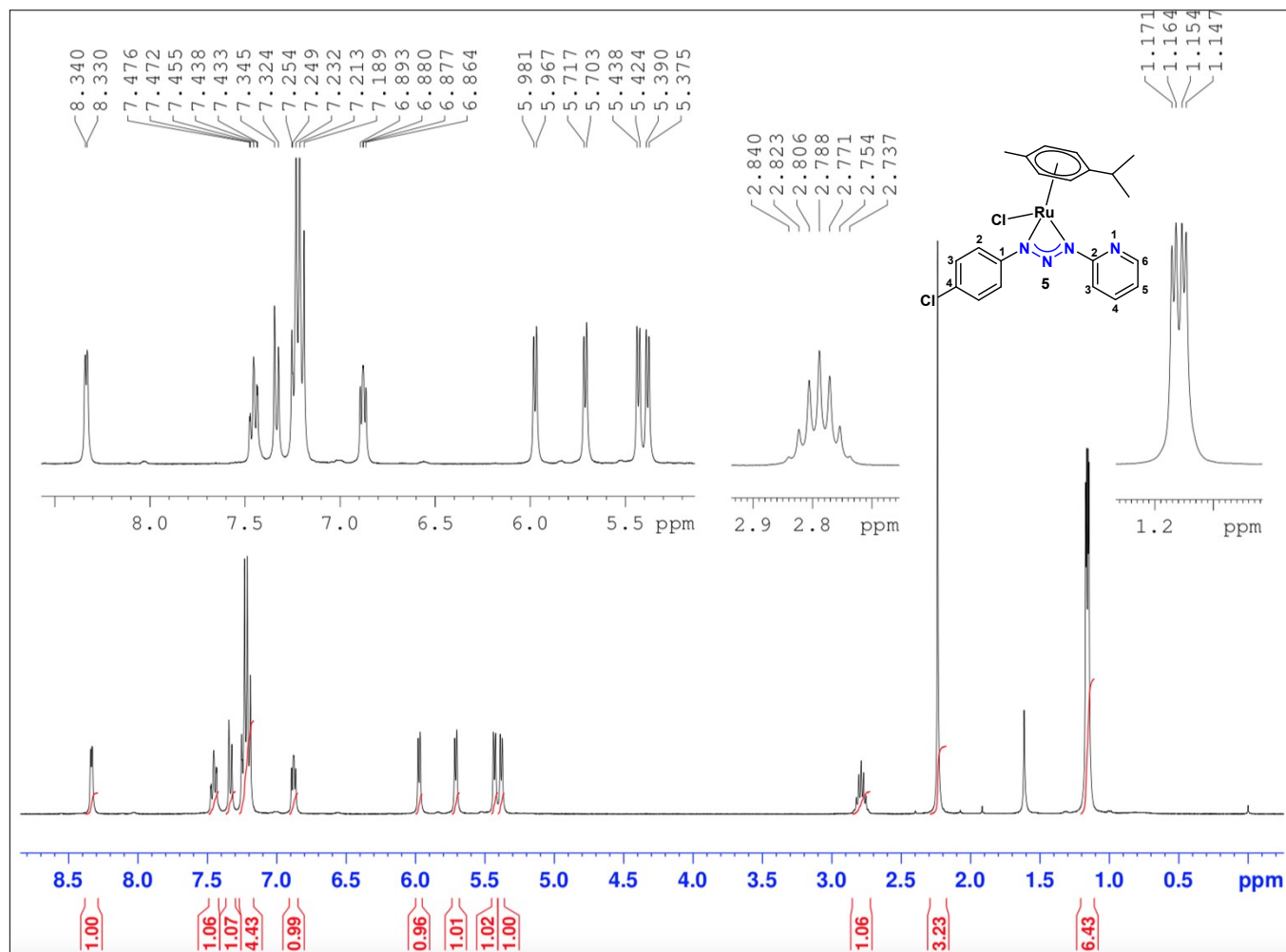
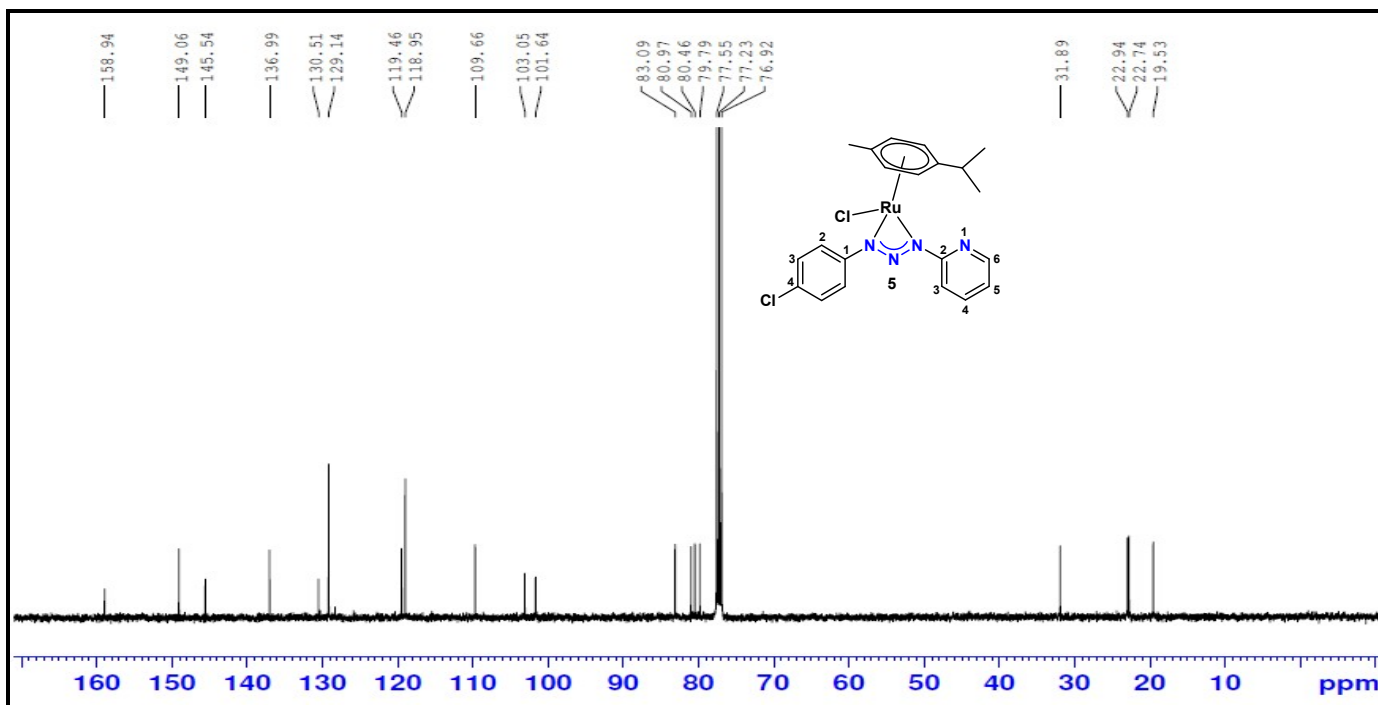
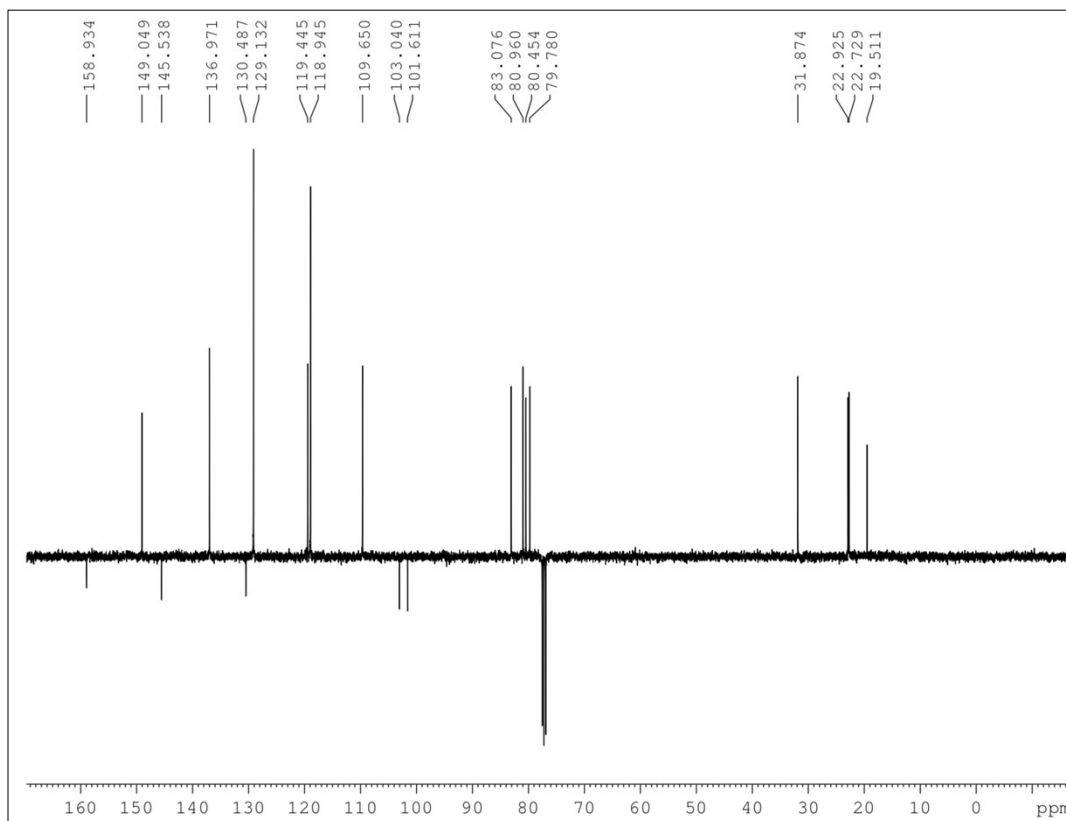


Figure S34. <sup>1</sup>H NMR spectrum of **5** in CDCl<sub>3</sub> (400 MHz).



**Figure S35.**  $^{13}\text{C}$  { $^1\text{H}$ } NMR spectrum of **5** in  $\text{CDCl}_3$  (100 MHz).



**Figure S36.** Partial  $^{13}\text{C}$  { $^1\text{H}$ } NMR-APT spectrum of **5** in  $\text{CDCl}_3$  (100 MHz).

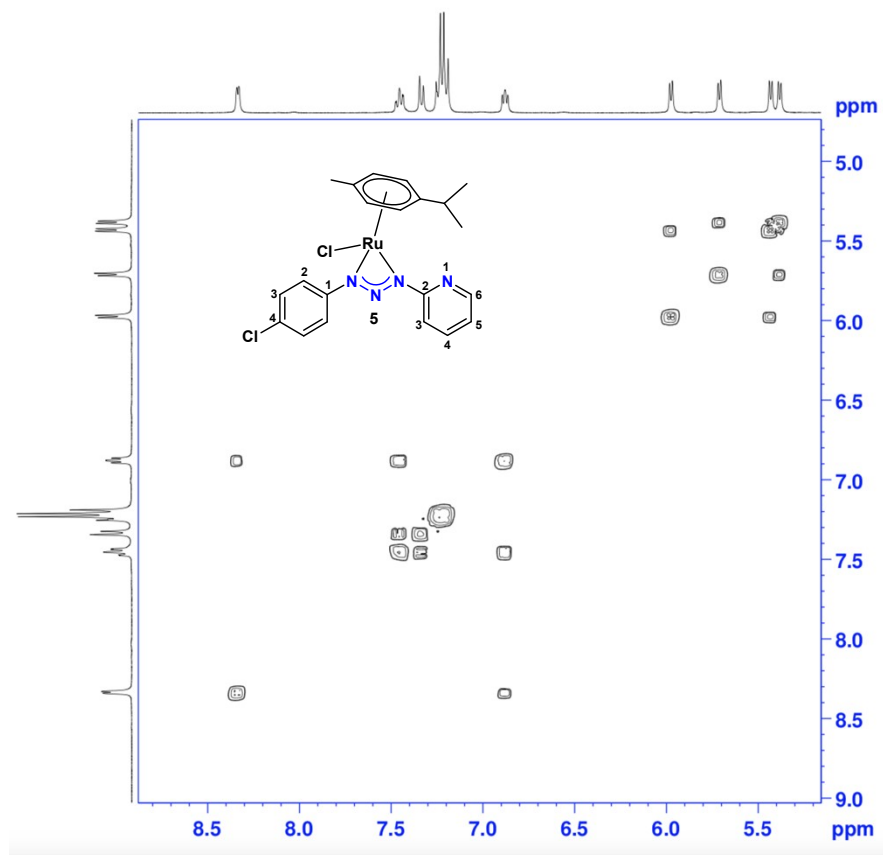


**Figure S37.** Partial  $^1\text{H}$ - $^1\text{H}$  gCOSY NMR spectrum of **5** in  $\text{CDCl}_3$ .

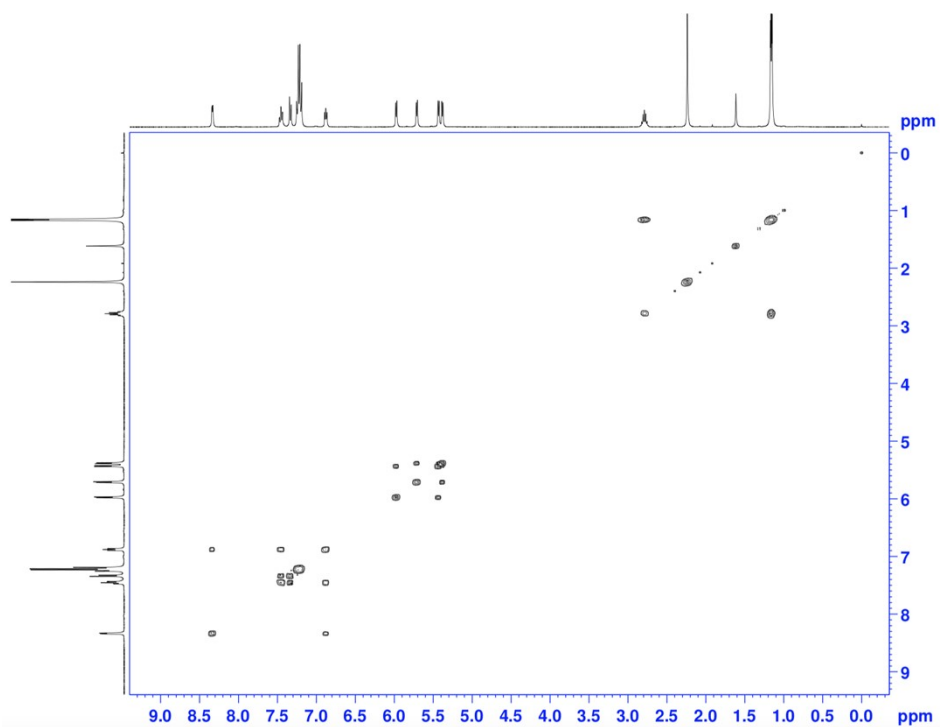


**Figure S38.** Full  $^1\text{H}$ - $^1\text{H}$  gCOSY NMR spectrum of **5** in  $\text{CDCl}_3$ .

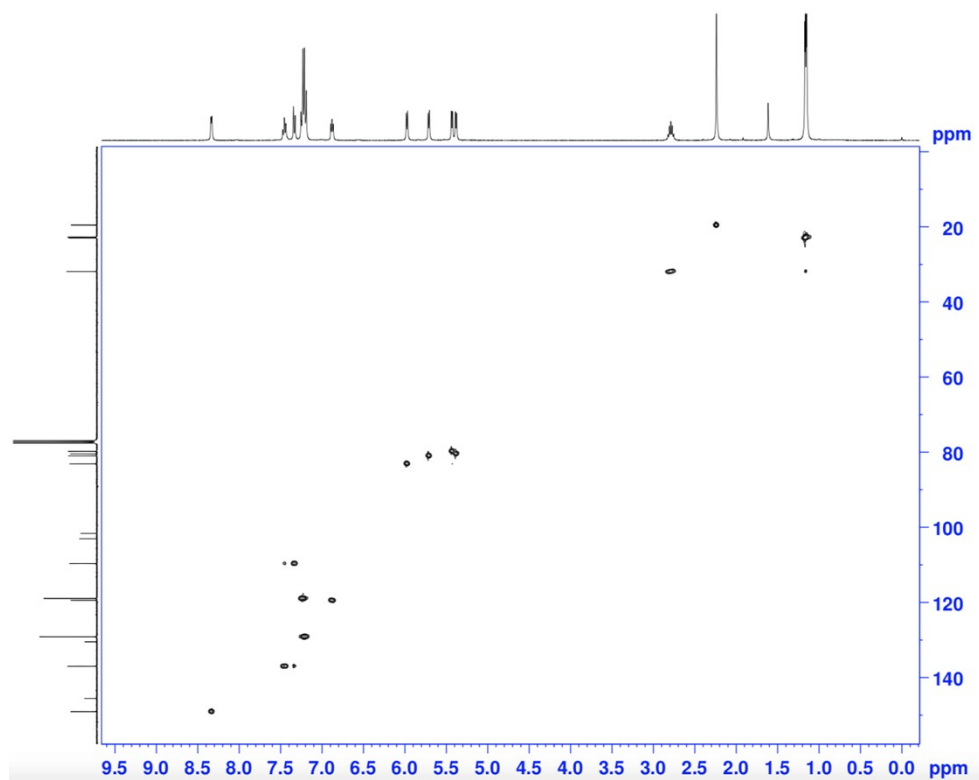


**Figure S39.**  $^1\text{H}$ - $^{13}\text{C}$  gHSQC NMR spectrum of **5** in  $\text{CDCl}_3$ .

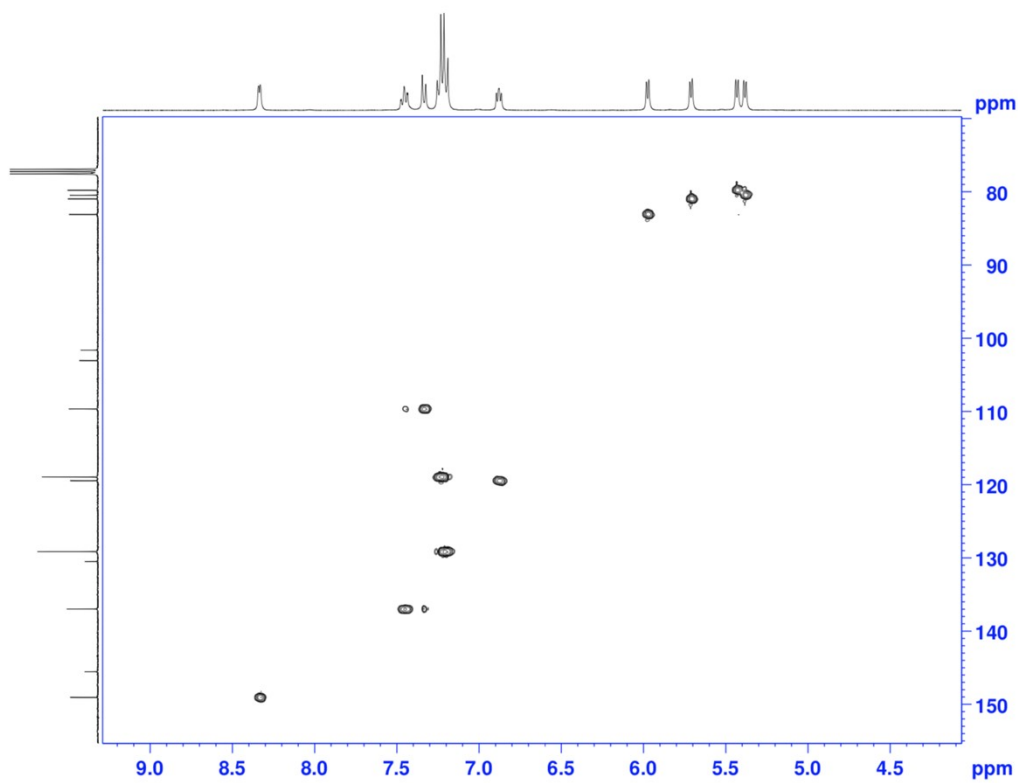


**Figure S40.** Partial  $^1\text{H}$ - $^{13}\text{C}$  gHSQC NMR spectrum of **5** in  $\text{CDCl}_3$ .

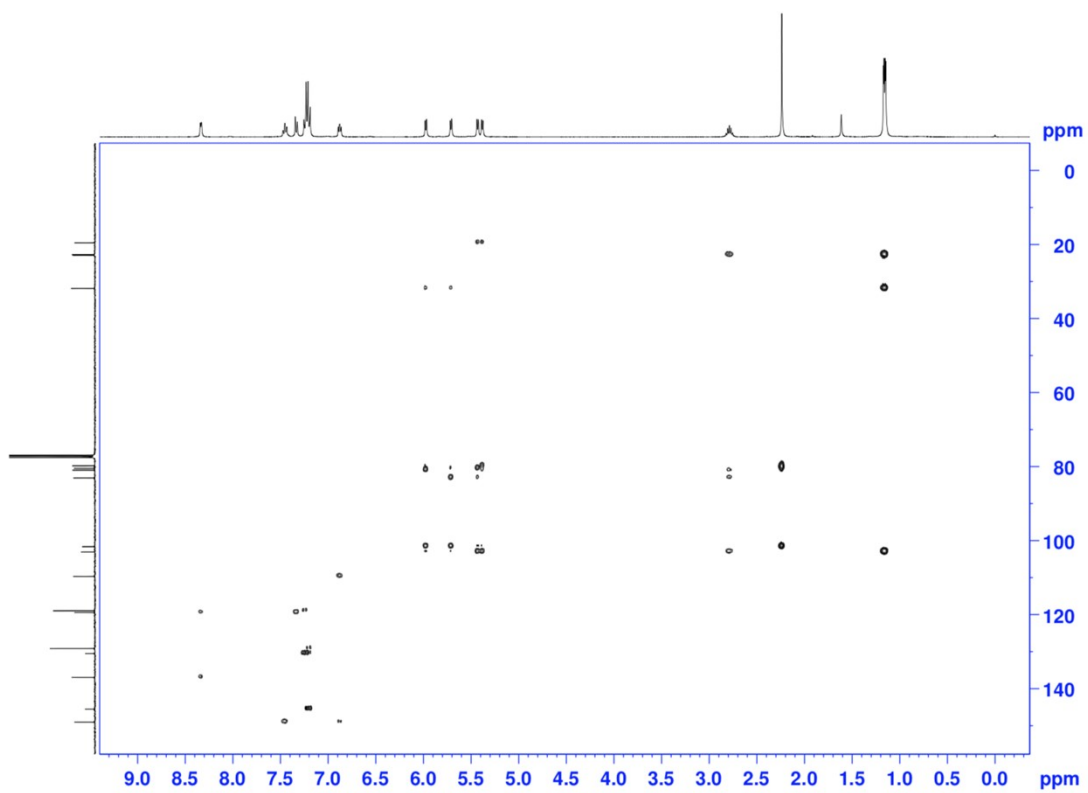


**Figure S41.**  $^1\text{H}$ - $^{13}\text{C}$  HMBC NMR spectrum of **5** in  $\text{CDCl}_3$ .

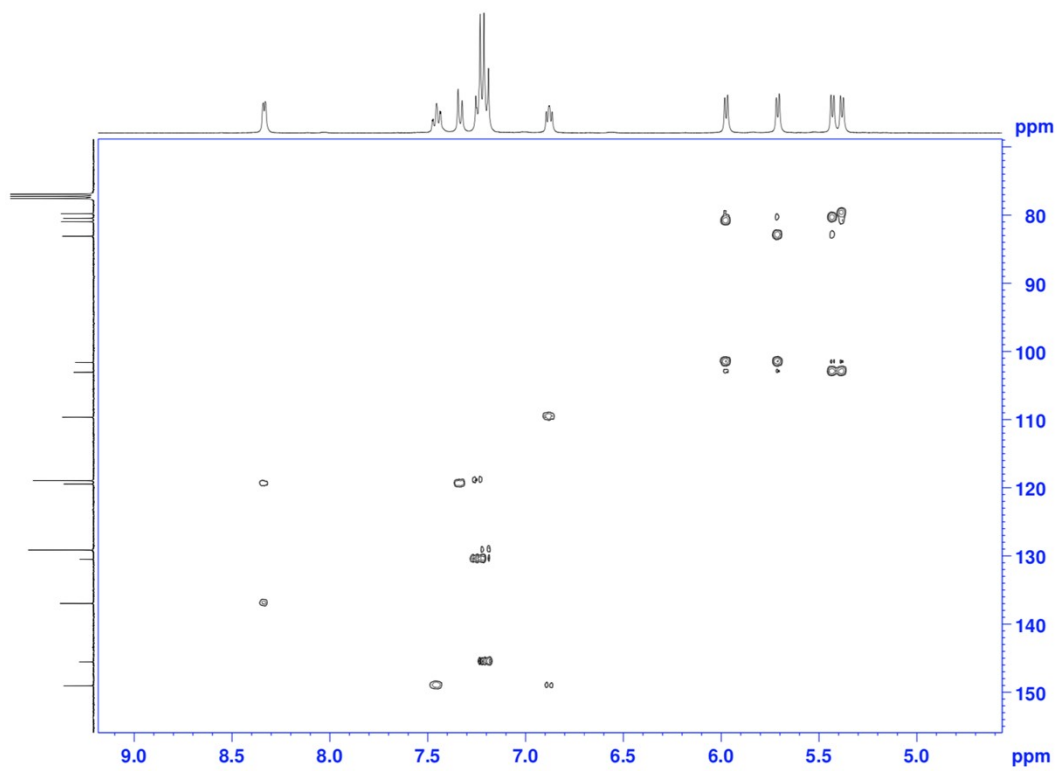


**Figure S42.** Partial  $^1\text{H}$ - $^{13}\text{C}$  HMBC NMR spectrum of **5** in  $\text{CDCl}_3$ .

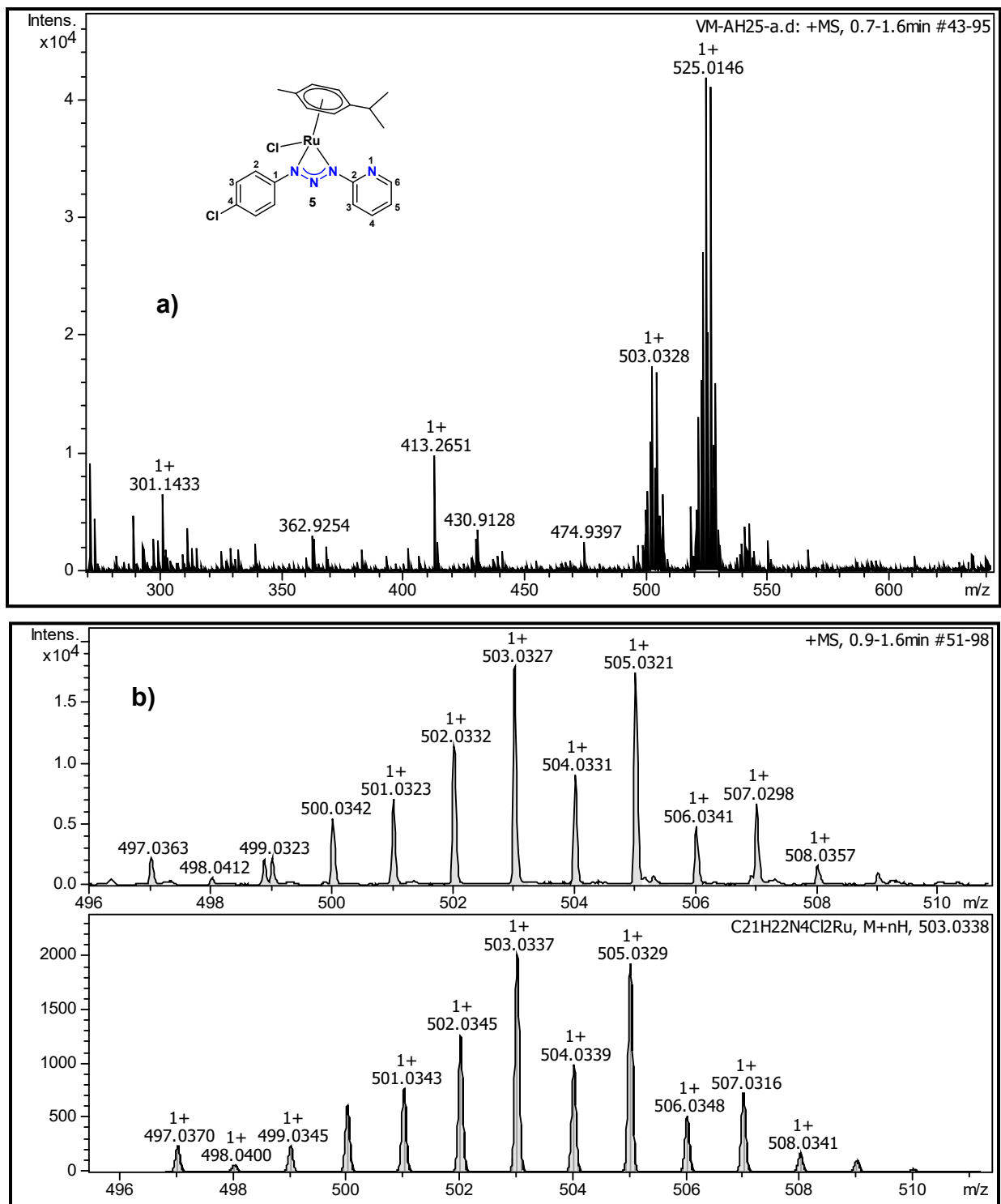


**Figure S43.** a) HRMS of **5**; b) HRMS of complex **5** (above) and simulated spectrum (below)  $[M+H]^+$ .



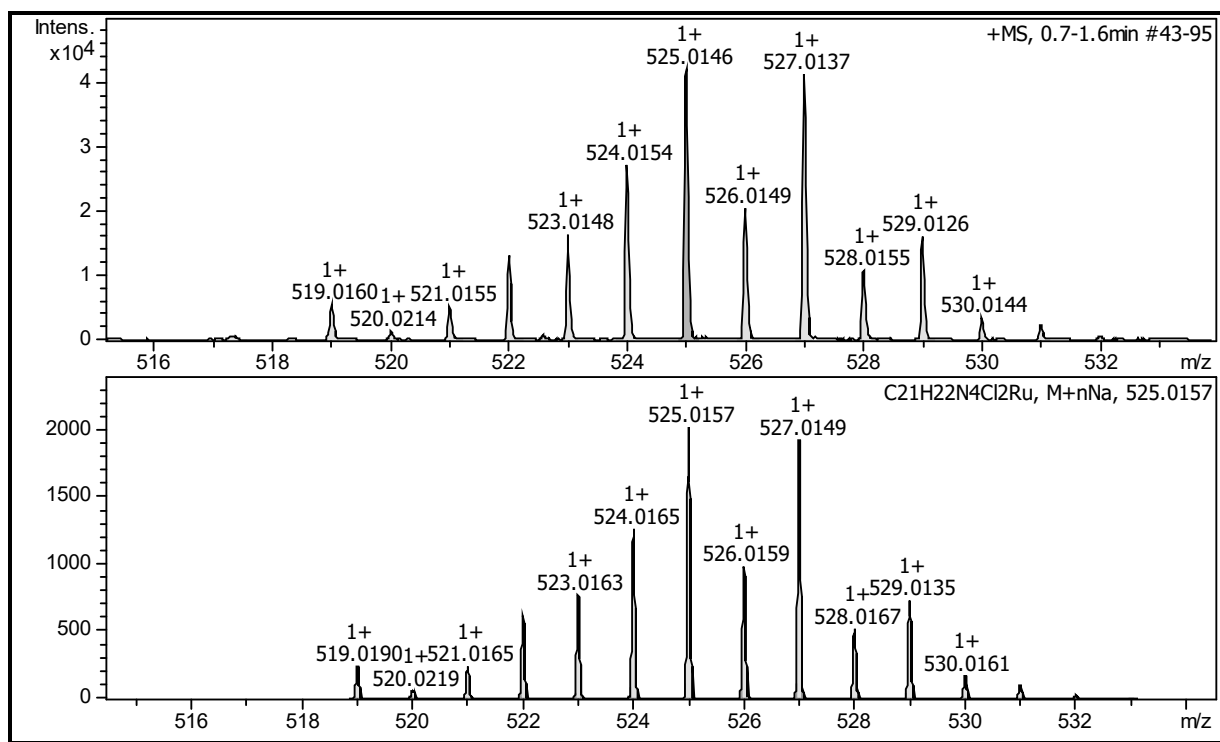


Figure S44. HRMS for **5** (above) and simulated spectrum (below) [M+Na] adduct.

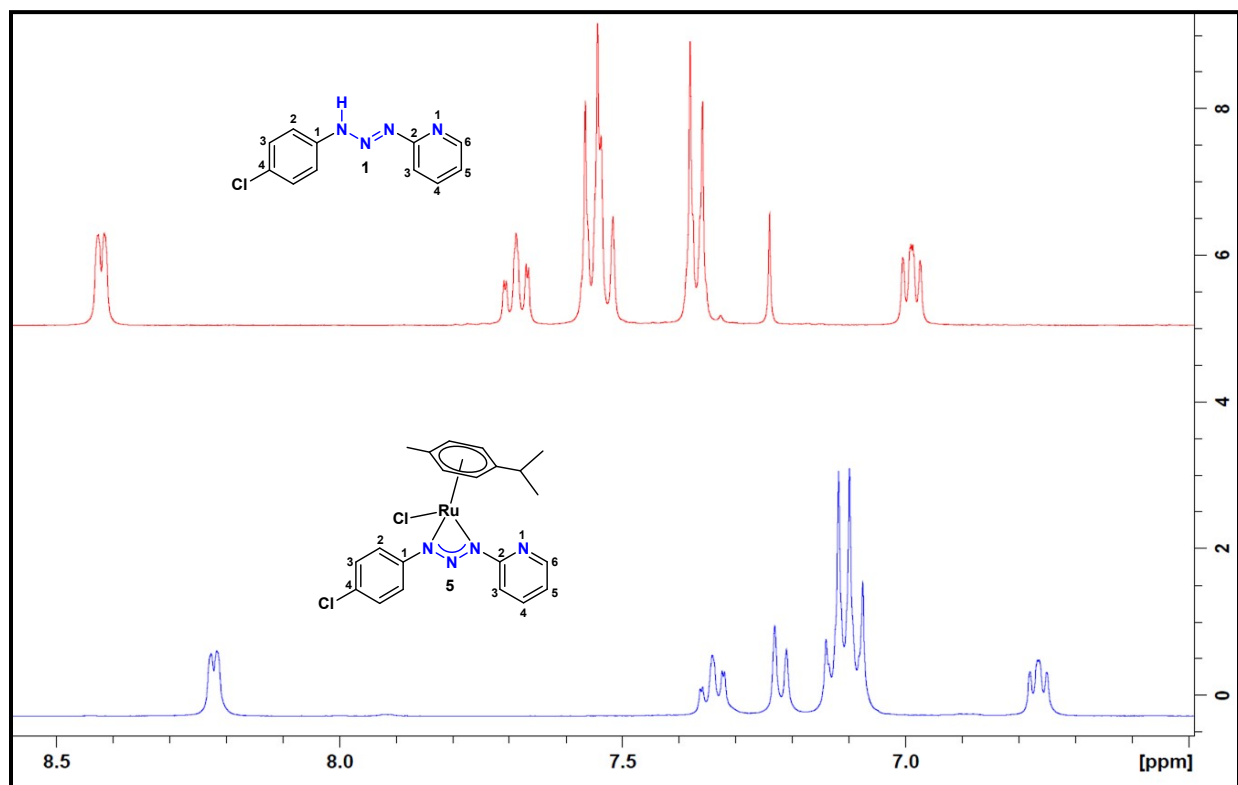
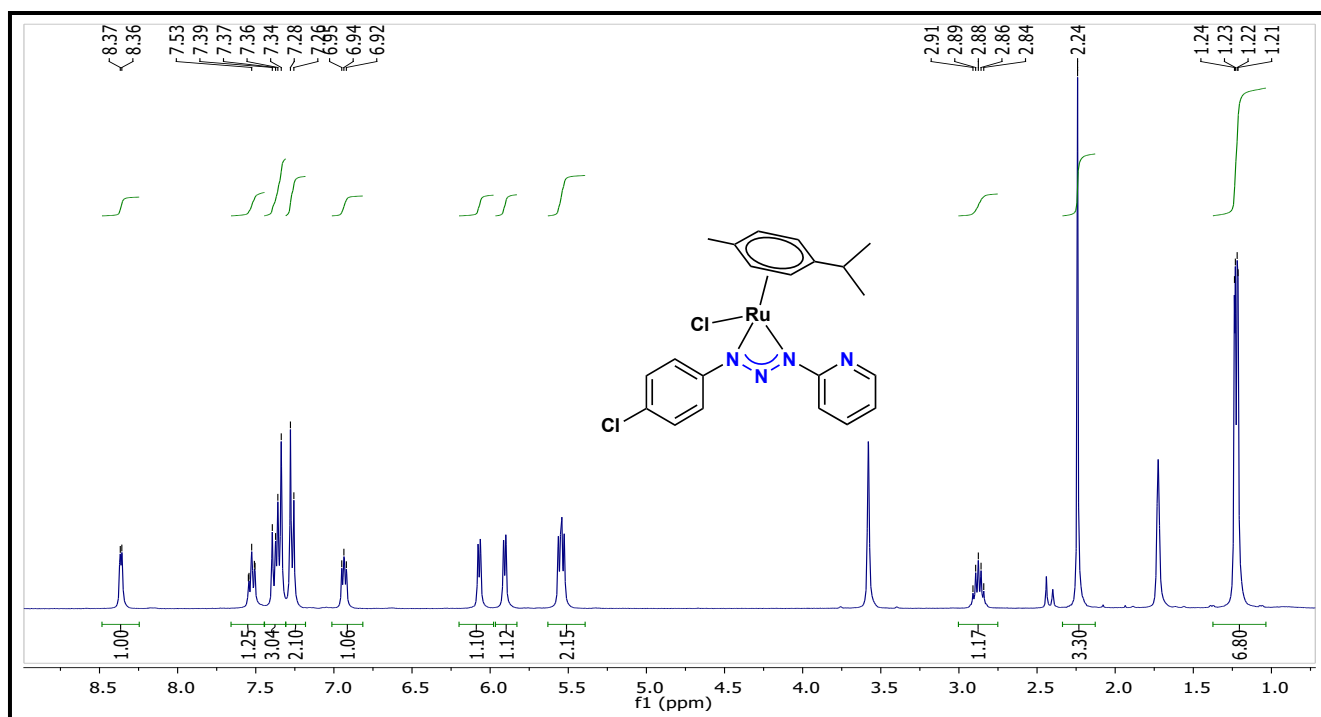
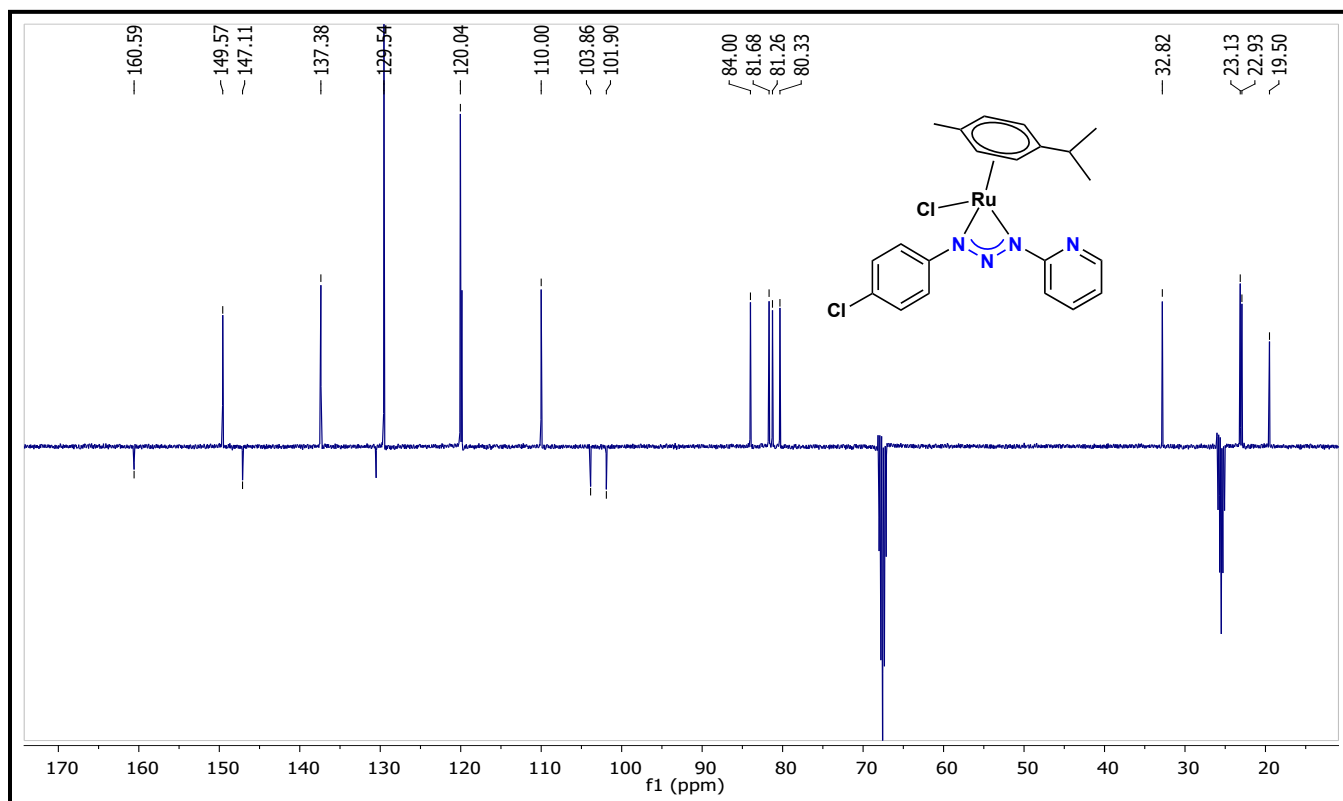


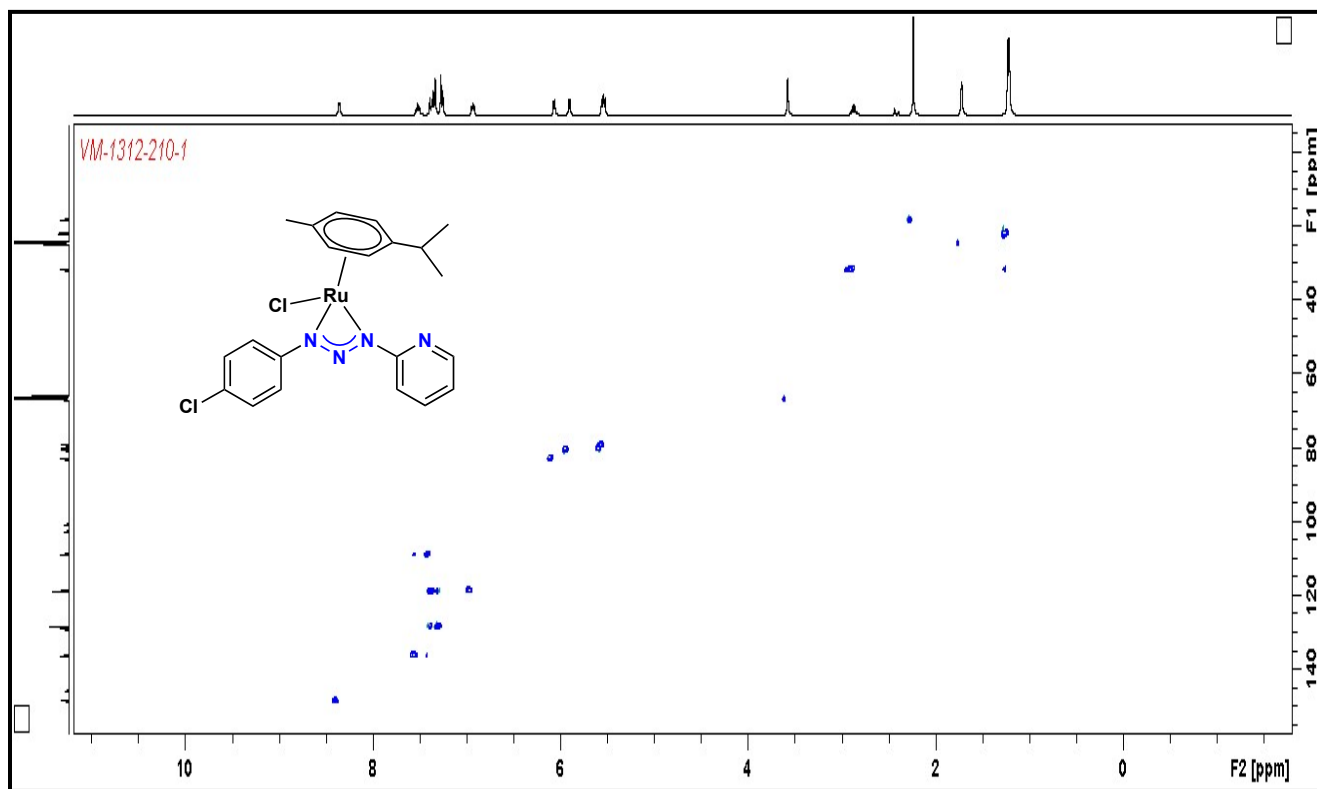
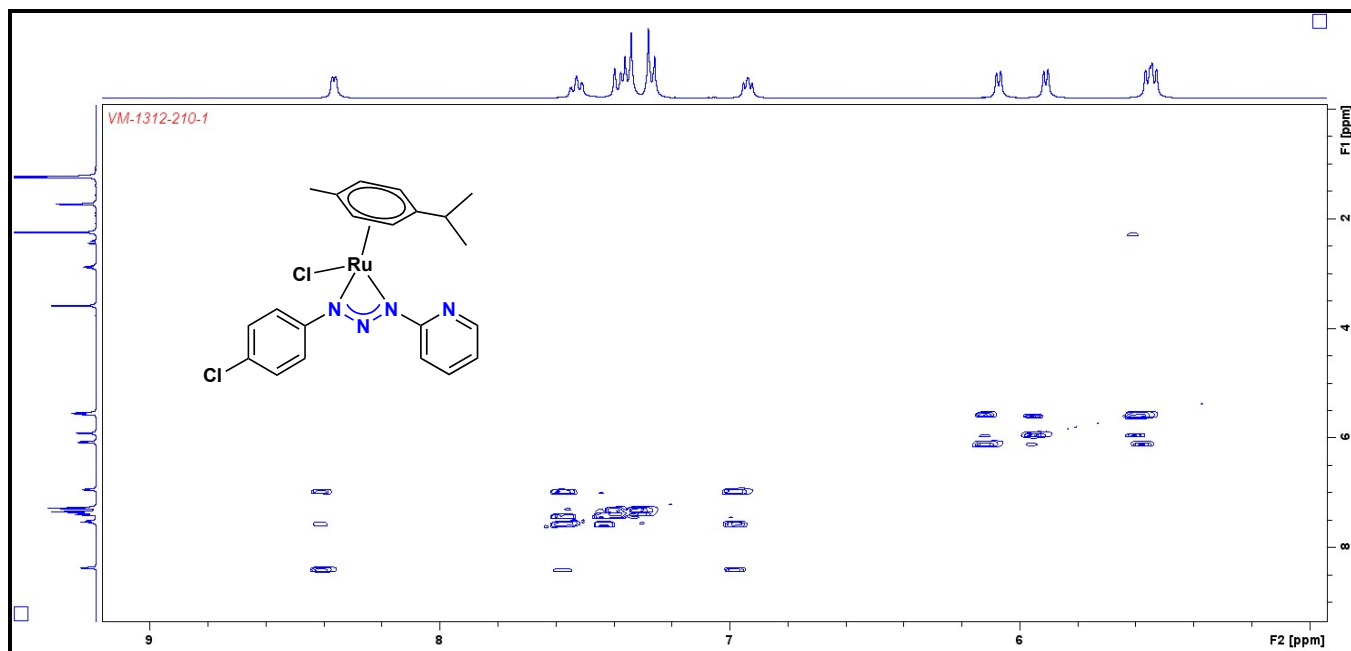
Figure S45. Partial <sup>1</sup>H NMR spectrum of complex **5** and free triazene **1** in CDCl<sub>3</sub>.



**Figure S46.**  $^1\text{H}$  NMR spectrum of **5** in  $\text{THF-d}_8$  (400 MHz).



**Figure S47.**  $^{13}\text{C}$   $\{^1\text{H}\}$  NMR-APT spectrum of **5** in  $\text{THF-d}_8$  (100 MHz).



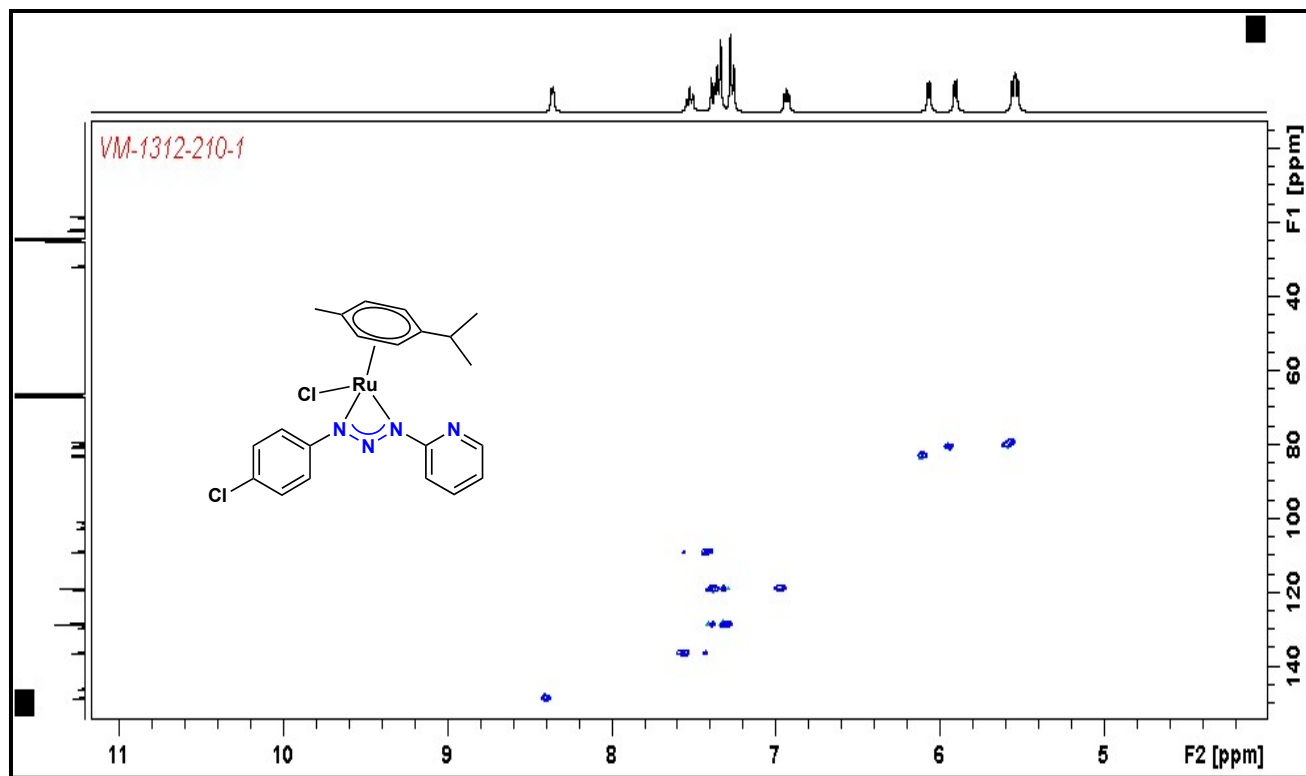


**Figure S50.** Partial  $^1\text{H}$ - $^{13}\text{C}$  gHSQC NMR spectrum of **5** in  $\text{THF-}d_8$ .

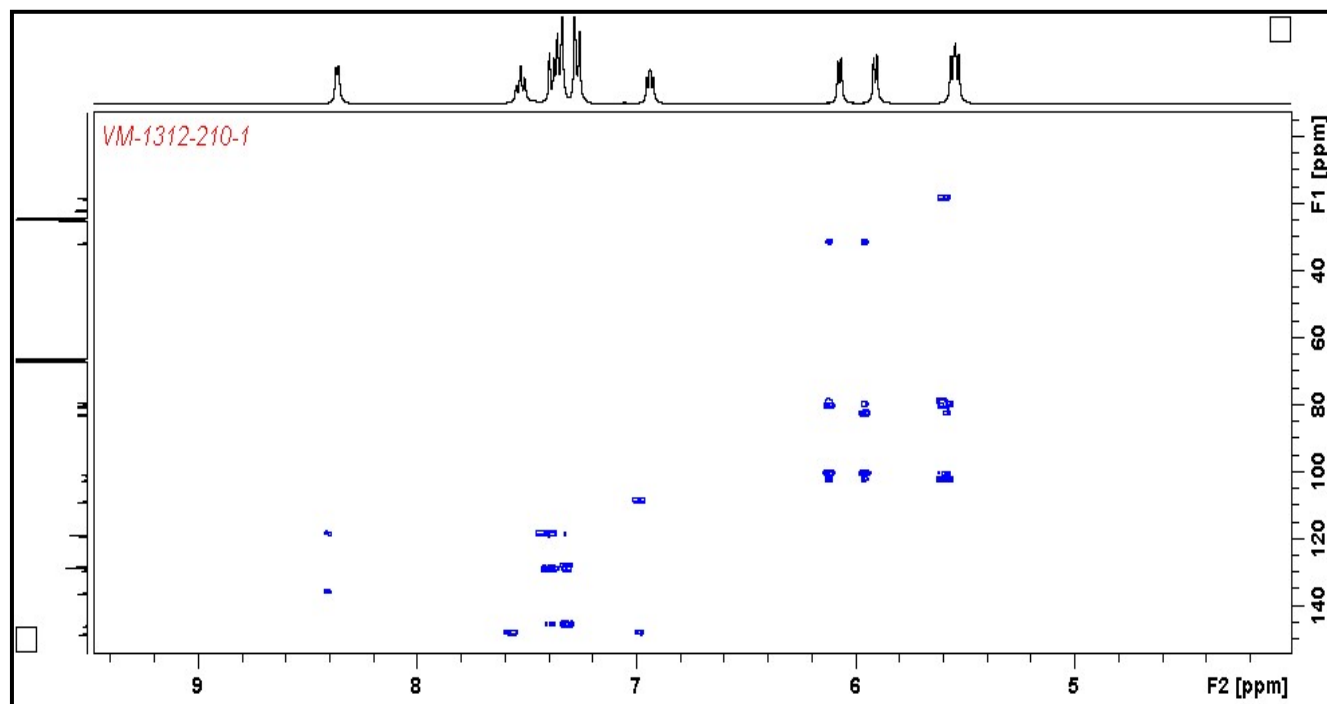


**Figure S51.** Partial  $^1\text{H}$ - $^{13}\text{C}$  HMBC NMR spectrum of **5** in  $\text{THF-}d_8$ .

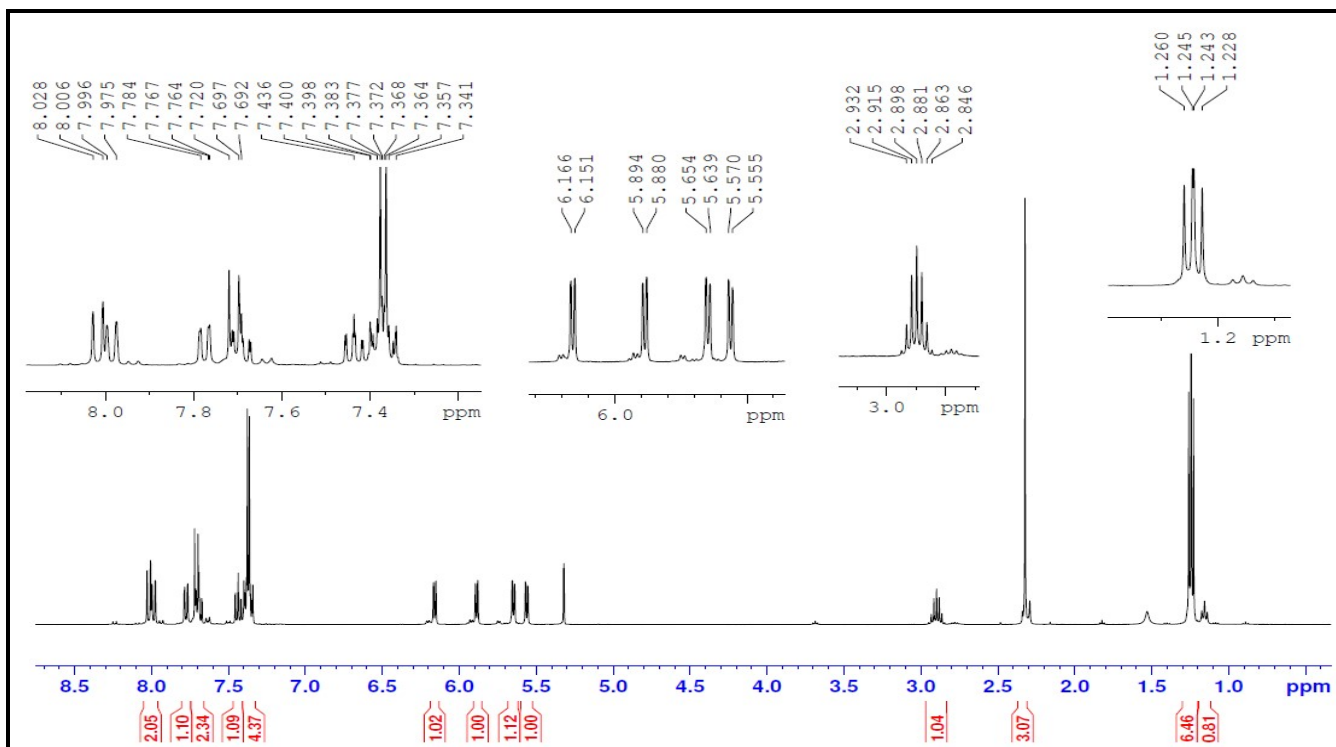


Figure S52.  $^1\text{H}$  NMR spectrum of complex **6** in  $\text{CD}_2\text{Cl}_2$  (400 MHz).

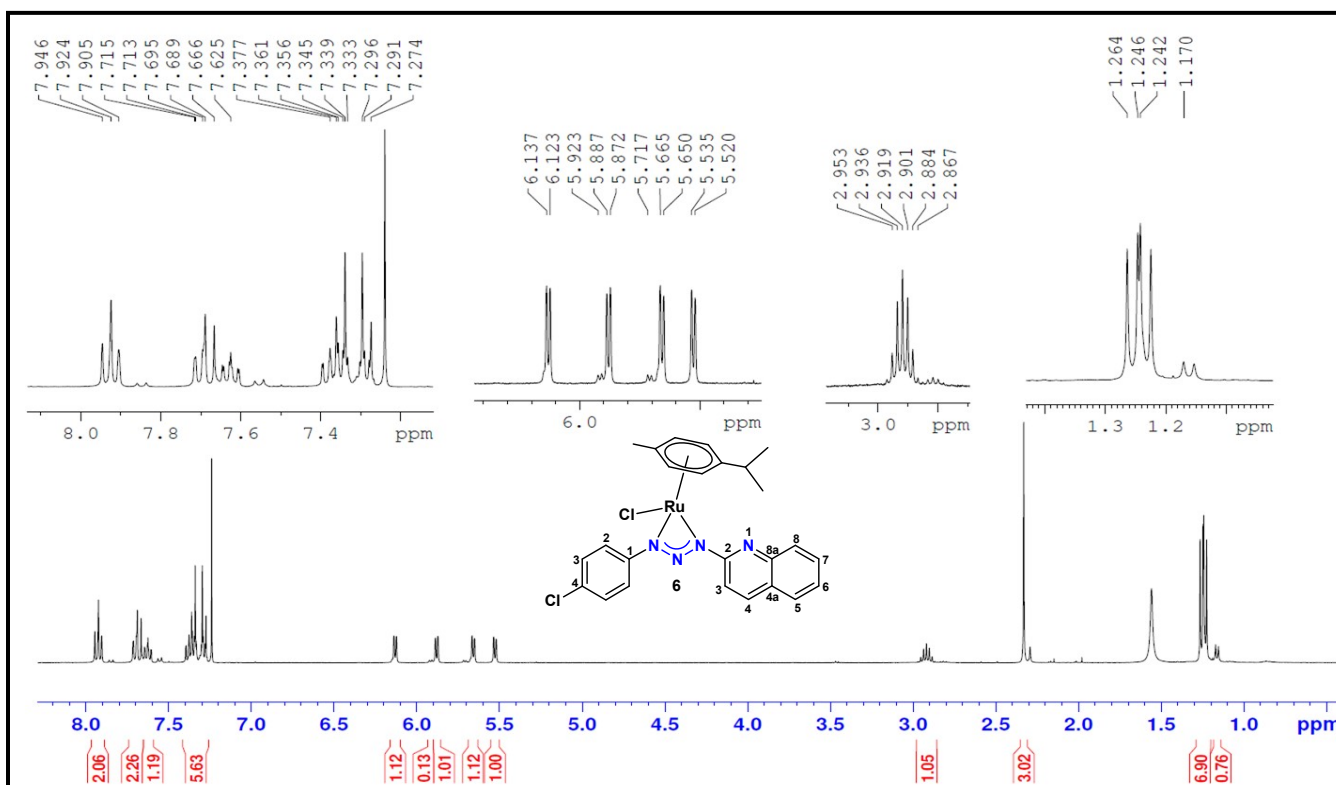
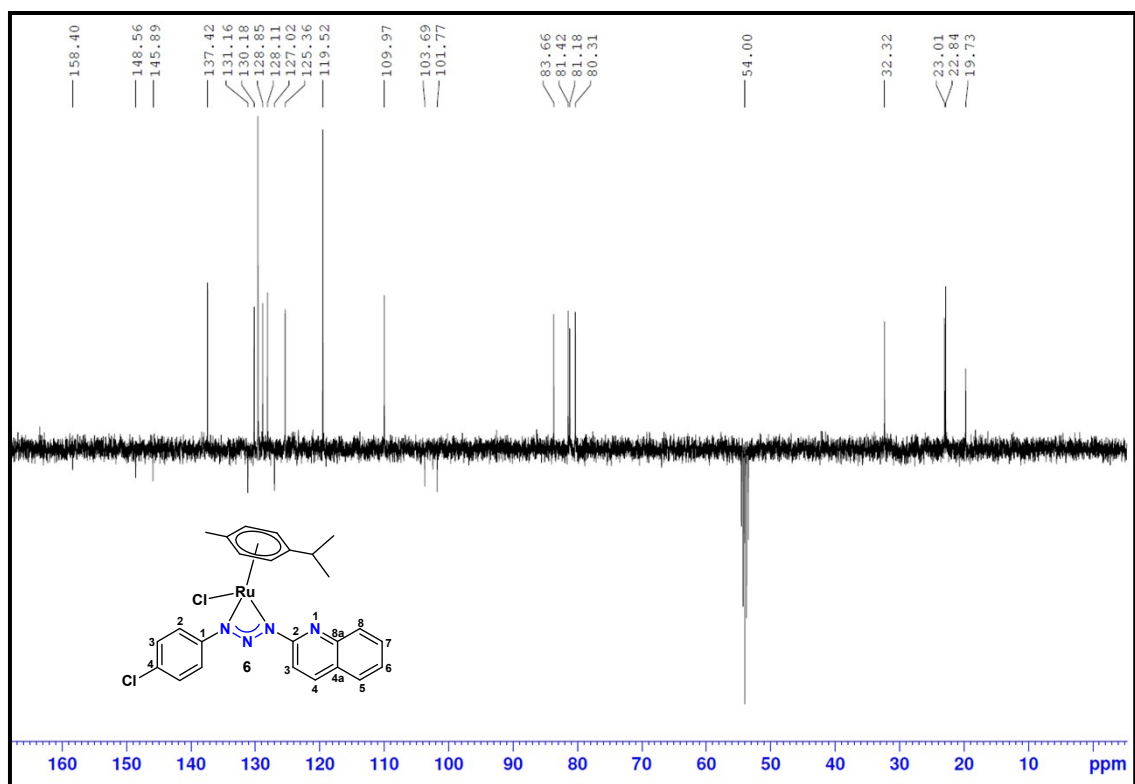
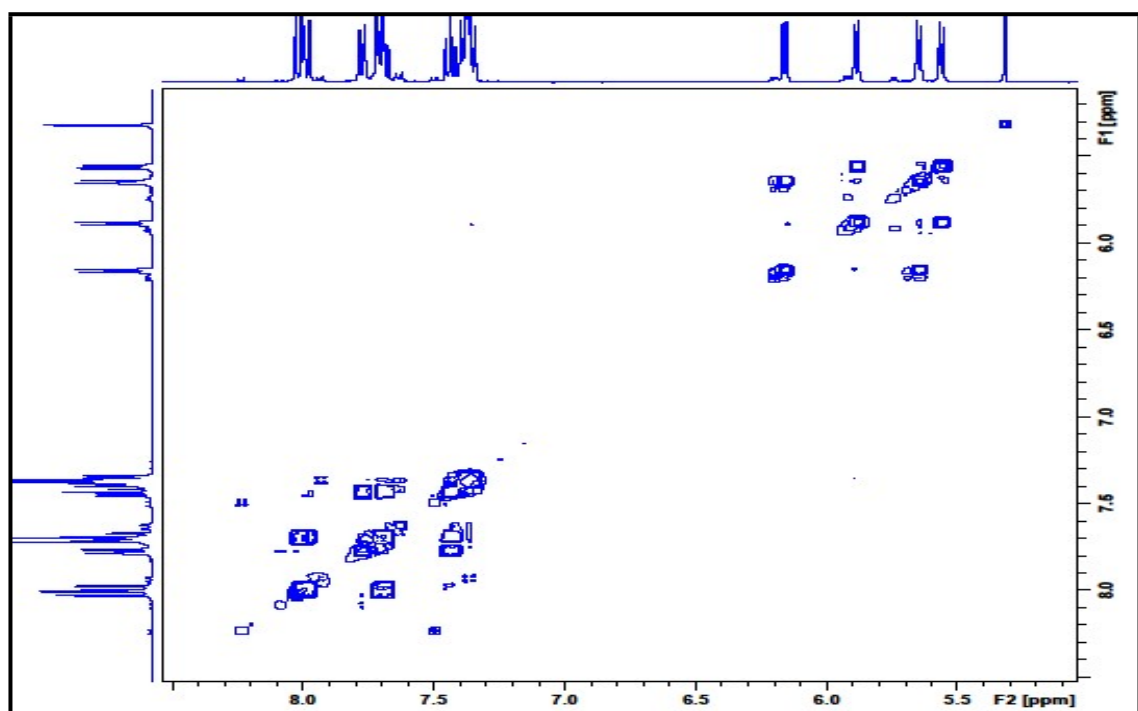


Figure S53.  $^1\text{H}$  NMR spectrum of **6** in  $\text{CDCl}_3$  (400 MHz).



**Figure S54.**  $^{13}\text{C}$  { $^1\text{H}$ } NMR-APT spectrum of complex **6** in  $\text{CD}_2\text{Cl}_2$  (100 MHz).



**Figure S55.** Partial  $^1\text{H}$ - $^1\text{H}$  gCOSY NMR spectrum of complex **6** in  $\text{CD}_2\text{Cl}_2$ .

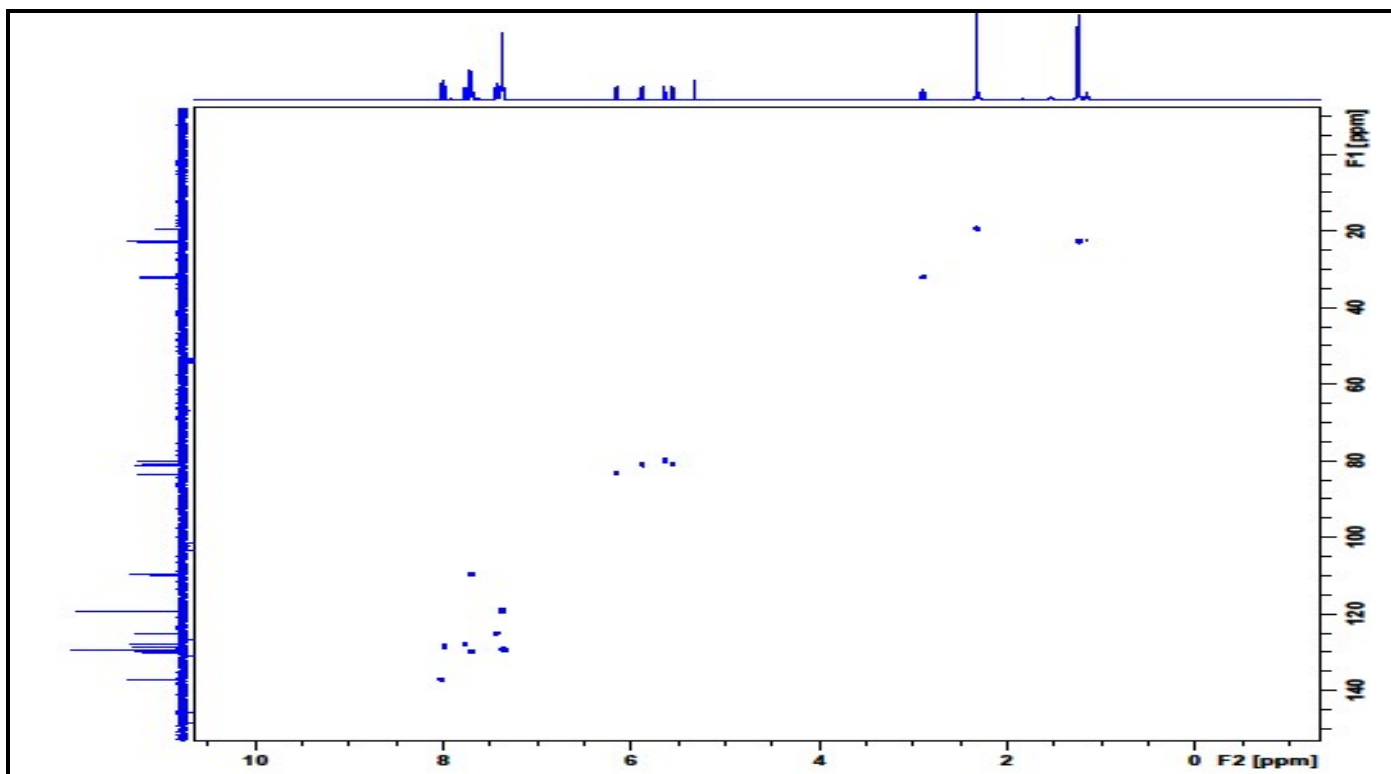


Figure S56.  $^1\text{H}$ - $^{13}\text{C}$  HSQC NMR spectrum of **6** in  $\text{CD}_2\text{Cl}_2$ .

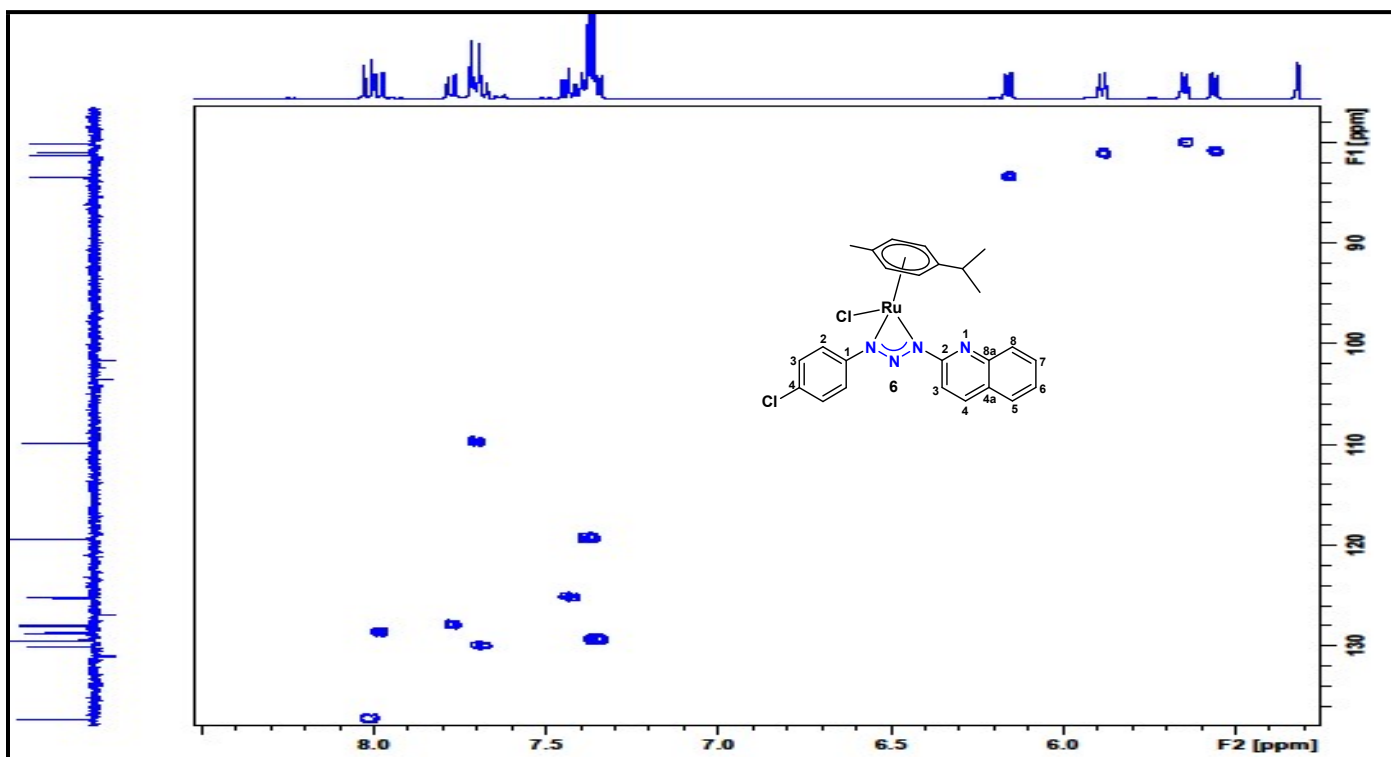


Figure S57. Partial  $^1\text{H}$ - $^{13}\text{C}$  HSQC NMR spectrum of **6** in  $\text{CD}_2\text{Cl}_2$ .

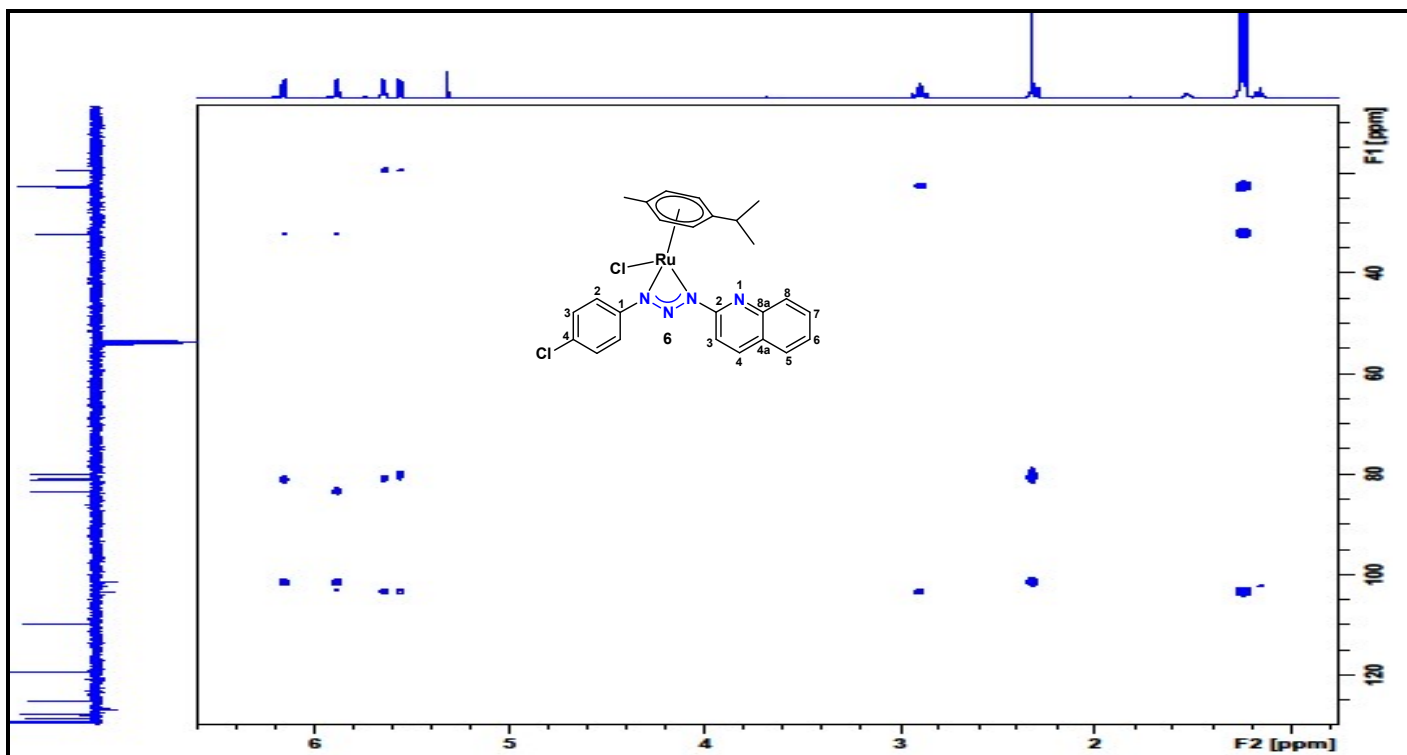


Figure S58.  $^1\text{H}$ - $^{13}\text{C}$  HMBC NMR spectrum of **6** in  $\text{CD}_2\text{Cl}_2$ .

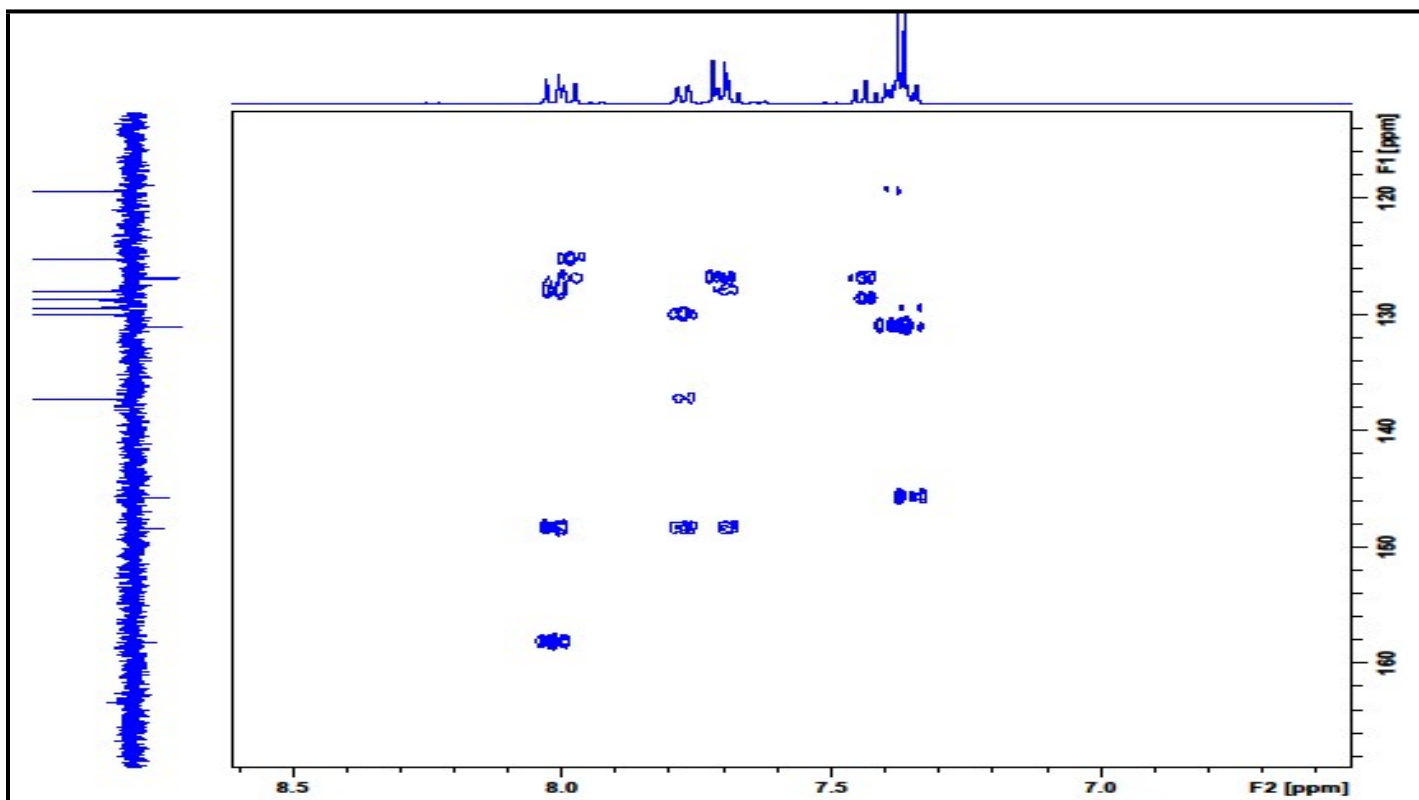


Figure S59. Partial  $^1\text{H}$ - $^{13}\text{C}$  HMBC NMR spectrum of **6** in  $\text{CD}_2\text{Cl}_2$ .



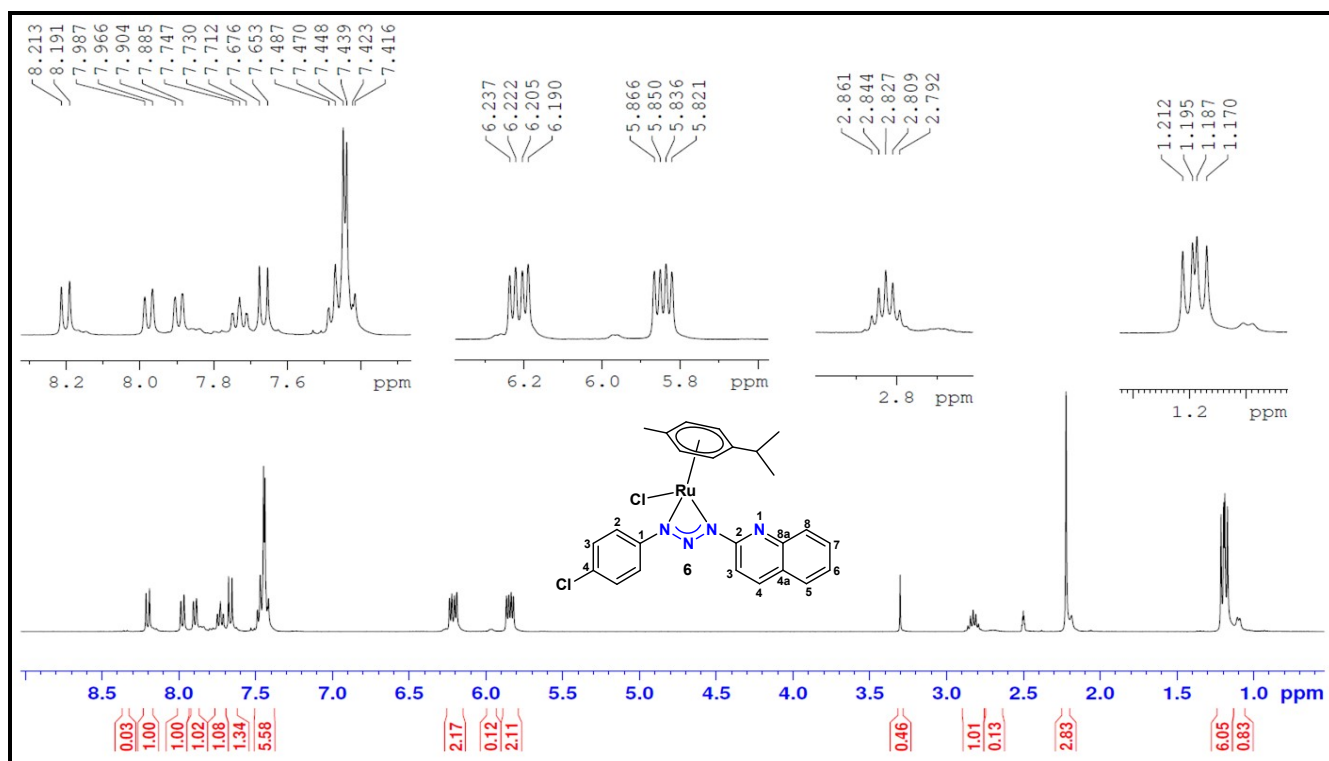


Figure S60.  $^1\text{H}$  NMR spectrum of **6** in  $\text{DMSO-}d_6$  (400 MHz).

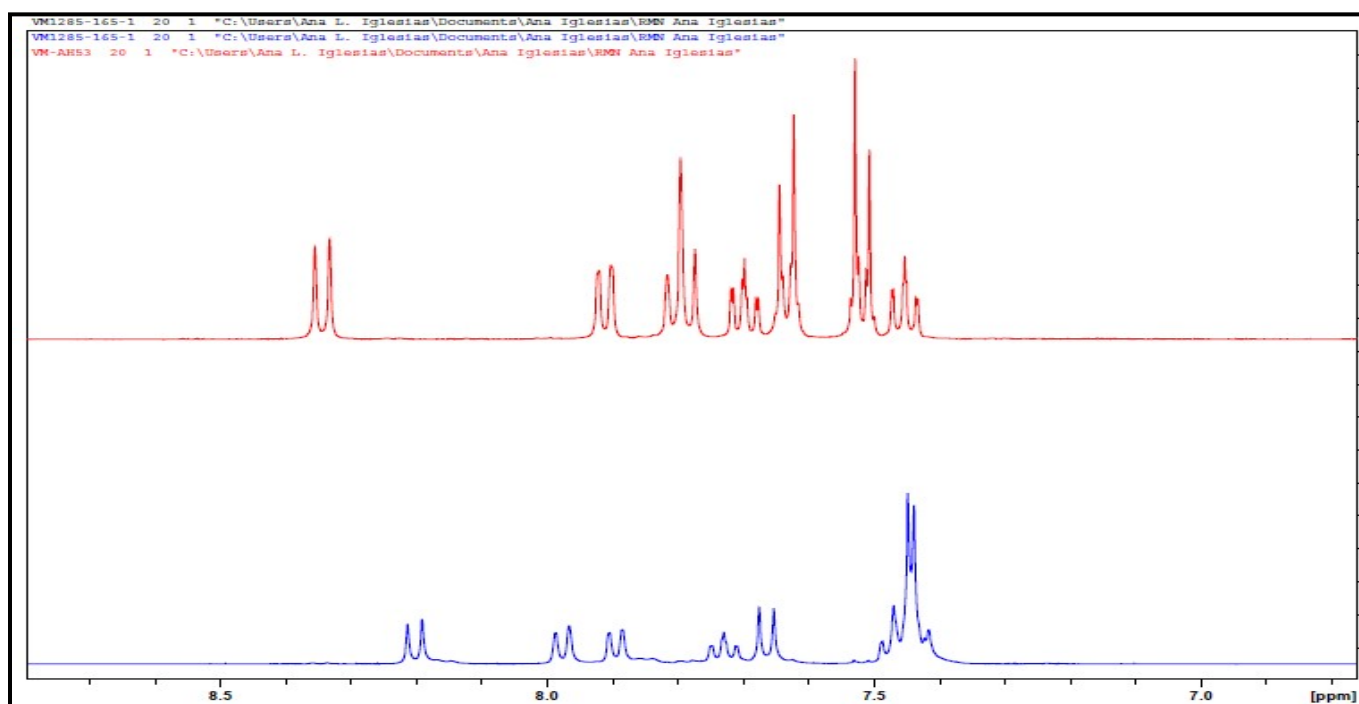


Figure S61. Partial  $^1\text{H}$  NMR spectrum of free triazene **2** (red) and complex **6** (blue) in  $\text{DMSO-}d_6$ .

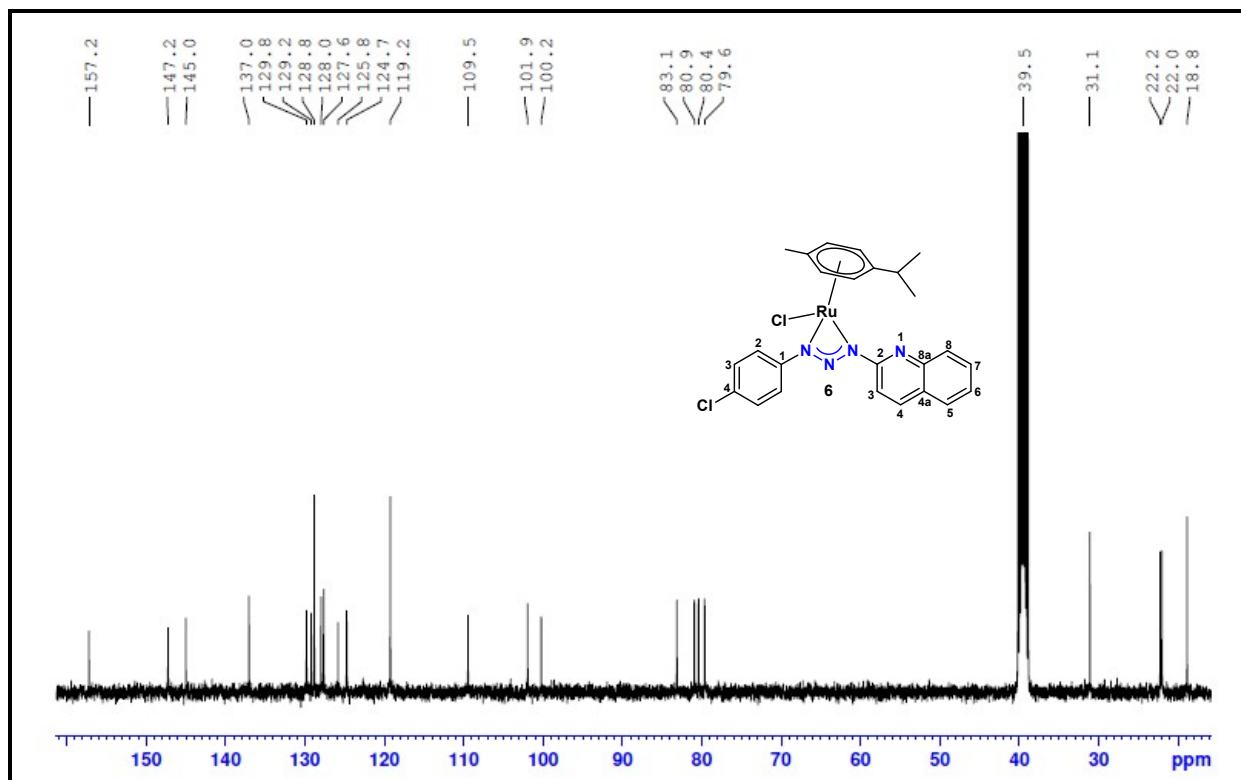


Figure S62.  $^{13}\text{C}$   $\{^1\text{H}\}$  NMR spectrum of **6** in  $\text{DMSO-}d_6$  (100 MHz).

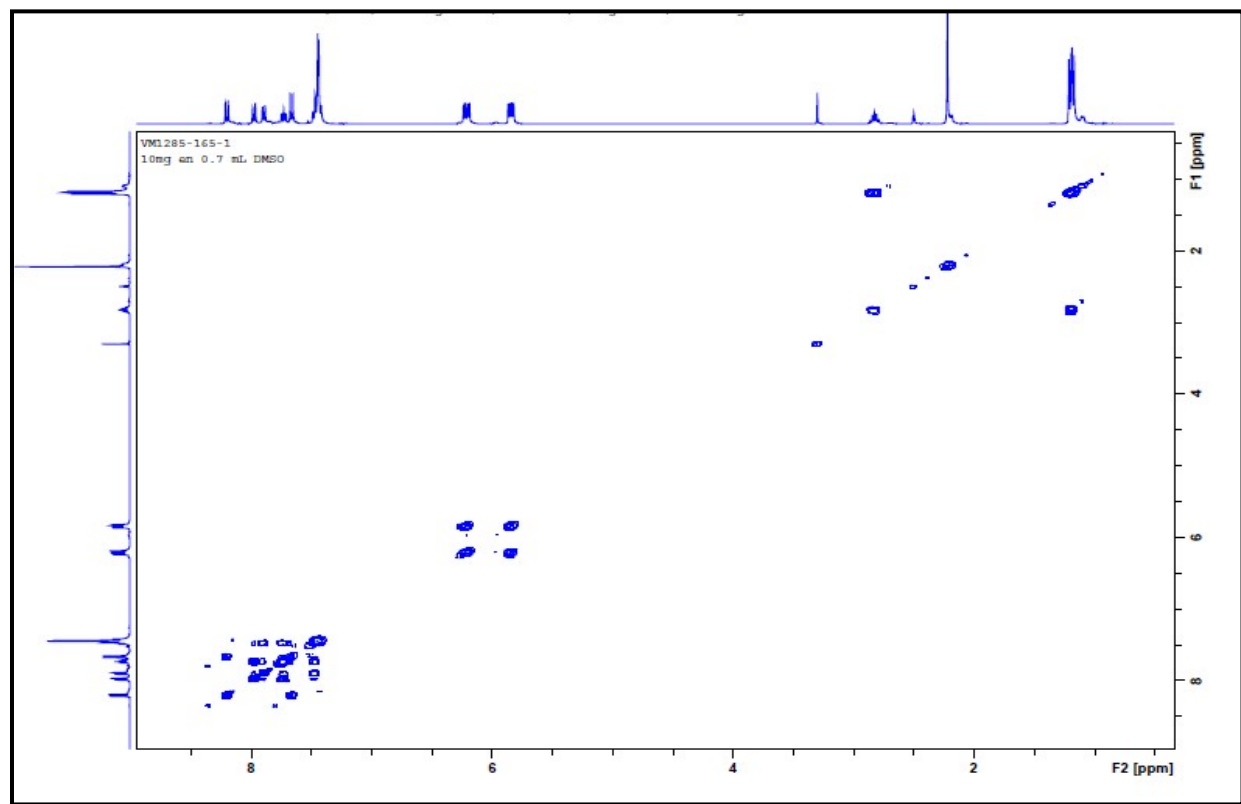


Figure S63.  $^1\text{H-}^1\text{H}$  gCOSY NMR spectrum of **6** in  $\text{DMSO-}d_6$ .

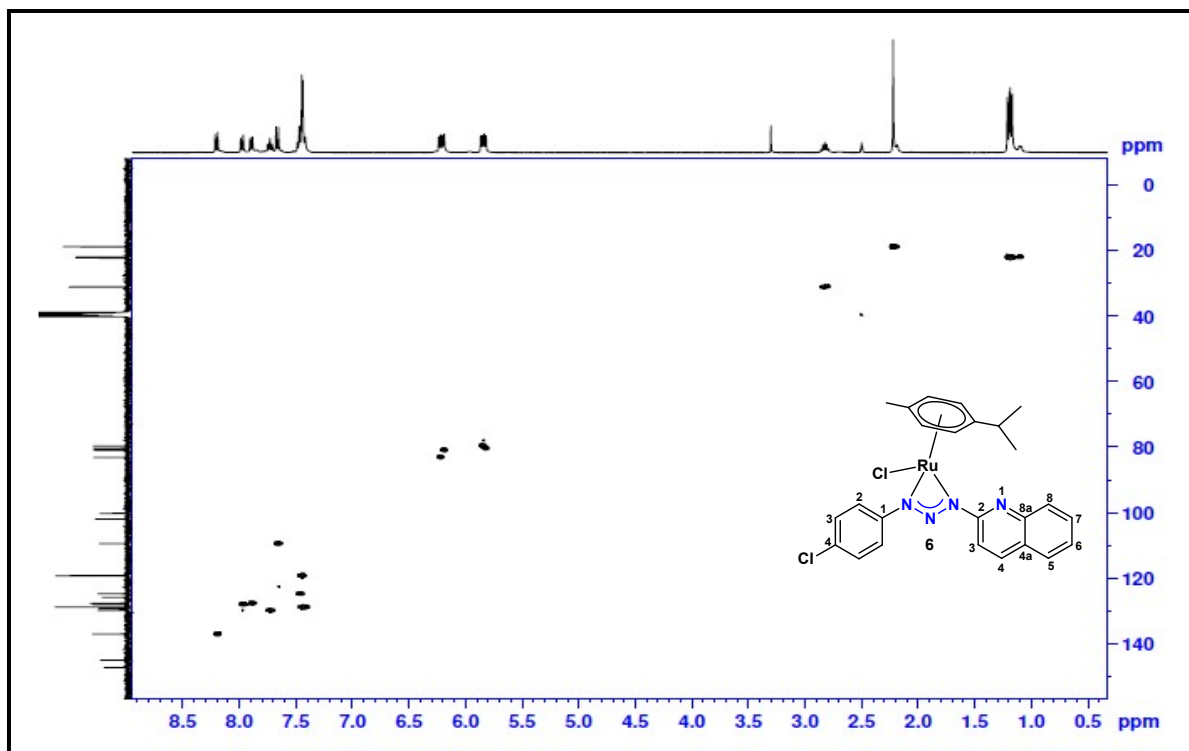


Figure S64.  $^1\text{H}$ - $^{13}\text{C}$  HSQC NMR spectrum of **6** in  $\text{DMSO-}d_6$ .

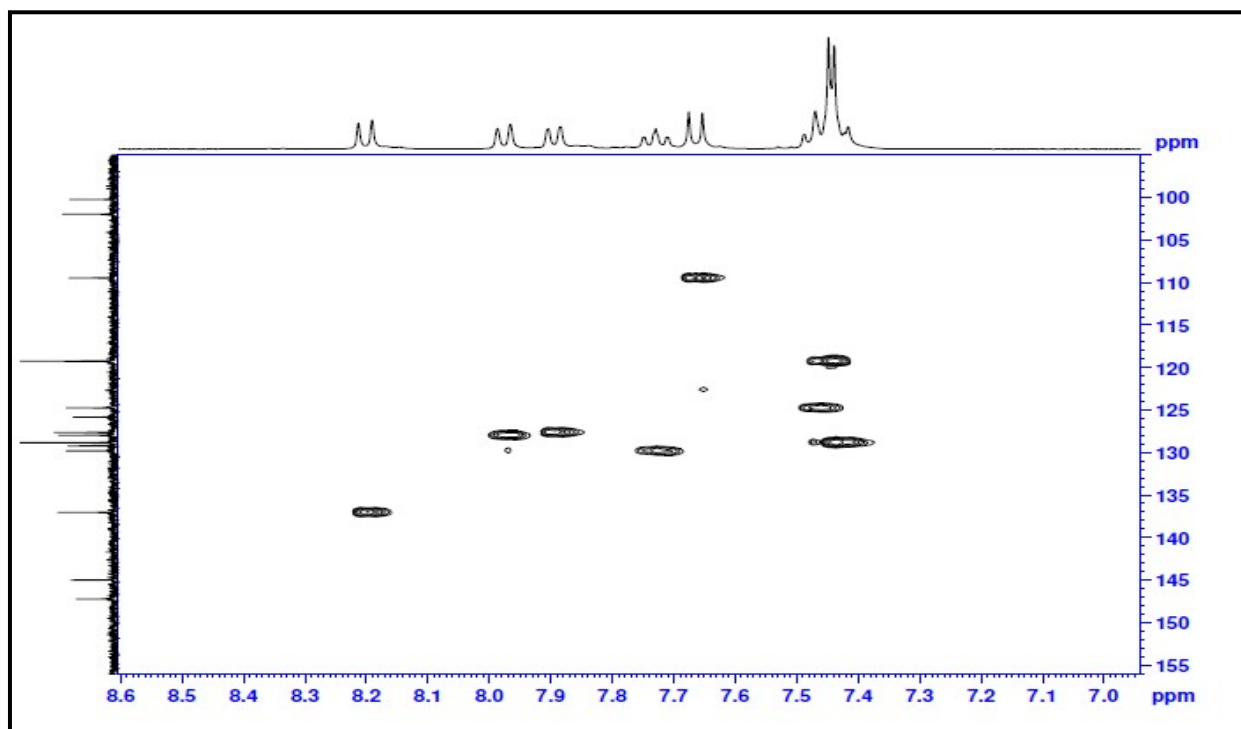


Figure S65. Partial  $^1\text{H}$ - $^{13}\text{C}$  HSQC NMR spectrum of **6** in  $\text{DMSO-}d_6$ .

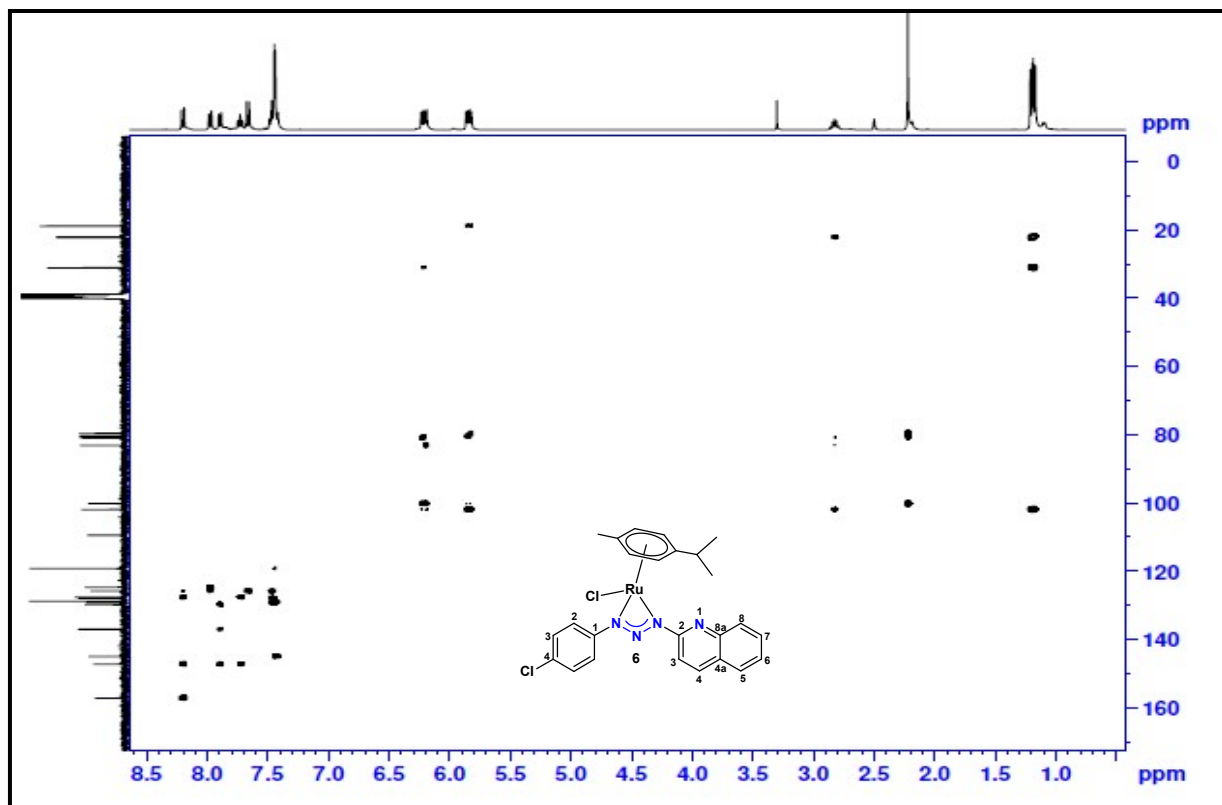


Figure S66.  $^1\text{H}$ - $^{13}\text{C}$  HMBC NMR spectrum of **6** in  $\text{DMSO-}d_6$ .

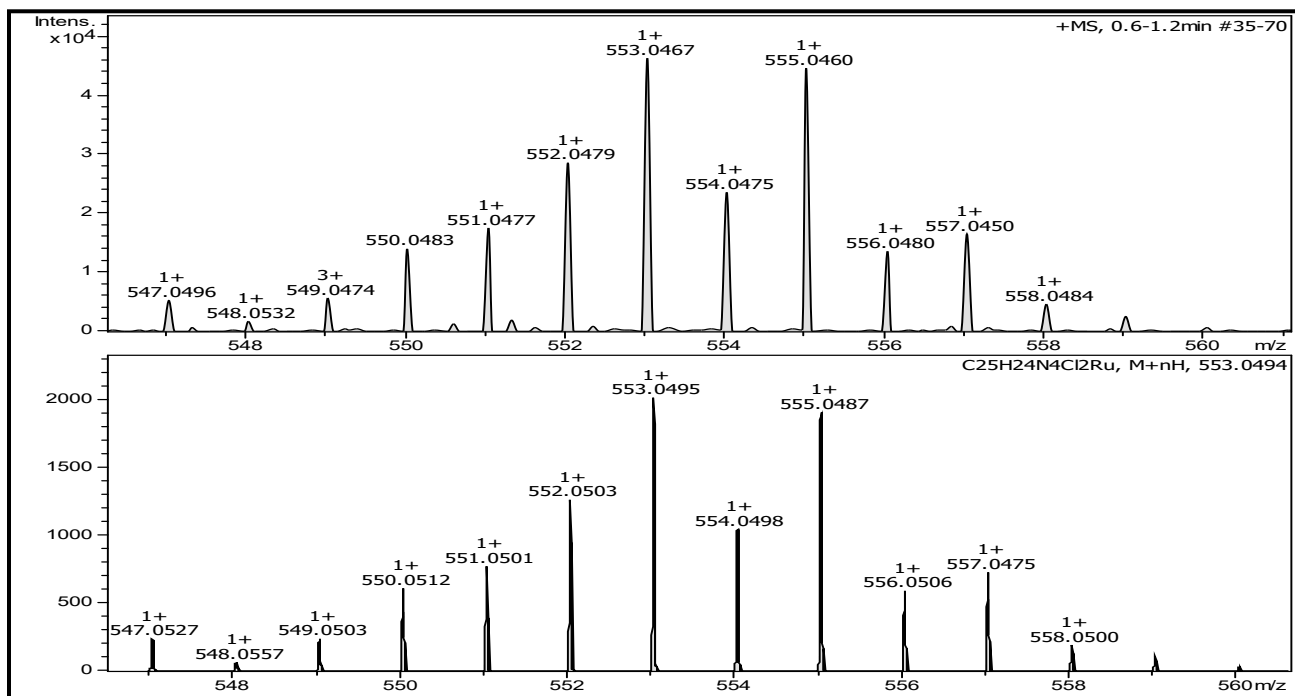
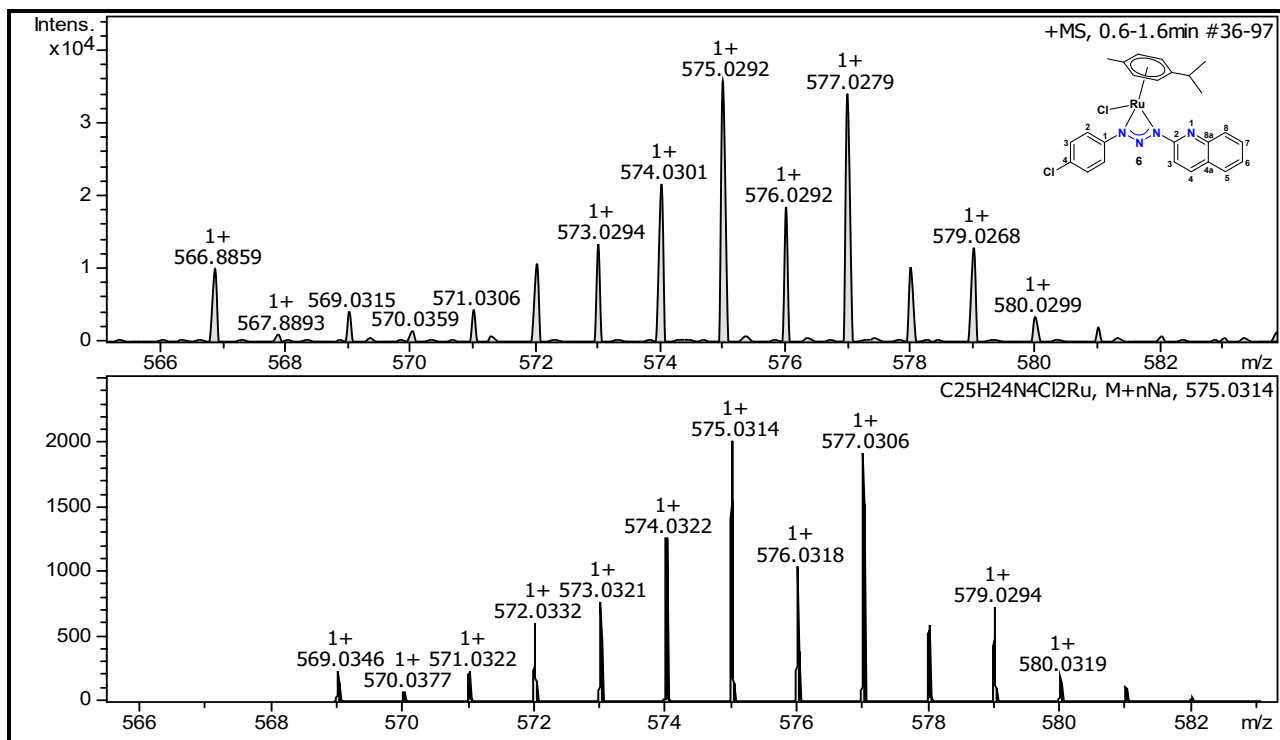
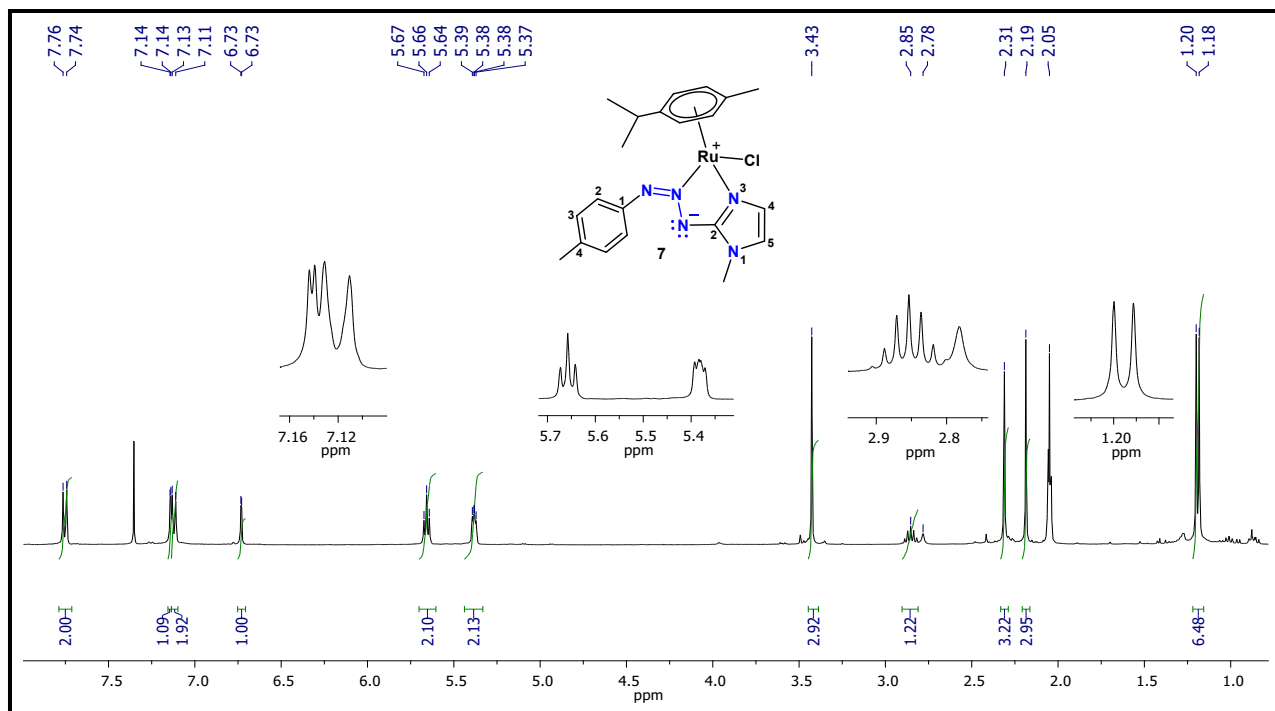


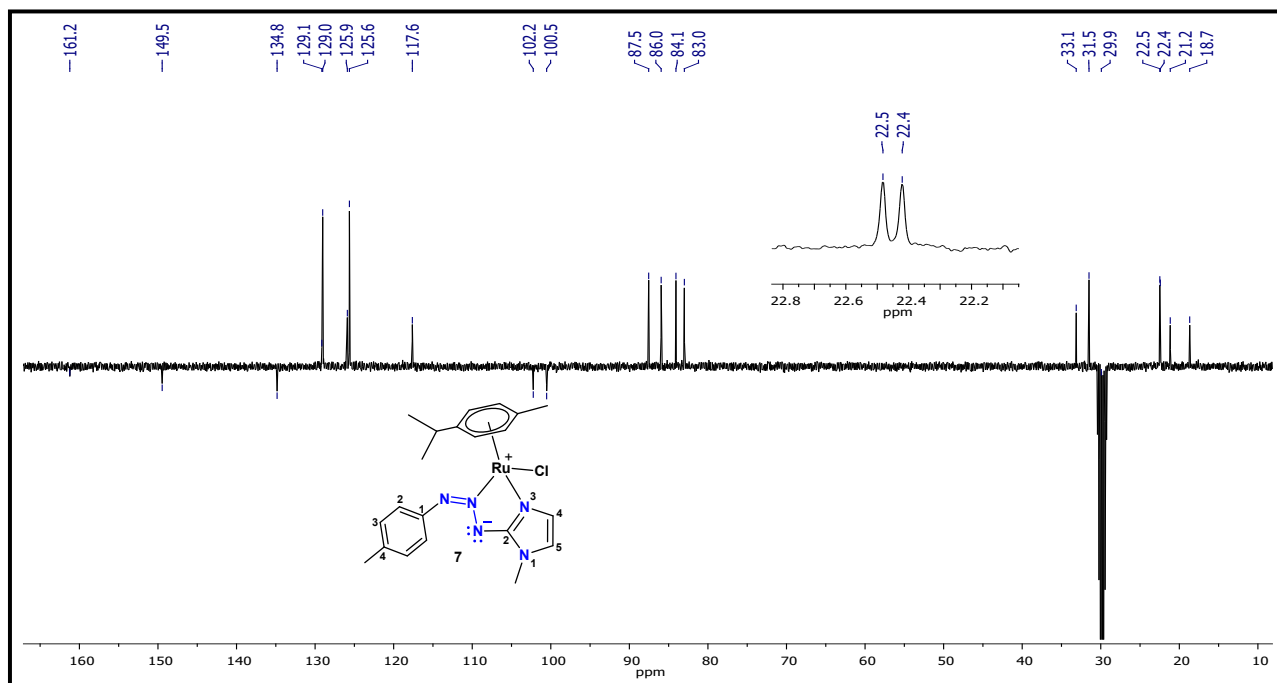
Figure S67. HRMS for **6** (above) and simulated spectrum (below)  $[\text{M}+\text{H}]^+$ .



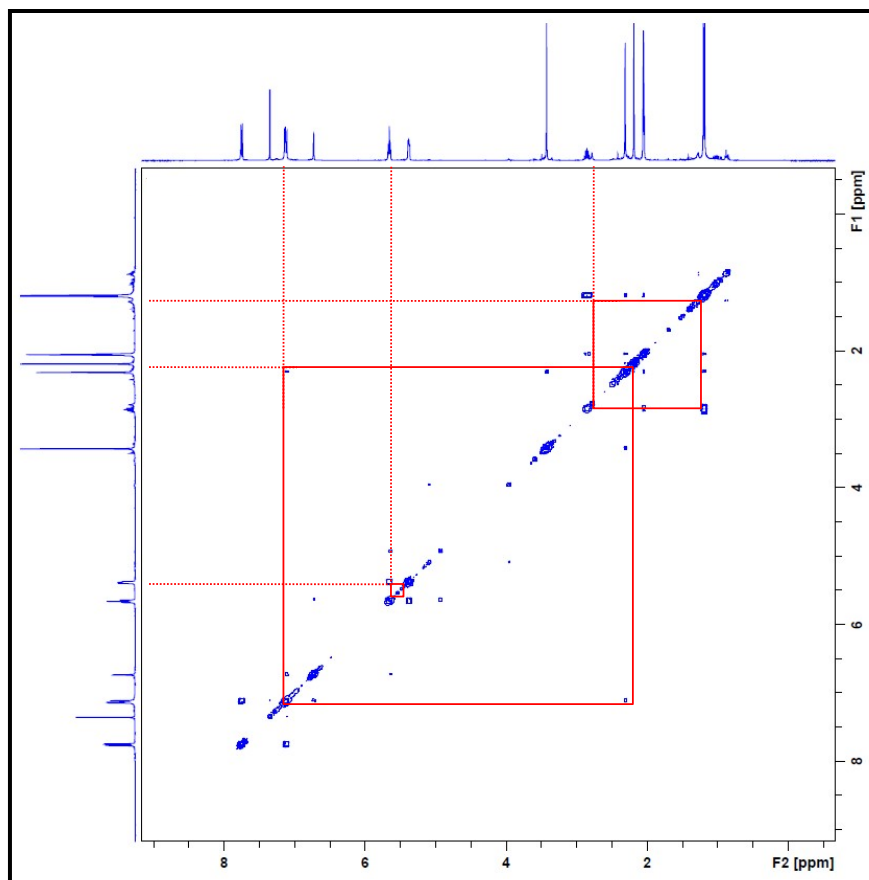
**Figure S68.** HRMS for **6** (above) and simulated spectrum (below) [M+Na]<sup>+</sup> adduct.



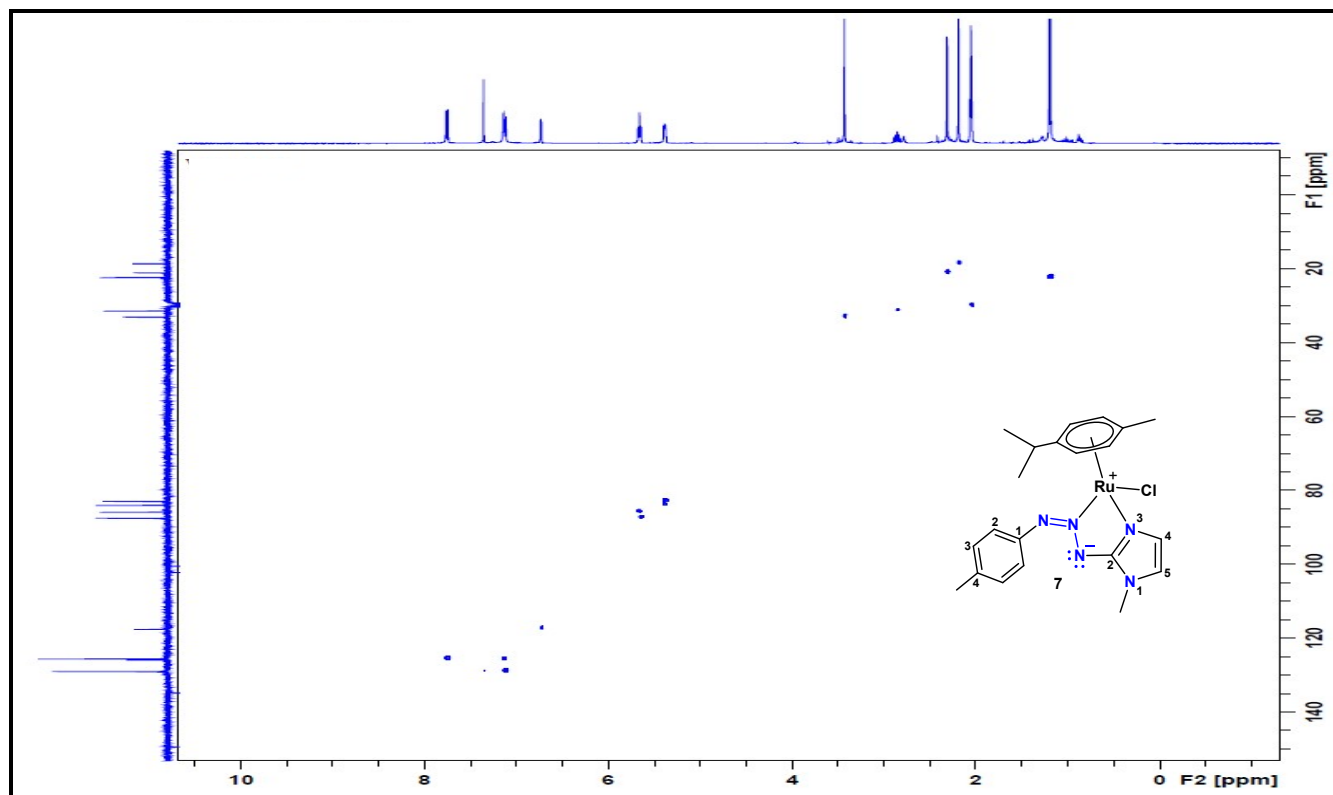
**Figure S69.**  $^1\text{H}$  NMR spectrum of **7** in acetone- $d_6$  (400 MHz).



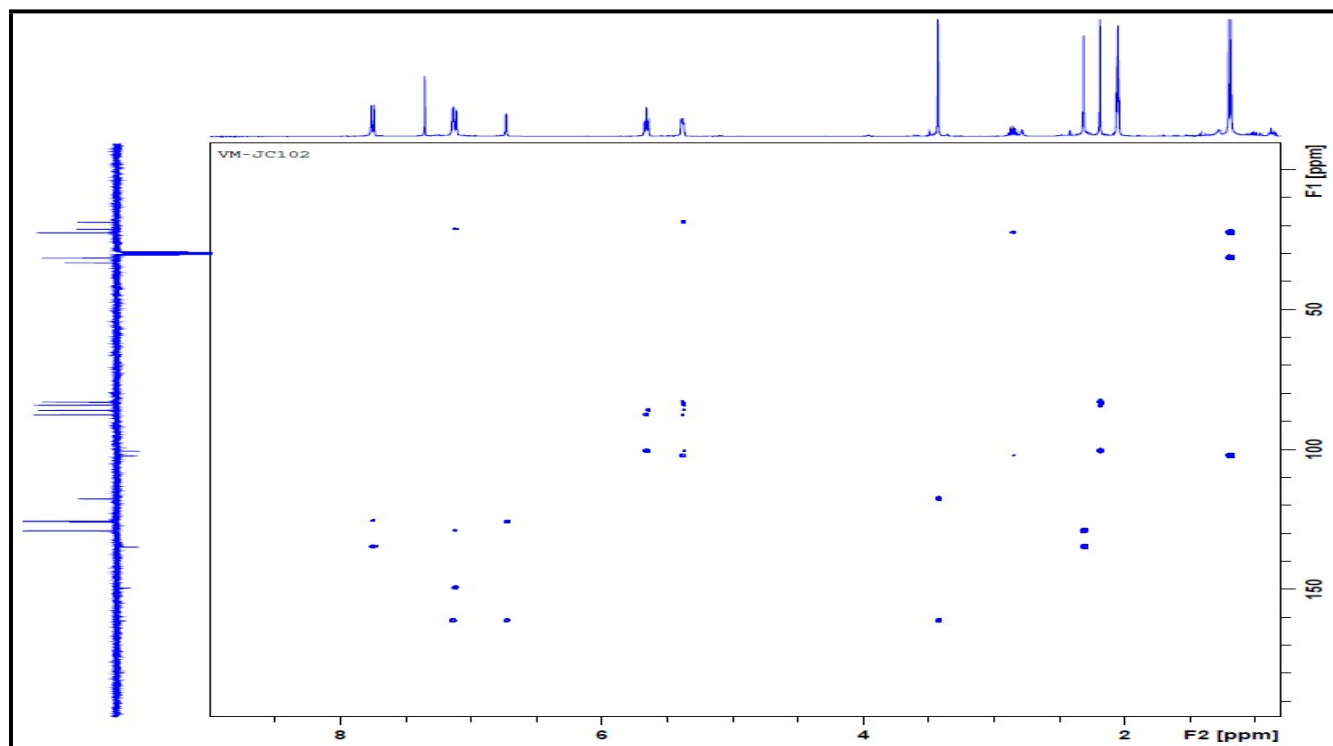
**Figure S70.**  $^{13}\text{C}$   $\{^1\text{H}\}$  NMR-APT spectrum of **7** in acetone- $d_6$  (100 MHz).



**Figure S71.**  $^1\text{H}$ - $^1\text{H}$  gCOSY NMR spectrum of **7** in acetone- $d_6$ .

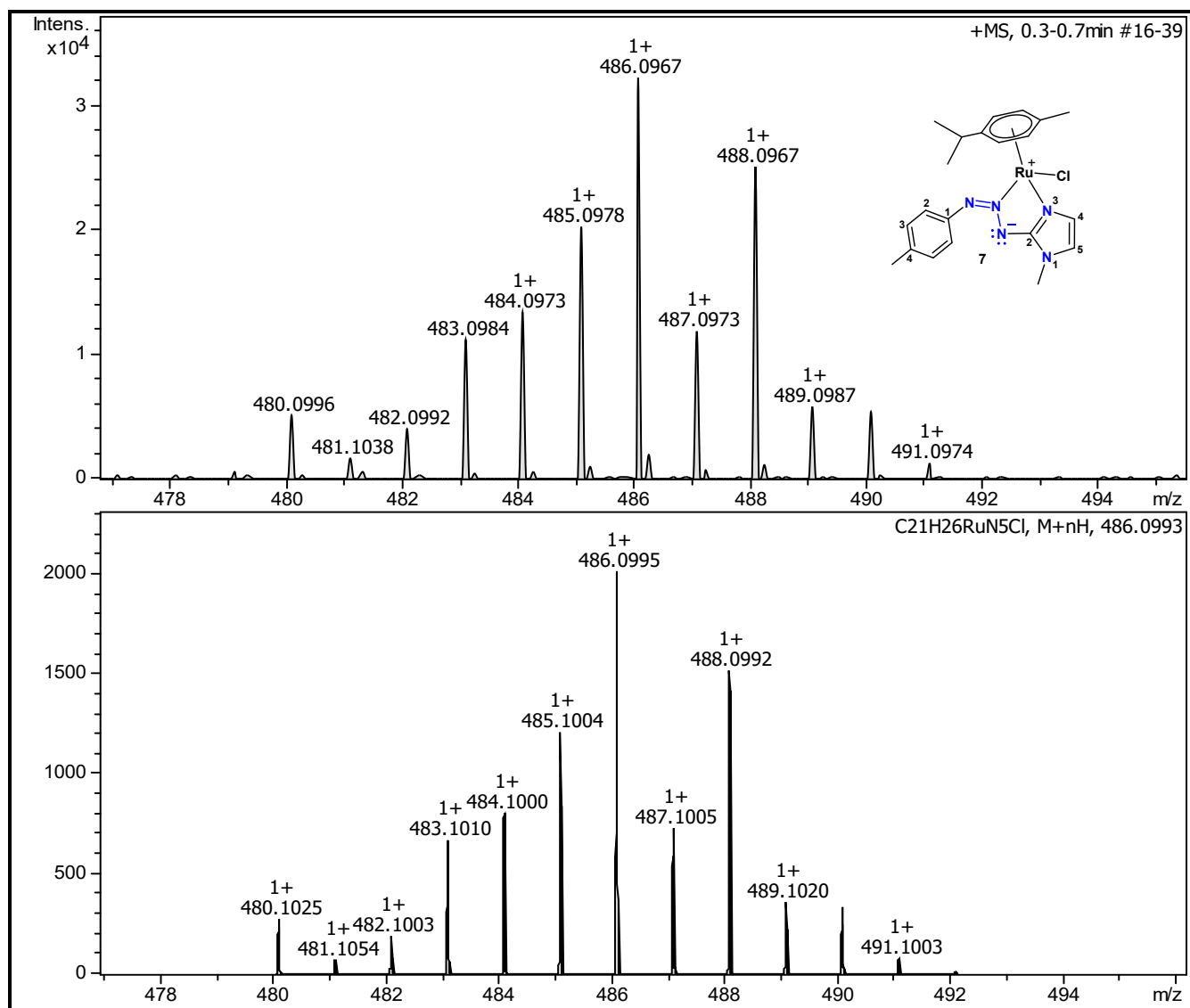


**Figure S72.**  $^1\text{H}$ - $^{13}\text{C}$  HSQC NMR spectrum of **7** in acetone- $d_6$ .

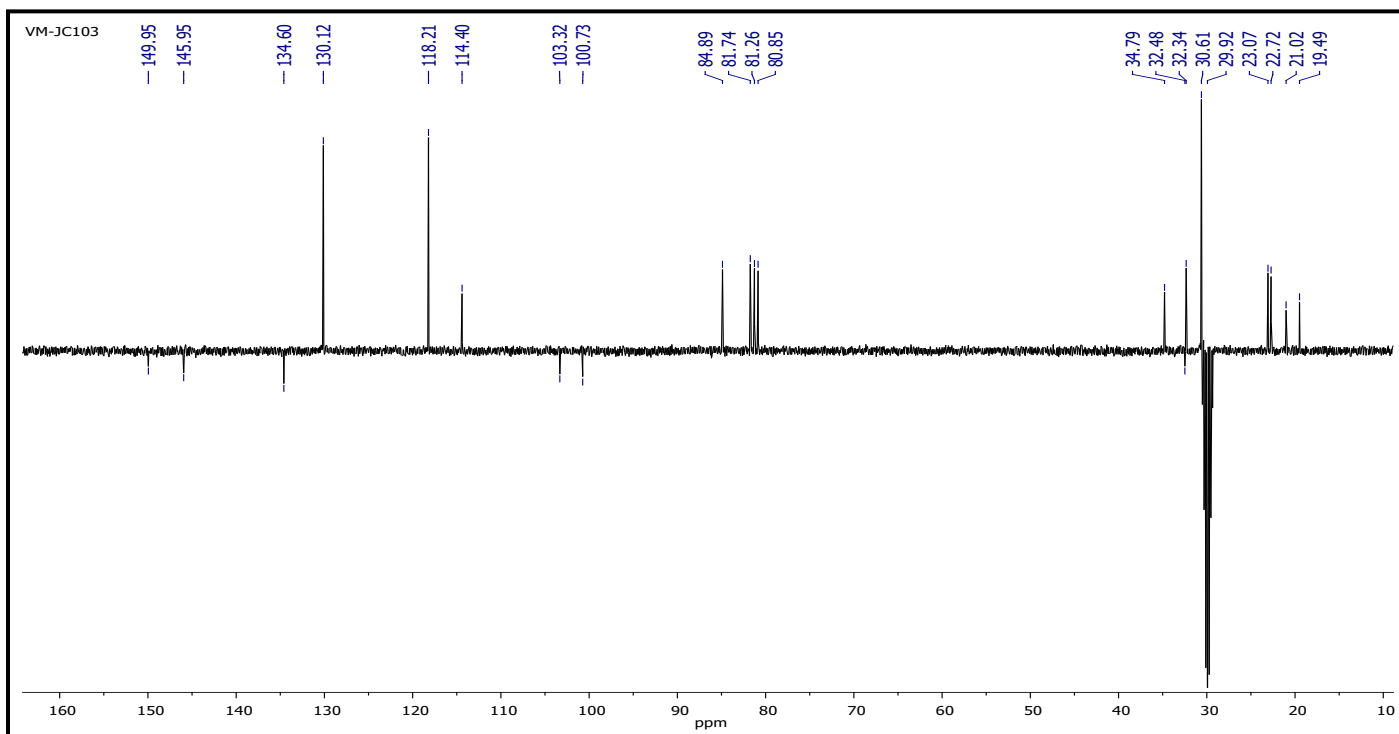
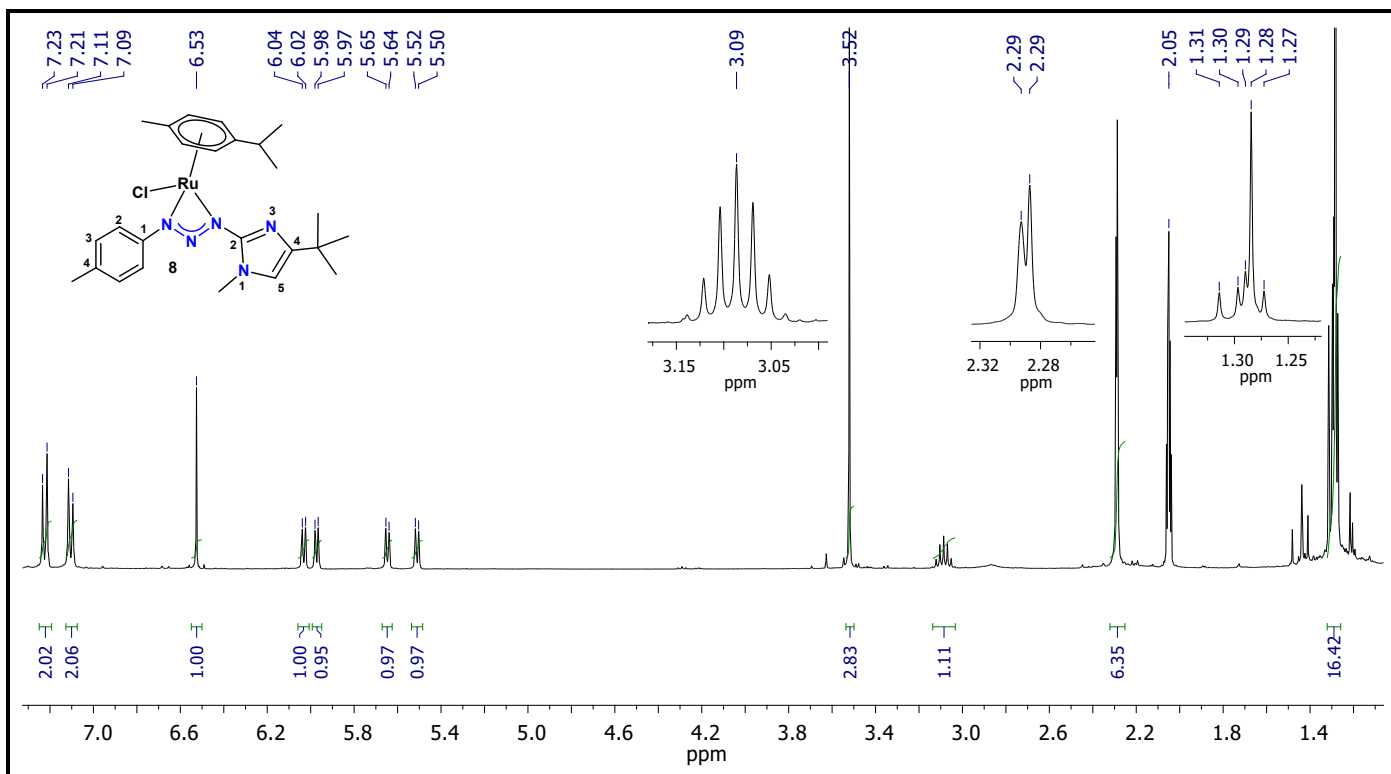


**Figure S73.**  $^1\text{H}$ - $^{13}\text{C}$  HMBC NMR spectrum of **7** in acetone- $d_6$ .





**Figure S74:** HRMS for complex **7** (above) and simulated spectrum (below)  $[M+H]^+$ .



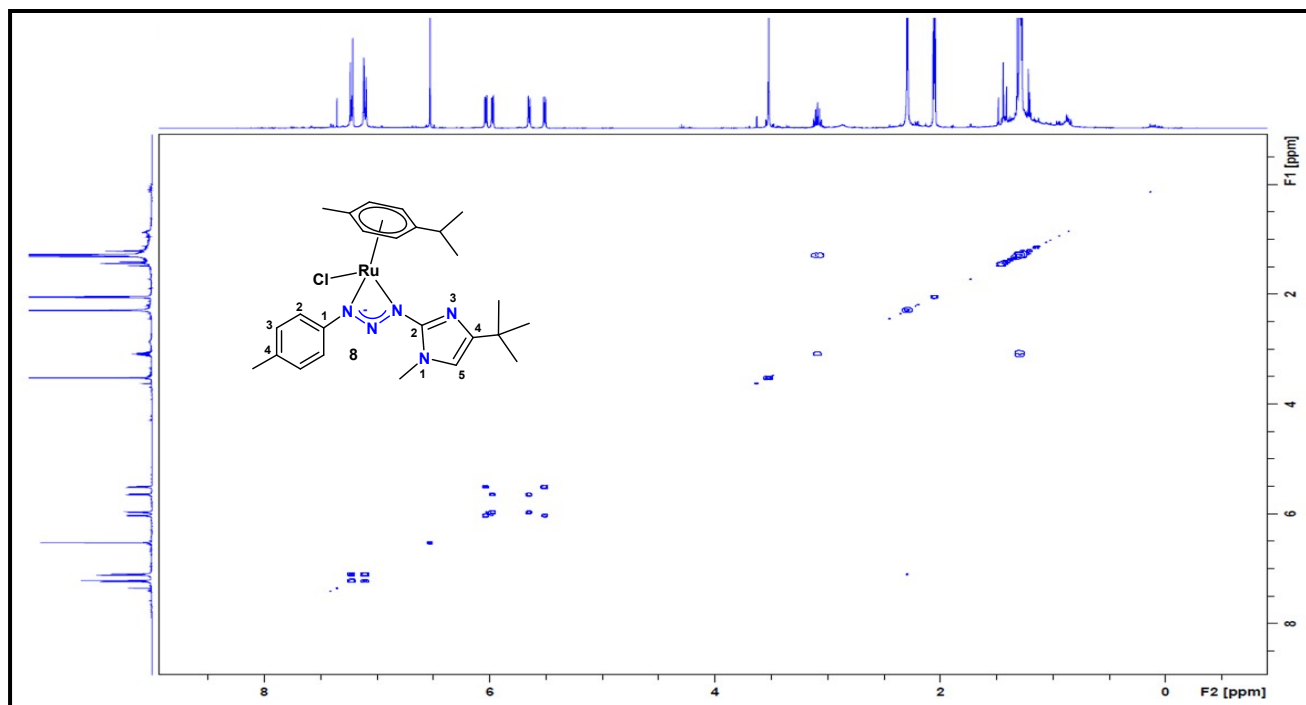


**Figure S77.**  $^1\text{H}$ - $^1\text{H}$  gCOSY NMR spectrum of **8** in acetone- $d_6$ .

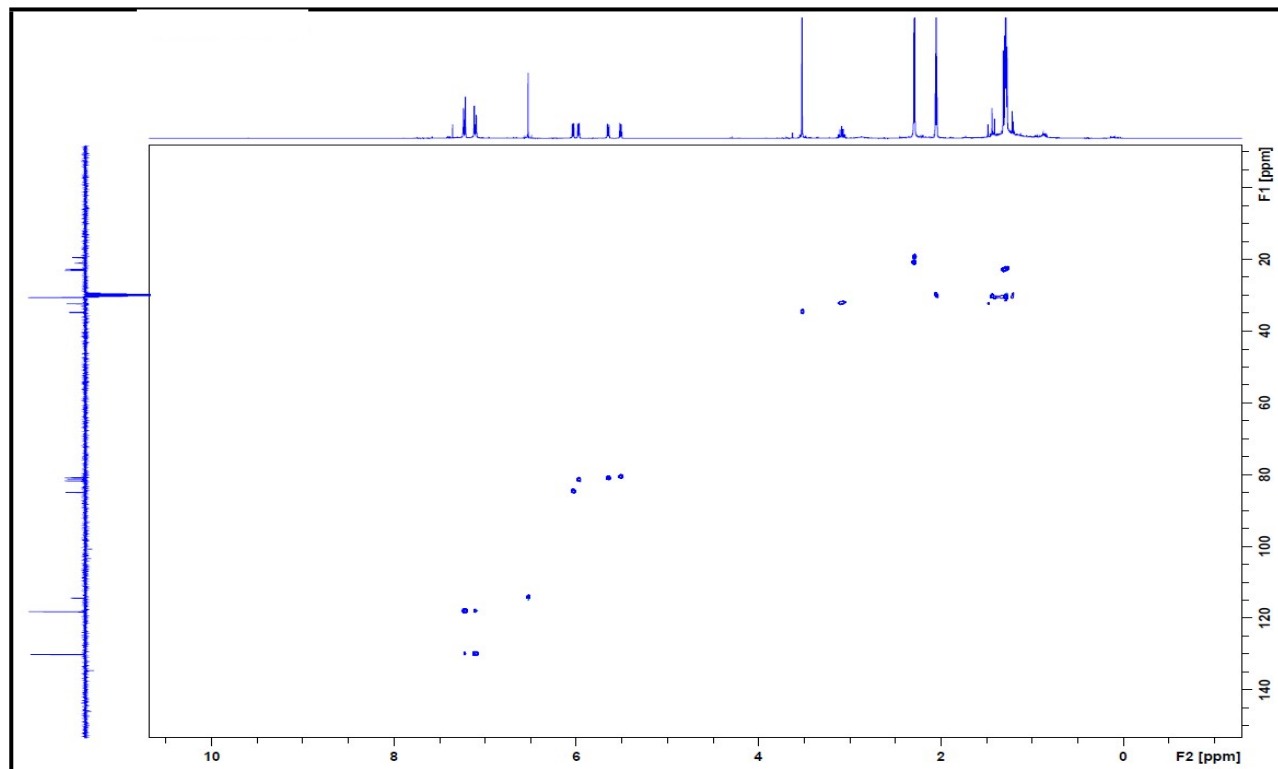


**Figure S78.**  $^1\text{H}$ - $^{13}\text{C}$  HSQC NMR spectrum of **8** in acetone- $d_6$ .

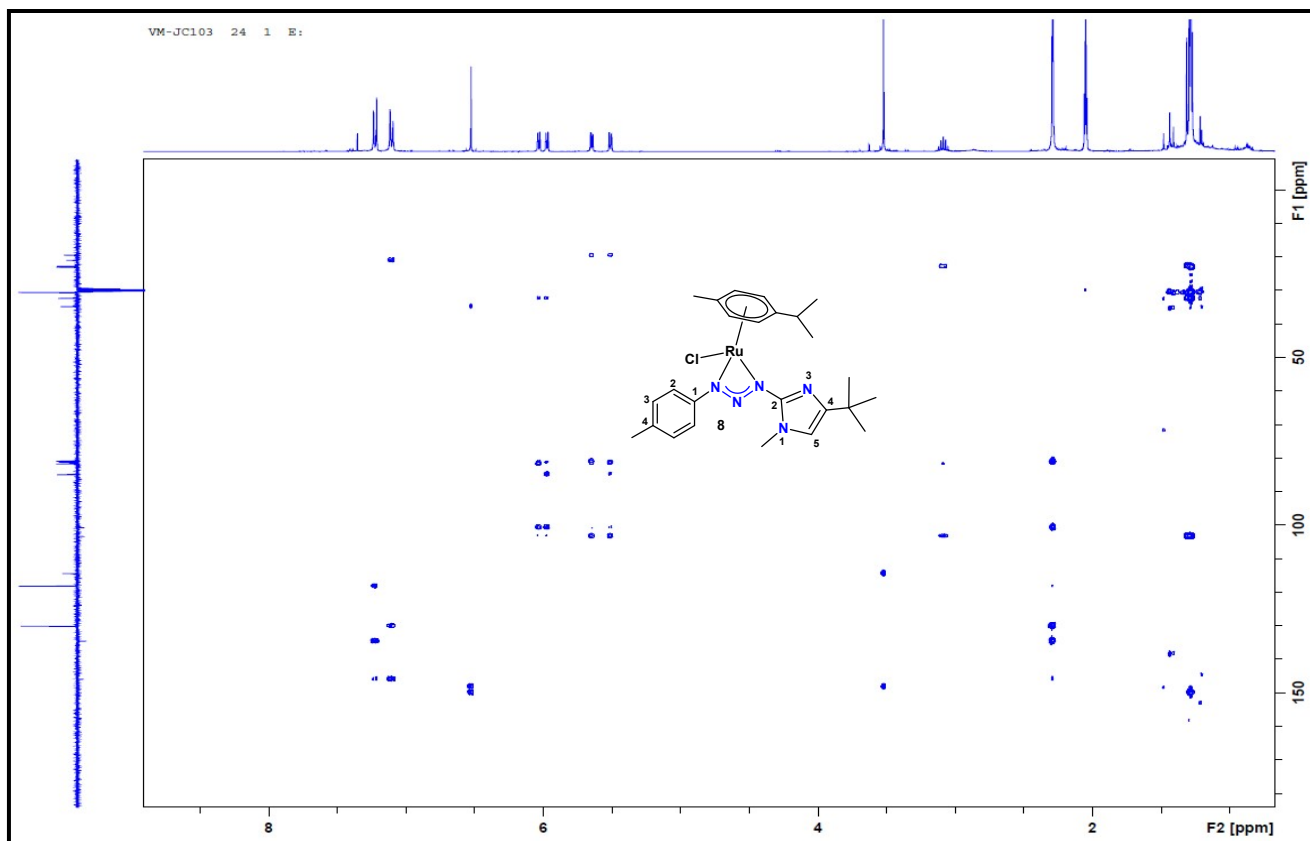


**Figure S79.**  $^1\text{H}$ - $^{13}\text{C}$  HMBC NMR spectrum of **8** in acetone- $d_6$ .

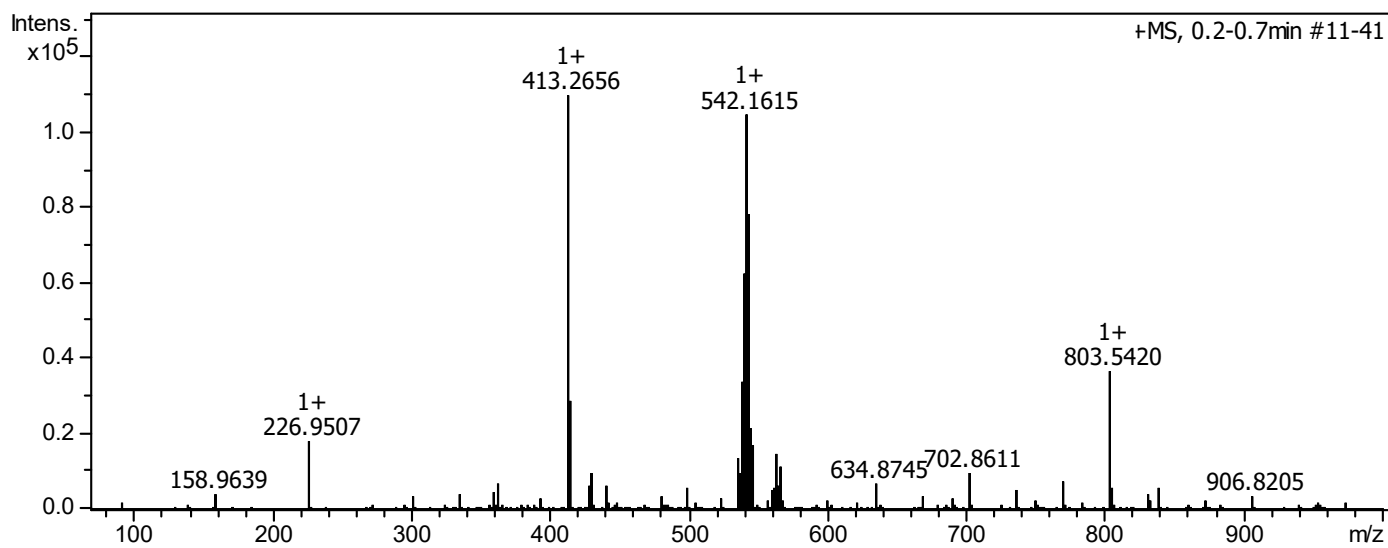


**Figure S80.** HRMS spectrum of complex **8**.

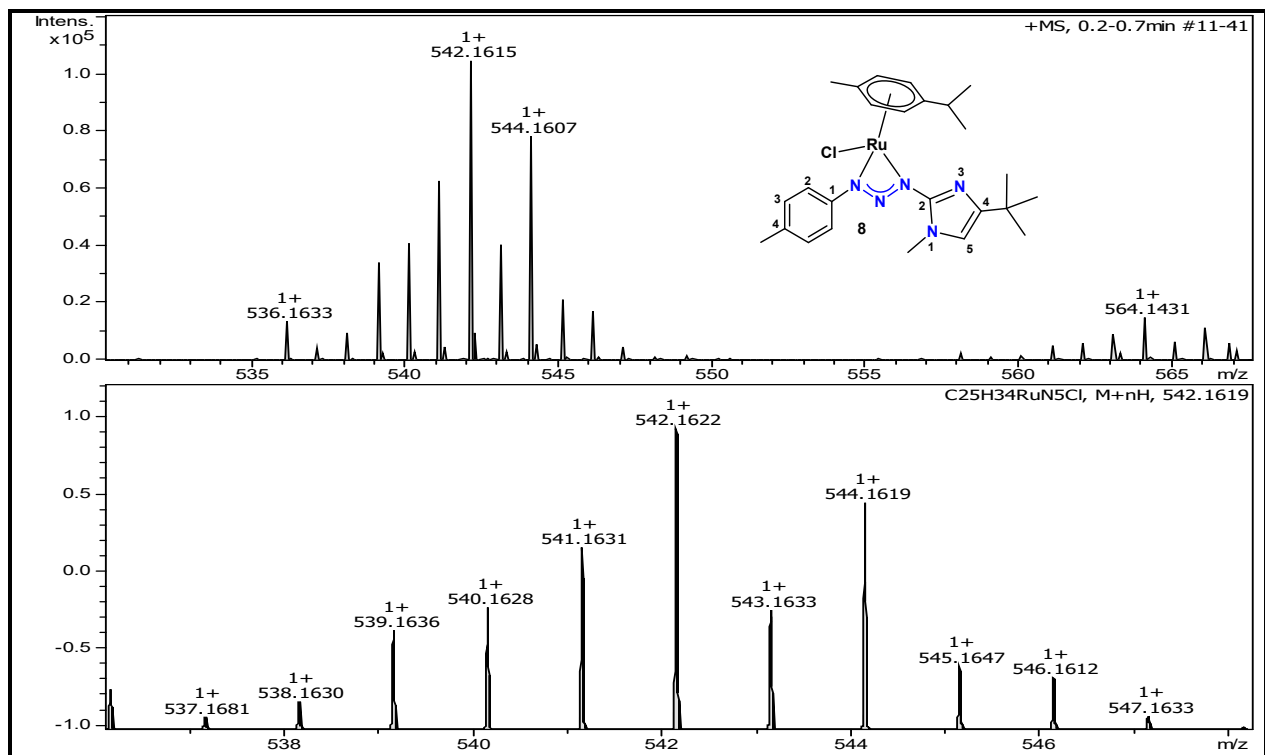


**Figure S81.** HRMS for **8** (above) and simulated spectrum (below) [M+H]<sup>+</sup>.

NMR, EIMS and HRMS spectra of complexes 10, 12, and 13

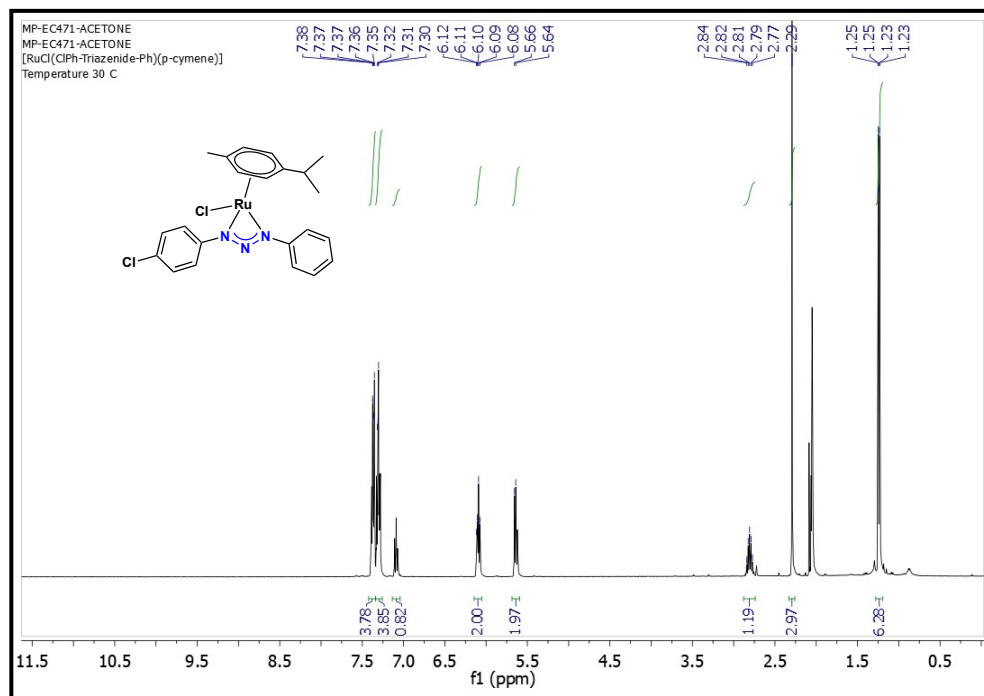


Figure S82.  $^1\text{H}$  NMR spectrum of complex 10 in acetone- $d_6$  (400 MHz).

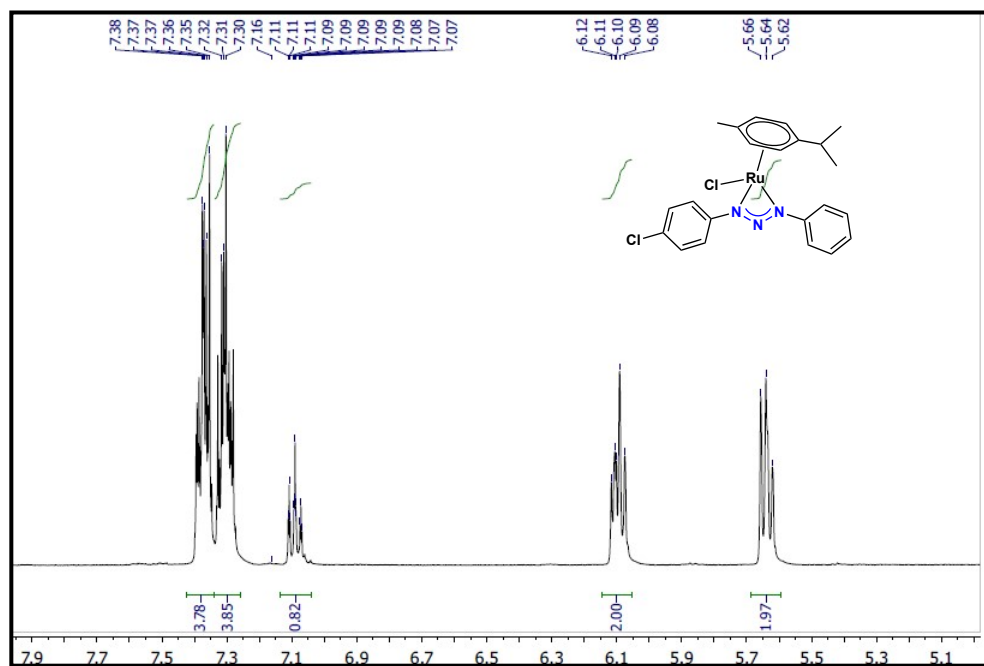


Figure 83. Partial  $^1\text{H}$  NMR spectrum of complex 10 in acetone- $d_6$ .

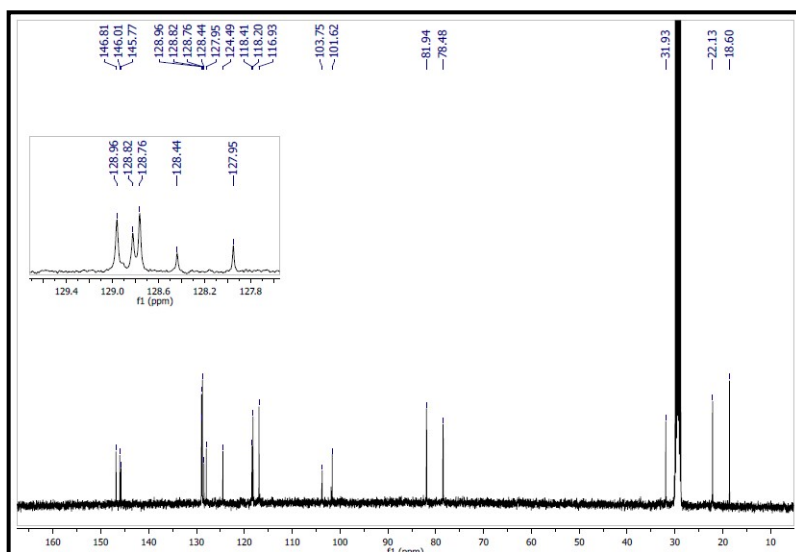


Figure S84.  $^{13}\text{C}$   $\{^1\text{H}\}$  NMR spectrum of complex **10** in acetone- $d_6$  (100 MHz).

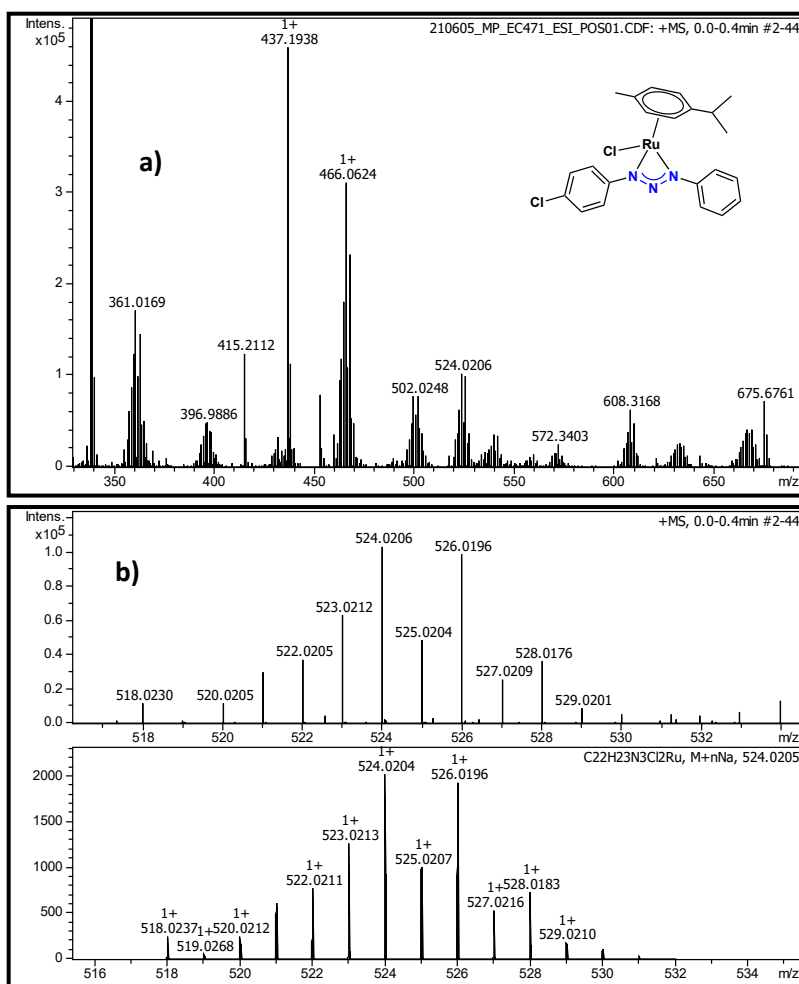


Figure S85. a) HRMS of **11**; b) HRMS of complex **10** (above) and simulated spectrum (below)  $[\text{M}+\text{Na}]^+$  adduct.

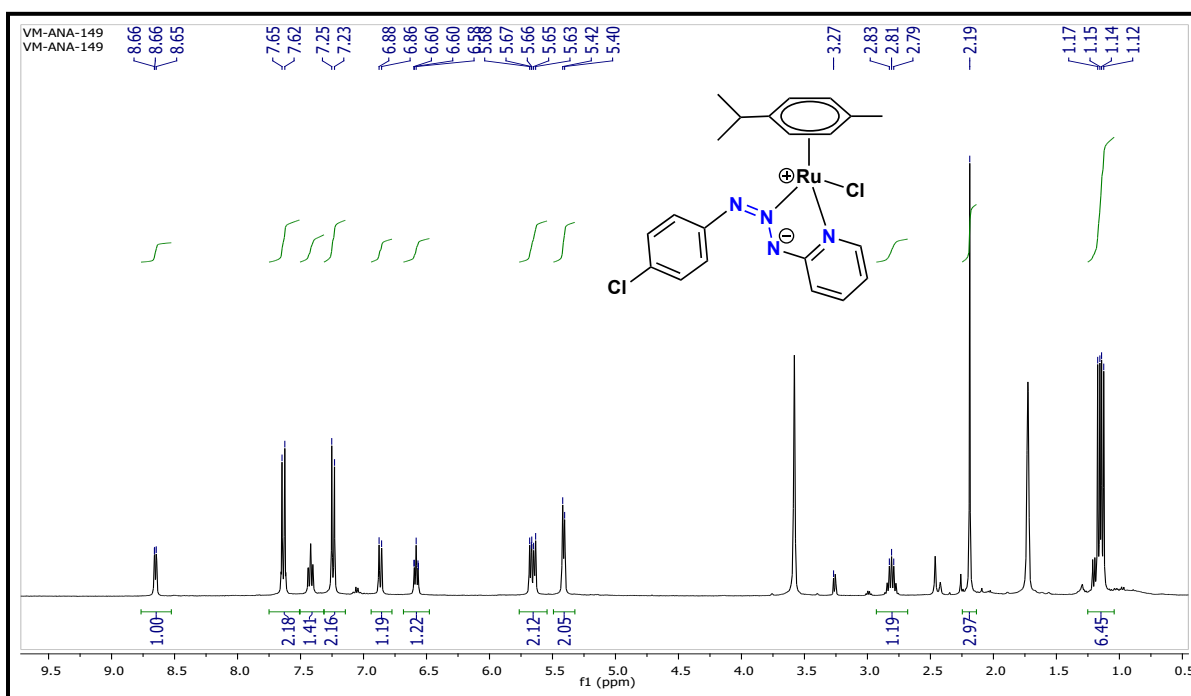


Figure S86.  $^1\text{H}$  NMR spectrum of **12** in  $\text{THF-}d_8$  (400 MHz).

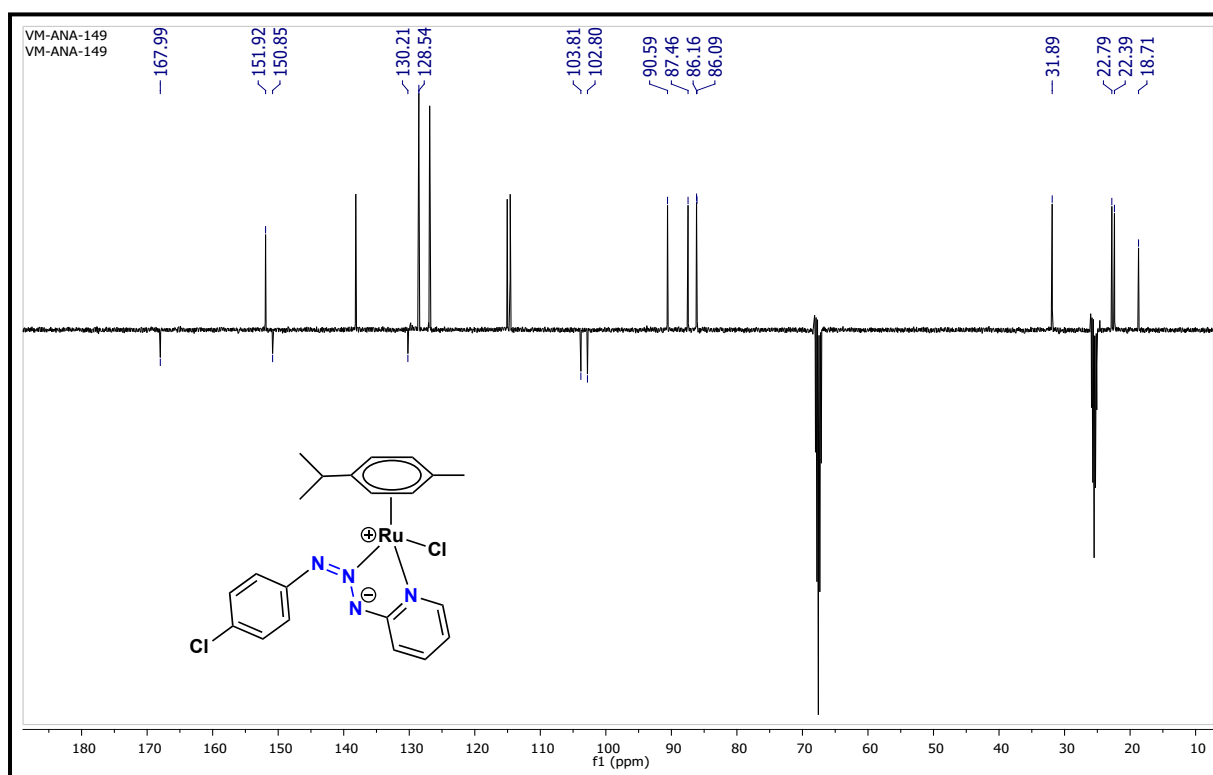


Figure S87.  $^{13}\text{C}$   $\{^1\text{H}\}$  NMR-APT spectrum of **12** in  $\text{THF-}d_8$  (100 MHz).



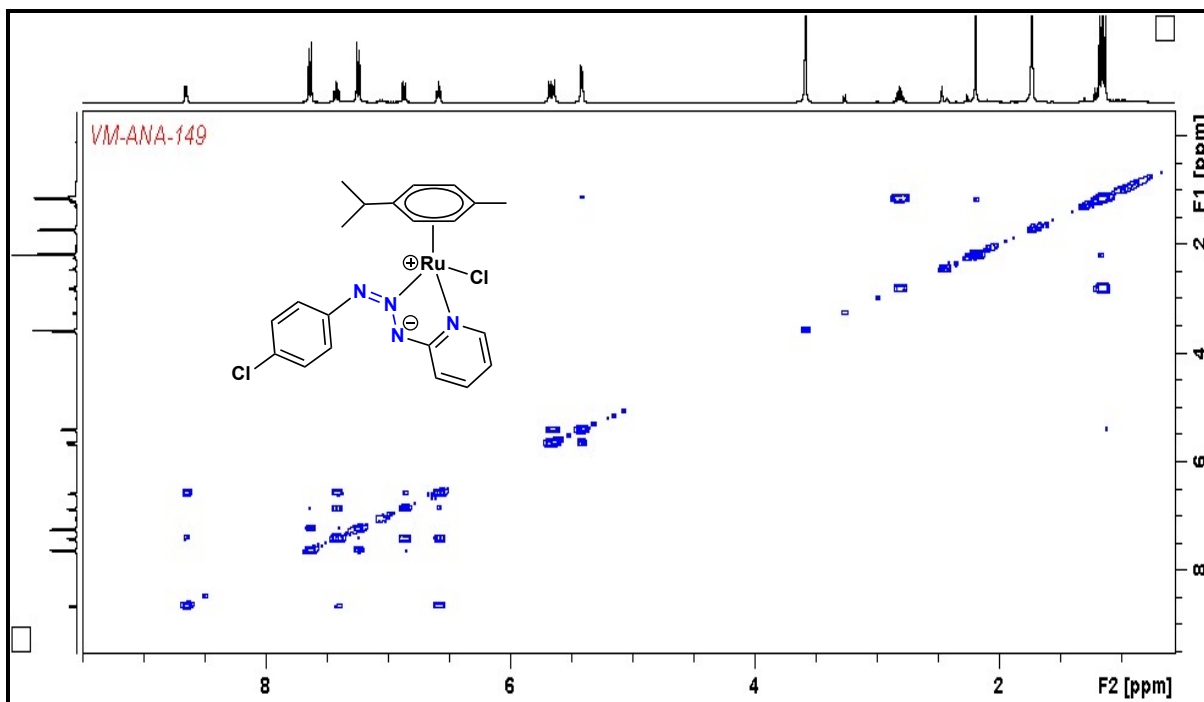


Figure S88.  $^1\text{H}$ - $^1\text{H}$  gCOSY NMR spectrum of **12** in  $\text{THF-}d_8$ .

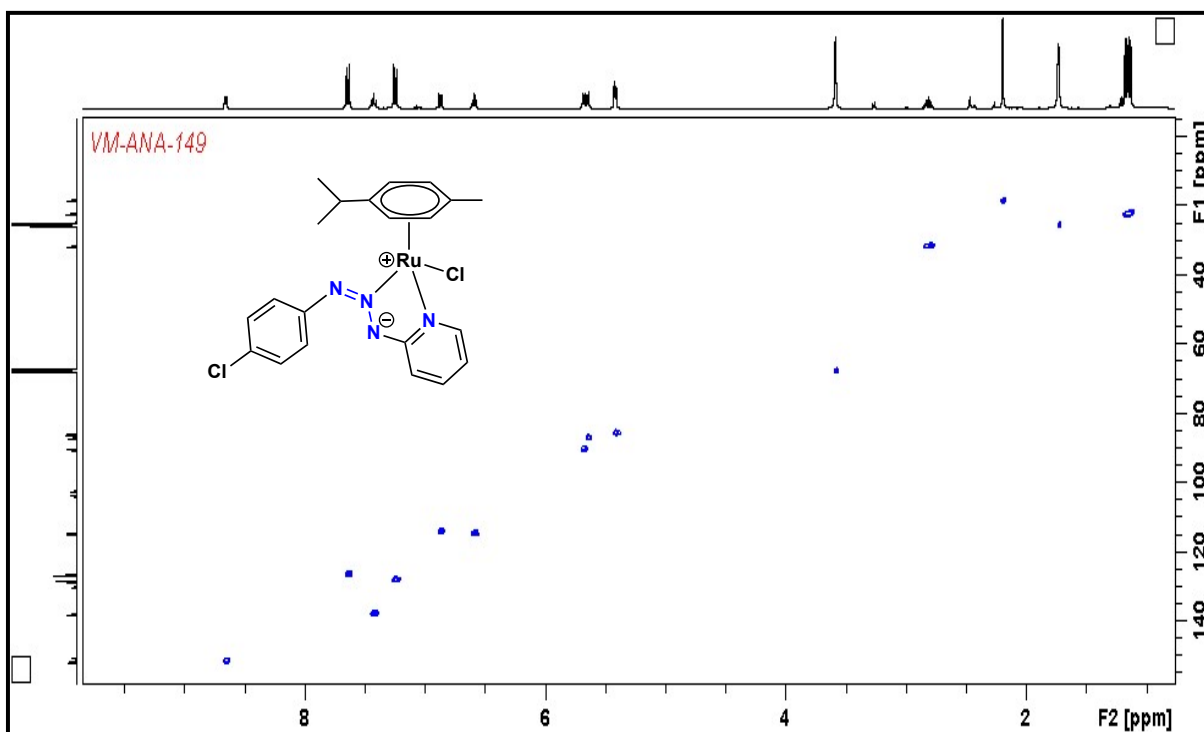
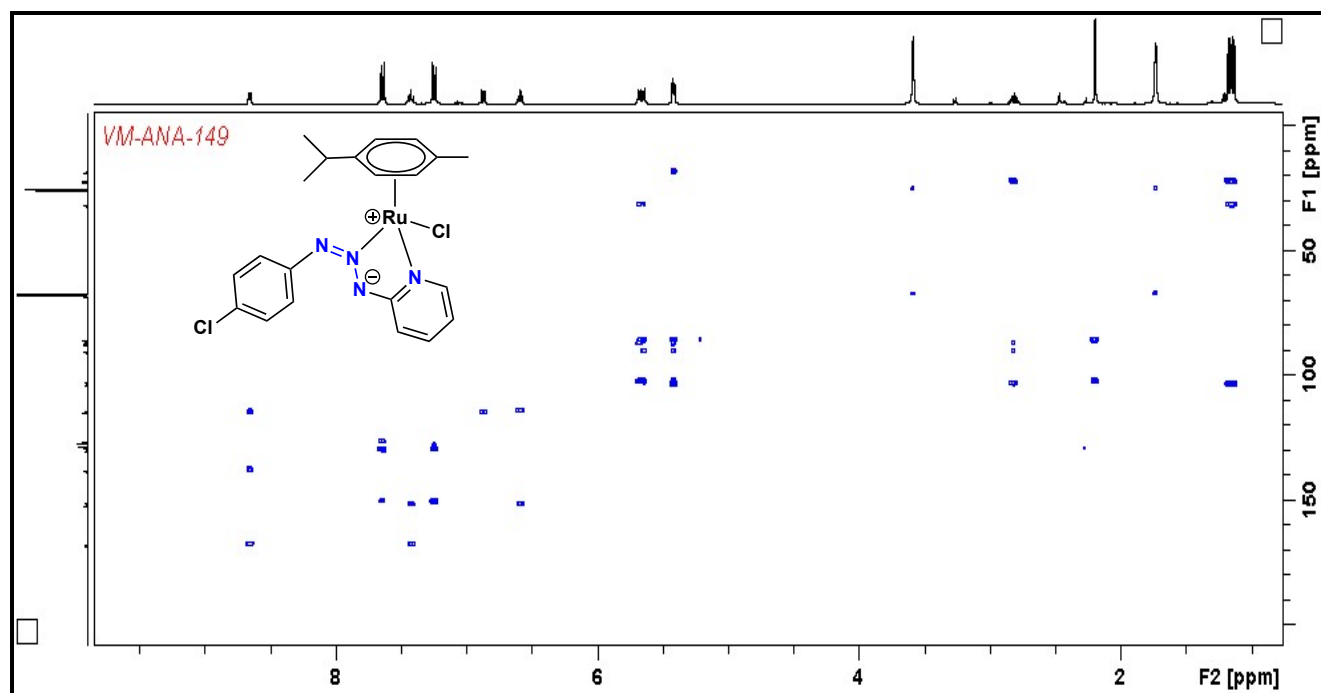
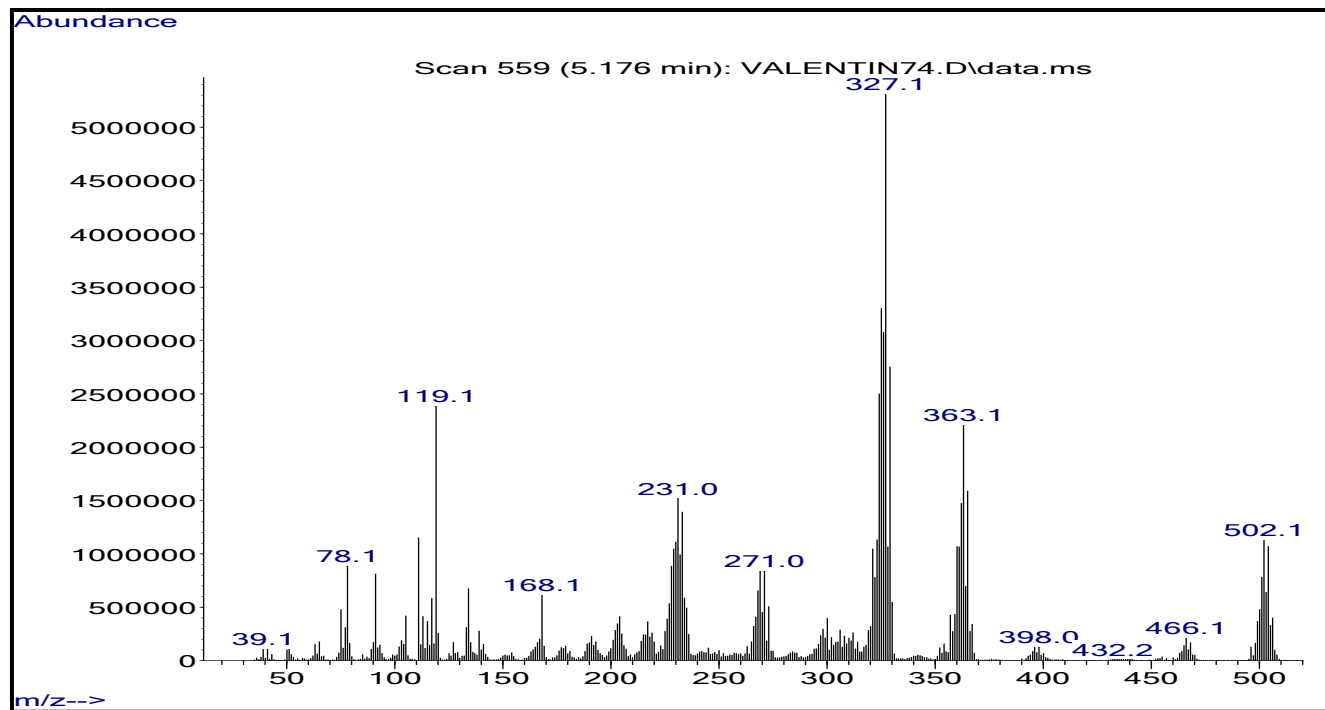


Figure S89.  $^1\text{H}$ - $^{13}\text{C}$  HSQC NMR spectrum of **12** in  $\text{THF-}d_8$ .



**Figure S90.**  $^1\text{H}$ - $^{13}\text{C}$  HMBC NMR spectrum of **12** in  $\text{THF-}d_8$ .



**Figure S91.** Electron Ionization-Mass spectrum of **12**.



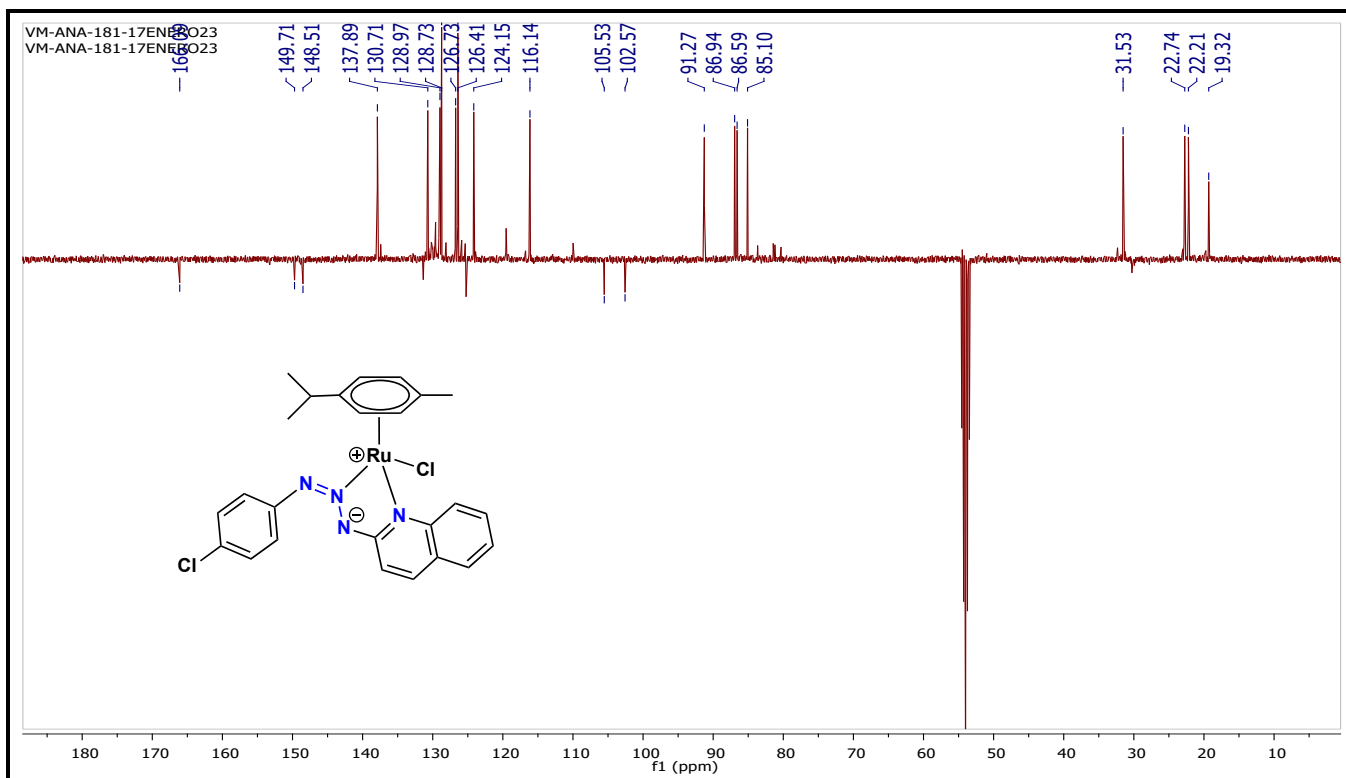


**Figure S94.** Full  $^{13}\text{C}$   $\{^1\text{H}\}$  NMR-APT spectrum of **13** in  $\text{CD}_2\text{Cl}_2$  (100 MHz).

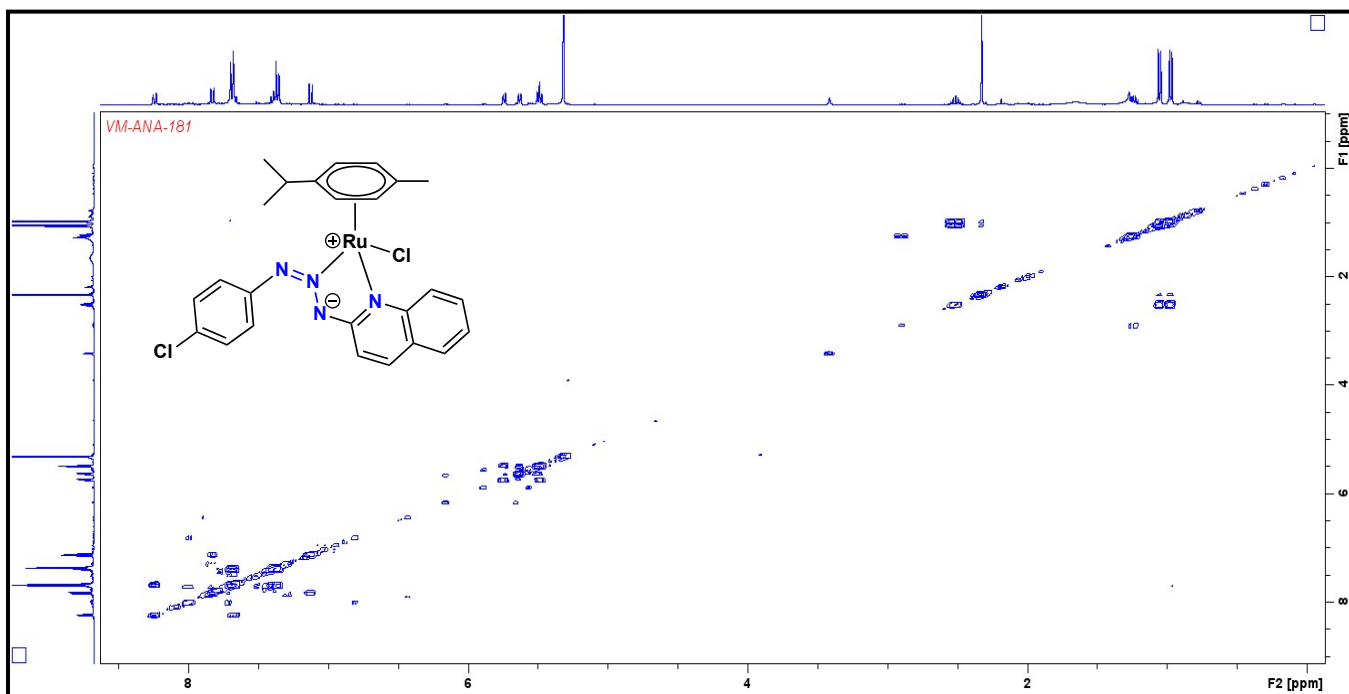


**Figure S95.** Full  $^1\text{H}$ - $^1\text{H}$  gCOSY NMR spectrum of **13** in  $\text{CD}_2\text{Cl}_2$ .

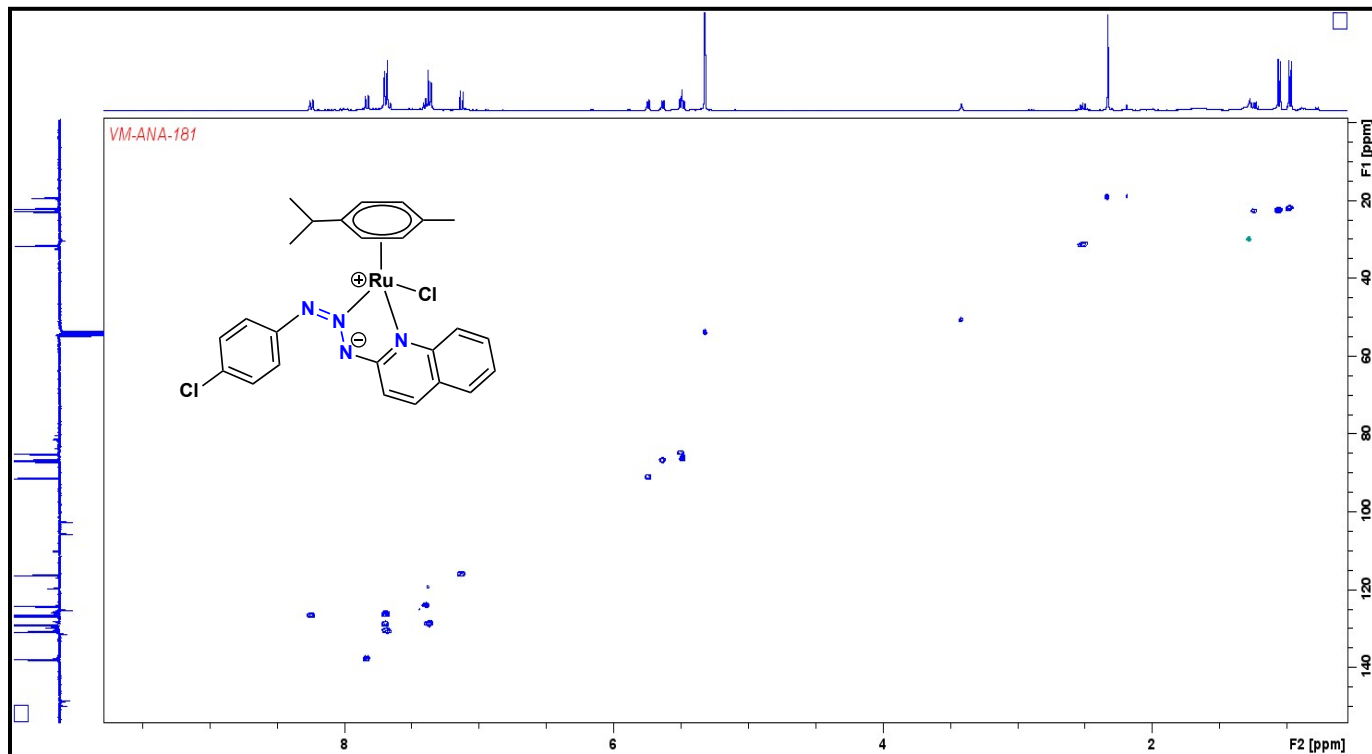


Figure S96. Full  $^1\text{H}$ - $^{13}\text{C}$  gHSQC NMR spectrum of **13** in  $\text{CD}_2\text{Cl}_2$ .

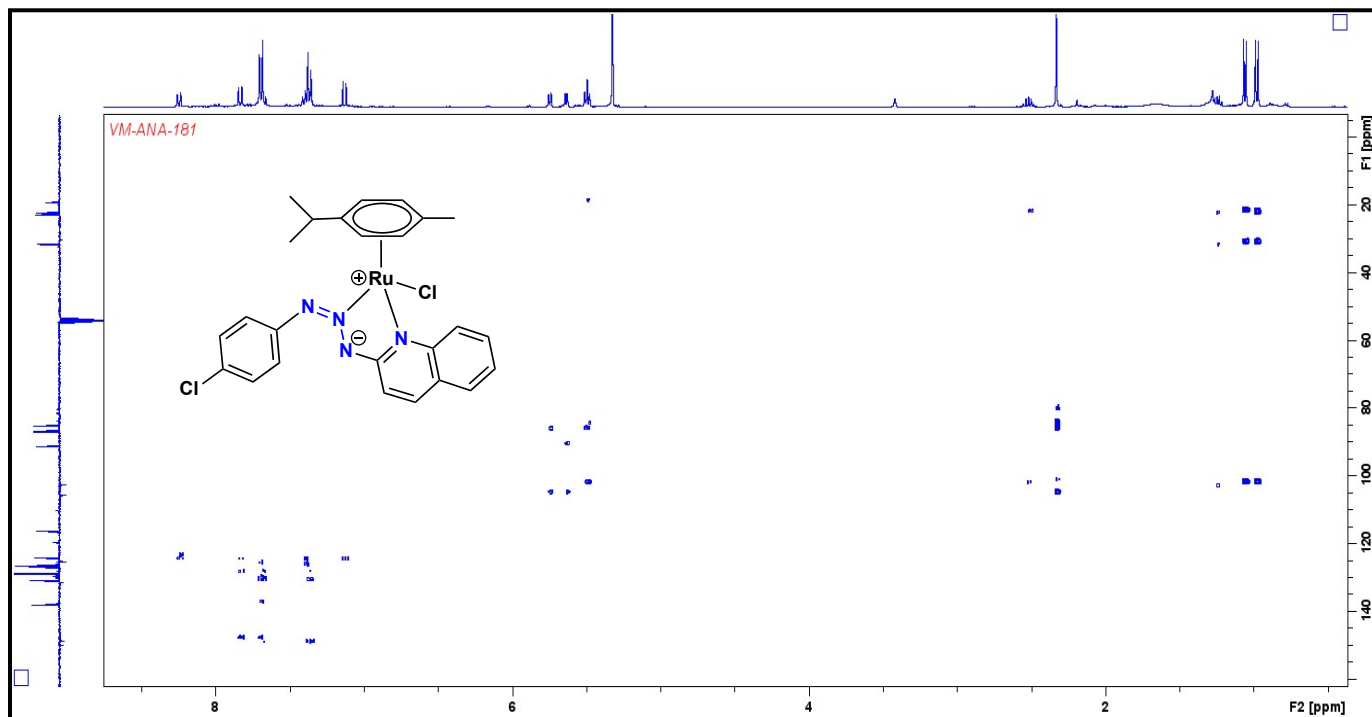


Figure S97. Full  $^1\text{H}$ - $^{13}\text{C}$  HMBC NMR spectrum of **13** in  $\text{CD}_2\text{Cl}_2$ .

**Table S1.** Crystallographic data for complex **5**.

Formula	C <sub>21</sub> H <sub>22</sub> Cl <sub>2</sub> N <sub>4</sub> Ru
<i>M<sub>w</sub></i> (g mol <sup>-1</sup> )	502.40
Crystal size (mm <sup>3</sup> )	0.28 x 0.12 x 0.08
Crystal system	Orthorhombic
Space group	P2 <sub>1</sub> 2 <sub>1</sub> 2 <sub>1</sub>
<i>a</i> (Å)	7.6210(14)
<i>b</i> (Å)	10.7471(18)
<i>c</i> (Å)	24.768(4)
$\alpha$ /°	90
$\beta$ /°	90
$\gamma$ /°	90
<i>V</i> (Å <sup>3</sup> )	2028.6(6)
<i>Z</i>	4
$\rho_{\text{calc}}$ (g cm <sup>-3</sup> )	1.645
$\lambda$ (Å)	0.71073
Temp (K)	100(2)
$2\theta_{\text{max}}$ (grados)	26.42
Reflections collected	13185
Independent reflections	4182 [R(int) = 0.0487]
No. de parámetros	256
wR2 [ <i>I</i> >2 $\sigma$ ( <i>I</i> )]	R1 = 0.0329, wR2 = 0.0578
R1 (all data)	R1 = 0.0409, wR2 = 0.0601
Goof (F <sup>2</sup> )	1.037

**Table S2.** Crystallographic data for complex **6**.

Empirical formula	C <sub>25</sub> H <sub>24</sub> N <sub>4</sub> Cl <sub>2</sub> Ru
Formula weight	552.45
Temperature/K	293.4(3)
Crystal system	orthorhombic
Space group	P2 <sub>1</sub> 2 <sub>1</sub> 2 <sub>1</sub>
a/Å	7.96150(10)
b/Å	11.85520(10)
c/Å	25.7291(2)
α/°	90
β/°	90
γ/°	90
Volume/Å <sup>3</sup>	2428.45(4)
Z	4
ρ <sub>calc</sub> /cm <sup>3</sup>	1.511
μ/mm <sup>1</sup>	7.401
F(000)	1120.0
Crystal size/mm <sup>3</sup>	0.301 × 0.145 × 0.123
Radiation	CuKα (λ = 1.54184)
2θ range for data collection/°	6.872 to 141.616
Index ranges	-9 ≤ h ≤ 7, -14 ≤ k ≤ 14, -30 ≤ l ≤ 31
Reflections collected	12917
Independent reflections	4509 [R <sub>int</sub> = 0.0330, R <sub>sigma</sub> = 0.0340]
Data/restraints/parameters	4509/0/292
Goodness-of-fit on F <sup>2</sup>	1.043
Final R indexes [I ≥ 2σ (I)]	R <sub>1</sub> = 0.0309, wR <sub>2</sub> = 0.0779
Final R indexes [all data]	R <sub>1</sub> = 0.0321, wR <sub>2</sub> = 0.0787
Largest diff. peak/hole / e Å <sup>-3</sup>	0.38/-0.67

**Table S3.** Crystallographic data for complex 7.

Empirical formula	C <sub>21</sub> H <sub>27</sub> ClN <sub>5</sub> Ru
Formula weight	486.00
Temperature/K	293.1(10)
Crystal system	monoclinic
Space group	P2 <sub>1</sub> /n
a/Å	12.9896(4)
b/Å	13.2753(4)
c/Å	14.0569(4)
α/°	90.000(2)
β/°	116.179(3)
γ/°	90.000(3)
Volume/Å <sup>3</sup>	2175.33(13)
Z	4
ρ <sub>calc</sub> /cm <sup>3</sup>	1.4839
μ/mm <sup>-1</sup>	0.860
F(000)	991.9
Crystal size/mm <sup>3</sup>	0.185 × 0.123 × 0.062
Radiation	Mo Kα (λ = 0.71073)
2θ range for data collection/°	3.56 to 59.18
Index ranges	-17 ≤ h ≤ 17, -18 ≤ k ≤ 17, -19 ≤ l ≤ 19
Reflections collected	26543
Independent reflections	5732 [R <sub>int</sub> = 0.0298, R <sub>sigma</sub> = 0.0254]
Data/restraints/parameters	5732/0/258
Goodness-of-fit on F <sup>2</sup>	1.032
Final R indexes [I >= 2σ (I)]	R <sub>1</sub> = 0.0296, wR <sub>2</sub> = 0.0667
Final R indexes [all data]	R <sub>1</sub> = 0.0398, wR <sub>2</sub> = 0.0721



**Table S4.** Crystallographic data for complex **12**.

Empirical formula	C <sub>21</sub> H <sub>22</sub> Cl <sub>2</sub> N <sub>4</sub> Ru
Formula weight	502.39
Temperature/K	293(2)
Crystal system	orthorhombic
Space group	Pbca
a/Å	20.5077(12)
b/Å	7.6529(3)
c/Å	26.1253(17)
α/°	90
β/°	90
γ/°	90
Volume/Å <sup>3</sup>	4100.2(4)
Z	8
ρ <sub>calc</sub> /cm <sup>3</sup>	1.628
μ/mm <sup>-1</sup>	1.040
F(000)	2032.0
Crystal size/mm <sup>3</sup>	0.332 × 0.112 × 0.071
Radiation	Mo Kα (λ = 0.71073)
2θ range for data collection/°	6.728 to 58.978
Index ranges	-25 ≤ h ≤ 28, -8 ≤ k ≤ 10, -35 ≤ l ≤ 33
Reflections collected	23842
Independent reflections	5198 [R <sub>int</sub> = 0.0476, R <sub>sigma</sub> = 0.0443]
Data/restraints/parameters	5198/0/256
Goodness-of-fit on F <sup>2</sup>	1.077
Final R indexes [I ≥ 2σ (I)]	R <sub>1</sub> = 0.0425, wR <sub>2</sub> = 0.0769
Final R indexes [all data]	R <sub>1</sub> = 0.0693, wR <sub>2</sub> = 0.0847

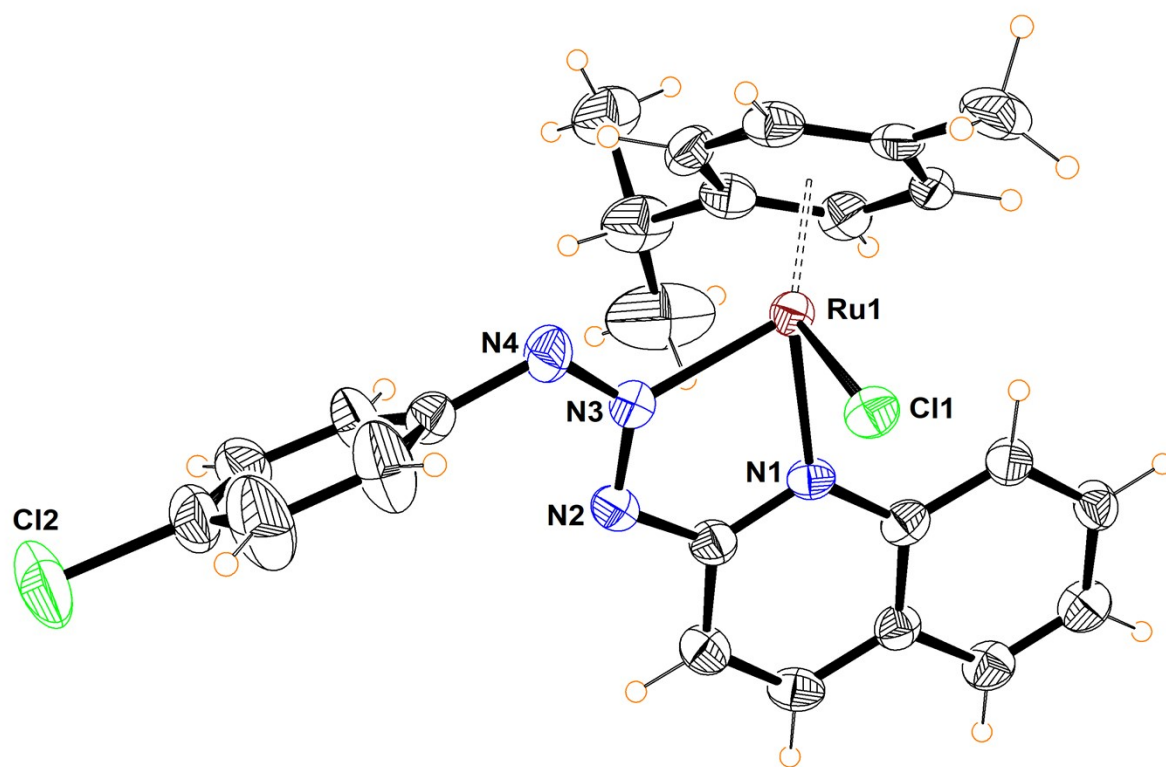
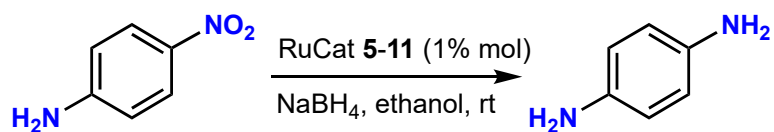


**Figure S98.** Molecular structure of **13**. Selected bond distances (Å): N(3)–N(4), 1.28(1); N(2)–N(3), 1.30(1); Ru(1)–N(3), 2.055(7); Ru(1)–N(1), 2.109(7); Ru(1)–Cl(1), 2.399(2). Selected bond angles (°): N(3)–Ru(1)–N(1), 75.1(2); N(3)–Ru(1)–Cl(1), 86.1(2); N(1)–Ru(1)–Cl(1), 87.3(2). N(2)–N(3)–N(4), 121.3(7).

**Table S5.** Crystallographic data for complex **13**.

Empirical formula	C <sub>25</sub> H <sub>24</sub> N <sub>4</sub> Cl <sub>2</sub> Ru
Formula weight	552.45
Temperature/K	294.7(7)
Crystal system	triclinic
Space group	P-1
a/Å	9.8885(8)
b/Å	14.1476(11)
c/Å	17.6592(11)
$\alpha$ /°	102.034(6)
$\beta$ /°	100.332(7)
$\gamma$ /°	94.941(7)
Volume/Å <sup>3</sup>	2357.4(3)
Z	4
$\rho_{\text{calc}}$ /g/cm <sup>3</sup>	1.557
$\mu$ /mm <sup>-1</sup>	0.912
F(000)	1120.0
Crystal size/mm <sup>3</sup>	0.187 × 0.168 × 0.054
Radiation	Mo K $\alpha$ ( $\lambda$ = 0.71073)
2 $\theta$ range for data collection/°	6.704 to 59.34
Index ranges	-13 ≤ h ≤ 13, -19 ≤ k ≤ 19, -22 ≤ l ≤ 24
Reflections collected	51887
Independent reflections	11636 [ $R_{\text{int}}$ = 0.1741, $R_{\text{sigma}}$ = 0.1640]
Data/restraints/parameters	11636/0/583
Goodness-of-fit on F <sup>2</sup>	1.022
Final R indexes [ $I \geq 2\sigma(I)$ ]	$R_1 = 0.0923$ , $wR_2 = 0.1928$
Final R indexes [all data]	$R1 = 0.1921$ , $wR2 = 0.2474$

**Table S6.** Screening of complexes **5-11** in the catalysis of 4-aminonitrobenzene.<sup>a</sup>



Entry	Catalyst	Time (min)	Yield (%)
1	<b>5</b>	30	45
2	<b>6</b>	30	34
3	<b>7</b>	30	22
4	<b>8</b>	30	32
5	<b>10</b>	30	22
6	<b>11</b>	30	33
7	<b>5</b>	60	87
8	<b>6</b>	60	76
9	<b>7</b>	60	51
10	<b>8</b>	60	76
11	<b>10</b>	60	56
12	<b>11</b>	60	53
13	<b>5</b>	90	100
14	<b>6</b>	90	96
15	<b>7</b>	90	80
16	<b>8</b>	90	95
17	<b>10</b>	90	84
18	<b>11</b>	90	88

<sup>[a]</sup>**Reaction conditions:** nitrobenzene (0.3 mmol), NaBH<sub>4</sub> (1.2 mmol), ethanol (2 mL), room temperature. Yields were determined by GC-MS.

Selected GC-MS data of the catalytic hydrogenation of nitrobenzene (Table 1)

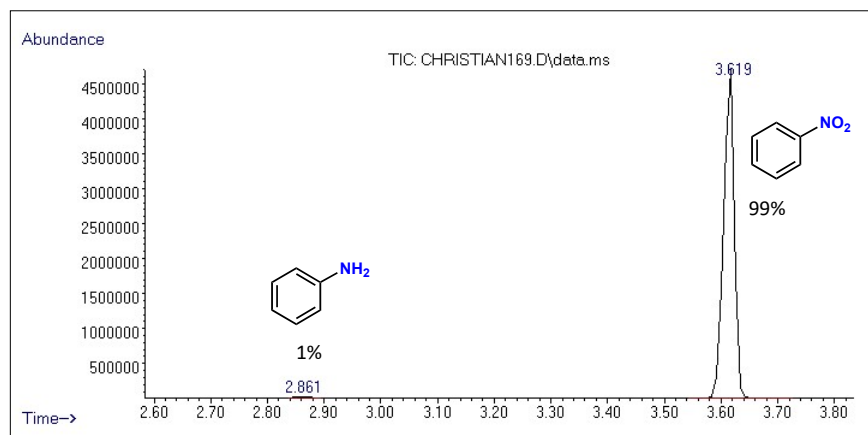


Figure S99. Chromatogram of the reduction of nitrobenzene (Table 1, entry 1).

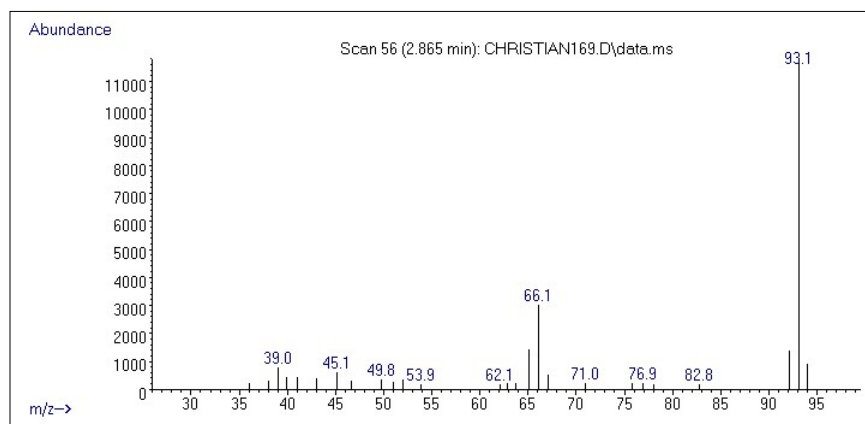


Figure S100. Mass spectrum of the component at 2.86 min identified as aniline.

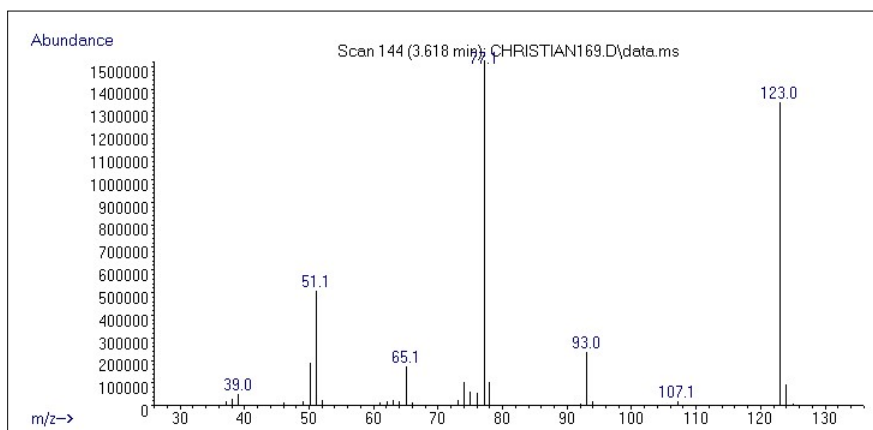
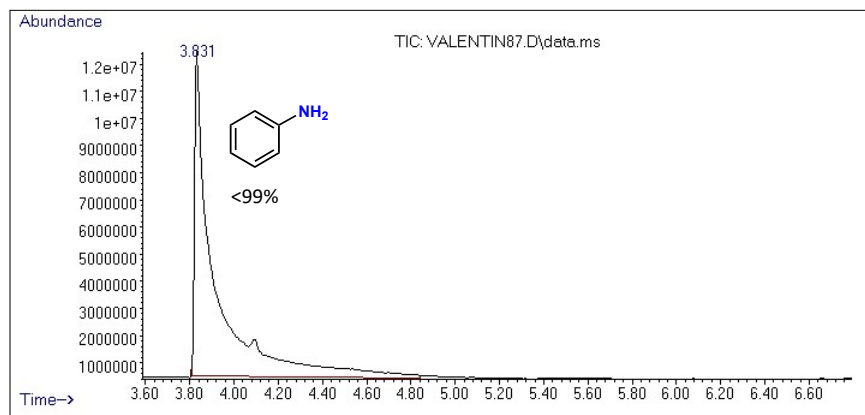
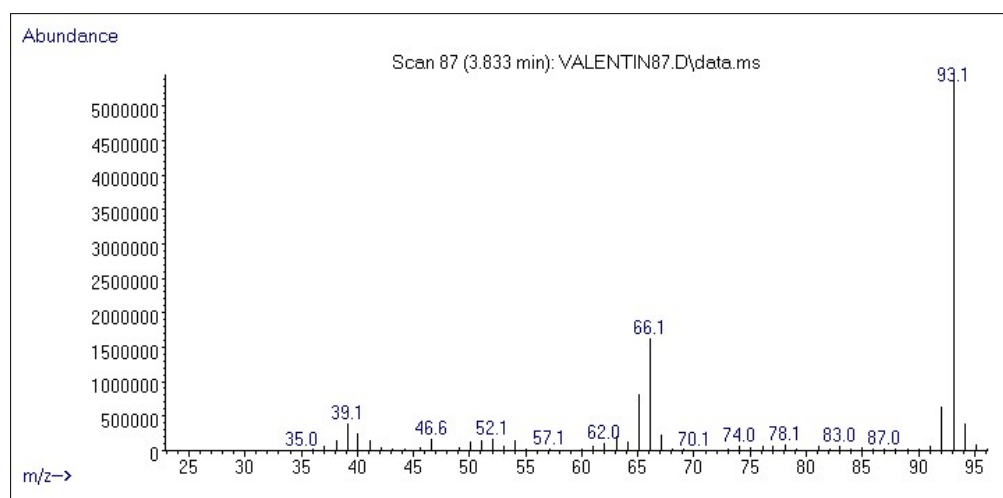


Figure S101. Mass spectrum of the component at 3.61 min identified as nitrobenzene.



**Figure S102.** Chromatogram of the reduction of nitrobenzene (Table 1, entry 2).



**Figure S103.** Mass spectrum of the component at 3.82 min identified as aniline.

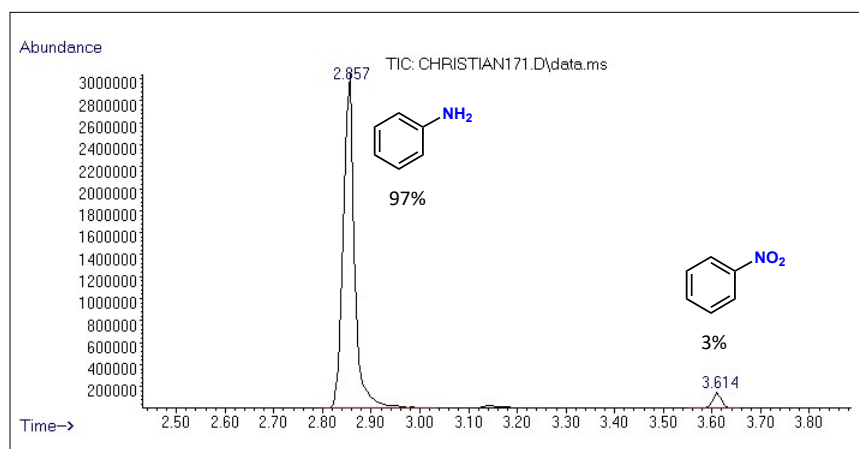


**Figure S104.** Chromatogram of the reduction of nitrobenzene (Table 1, entry 3).

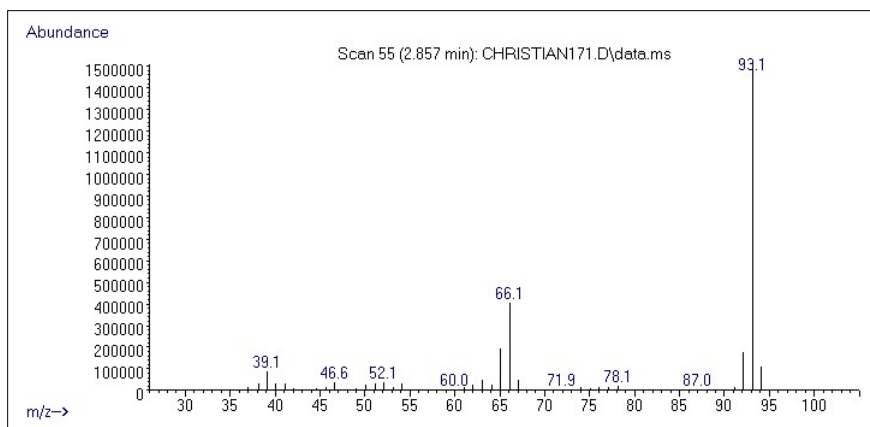


**Figure S105.** Mass spectrum of the component at 2.85 min identified as aniline.

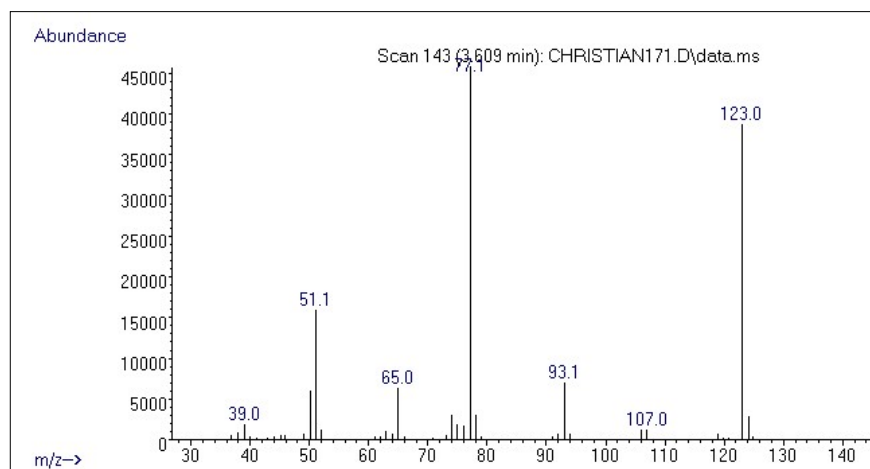


**Figure S106.** Mass spectrum of the component at 3.60 min identified as nitrobenzene.

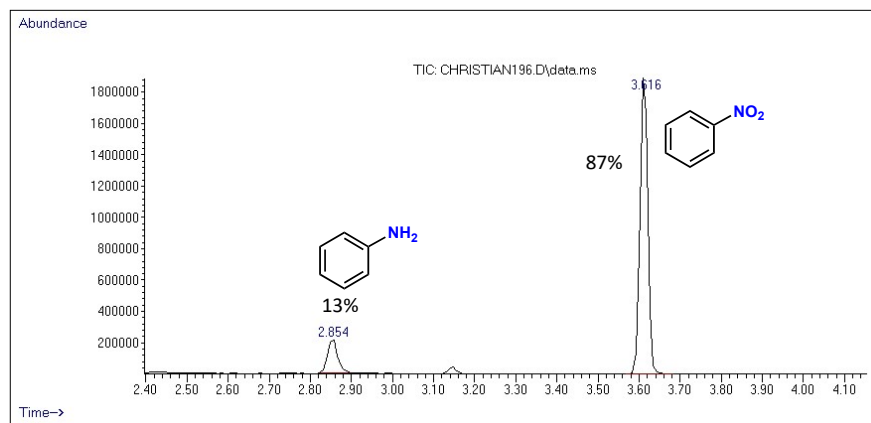


**Figure S107.** Chromatogram of the reduction of nitrobenzene (Table 1, entry 7).

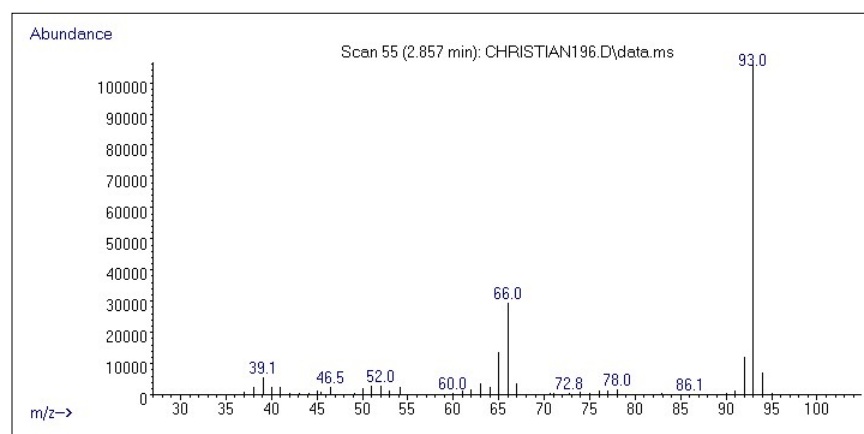


**Figure S108.** Mass spectrum of the component at 2.85 min identified as aniline.

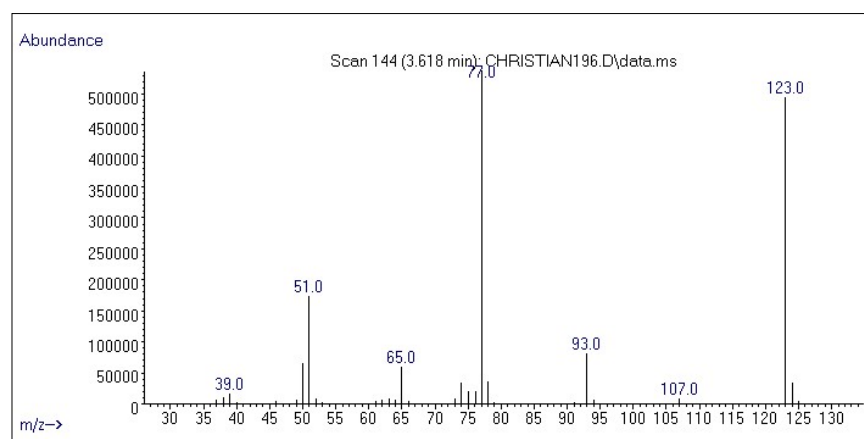


**Figure S109.** Mass spectrum of the component at 3.61 min identified as nitrobenzene.



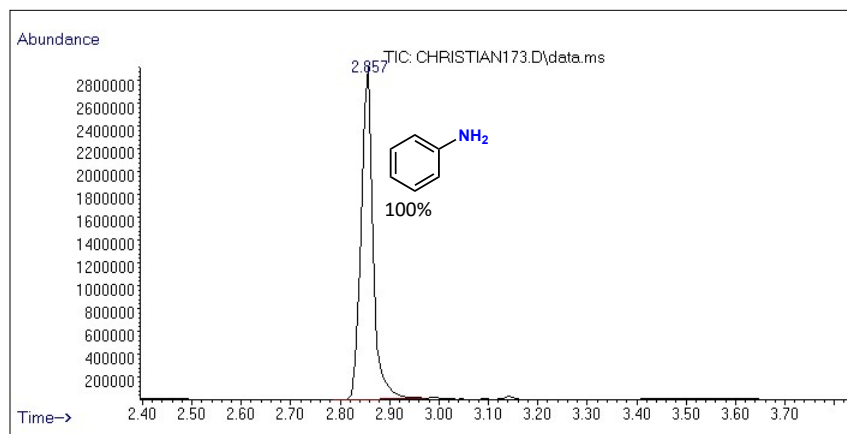


**Figure S110.** Chromatogram of the reduction of nitrobenzene (Table 1, entry 8).

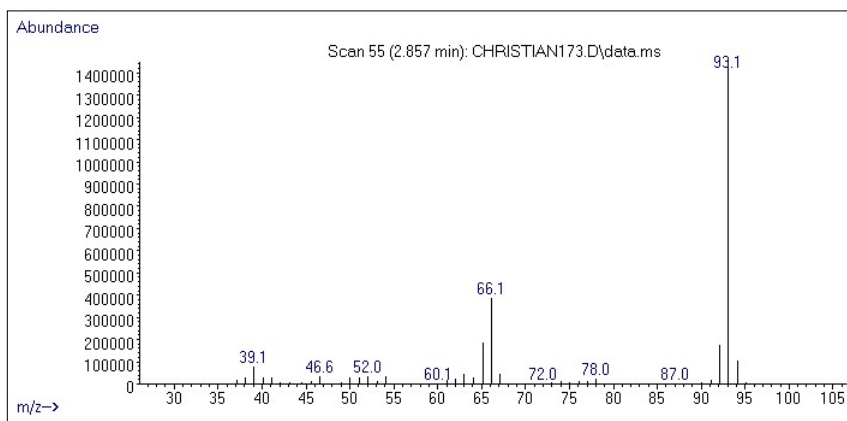


**Figure S111.** Mass spectrum of the component at 2.85 min identified as aniline.

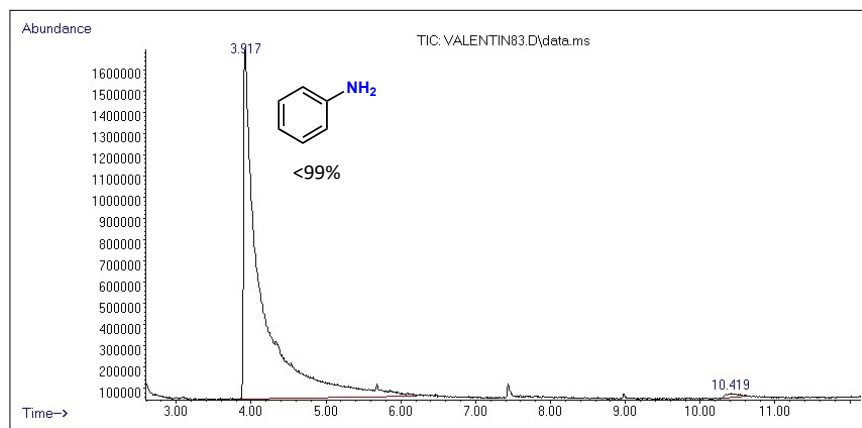


**Figure S112.** Mercury drop test in the reduction of nitrobenzene (Table 1, entry 12).

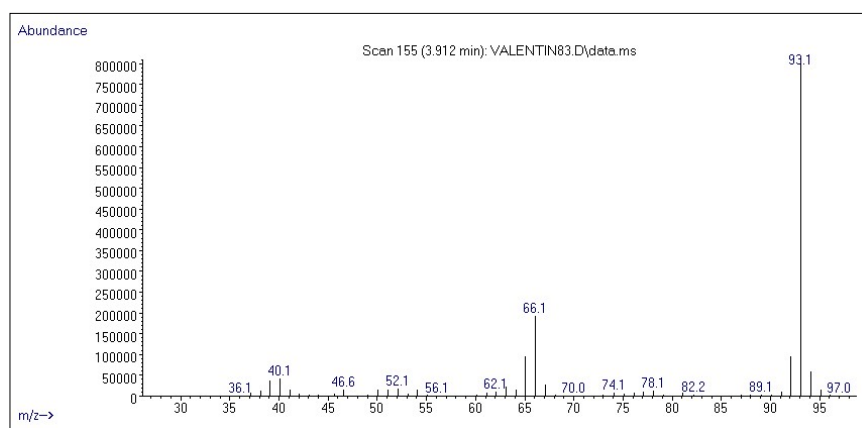


**Figure S113.** Mass spectrum of the component at 3.91 min identified as aniline.

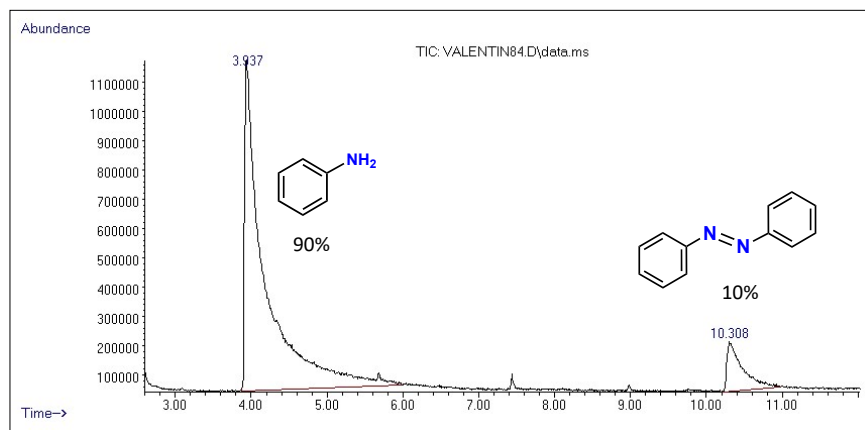


**Figure S114.** Chromatogram of the reduction of nitrobenzene with 0.5% mol of **5** (Table 1, entry 13).

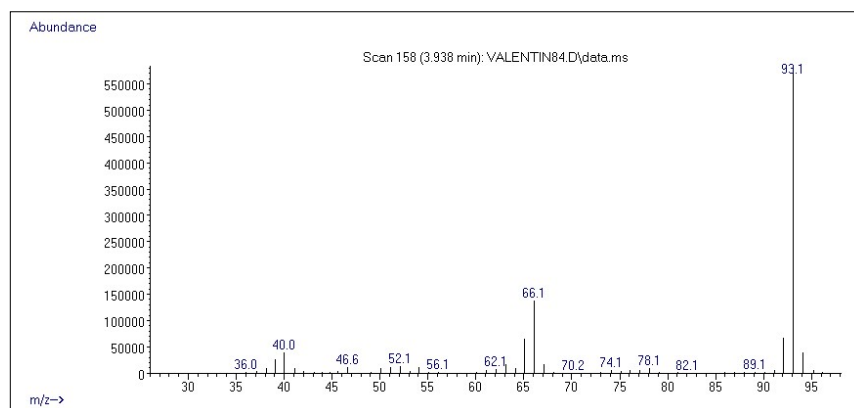


**Figure S115.** Mass spectrum of the component at 3.93 min identified as aniline.

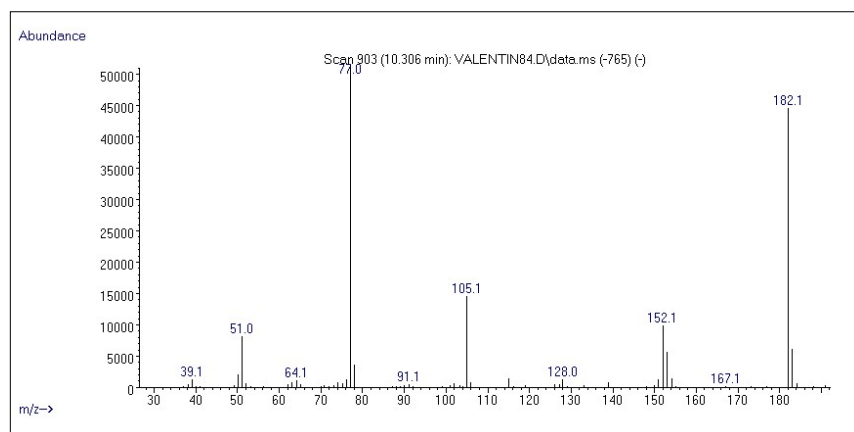


**Figure S116.** Mass spectrum of the component at 10.30 min identified as azobenzene.

Selected GC-MS data of the catalytic hydrogenation of 4-aminonitrobenzene (Table S6)

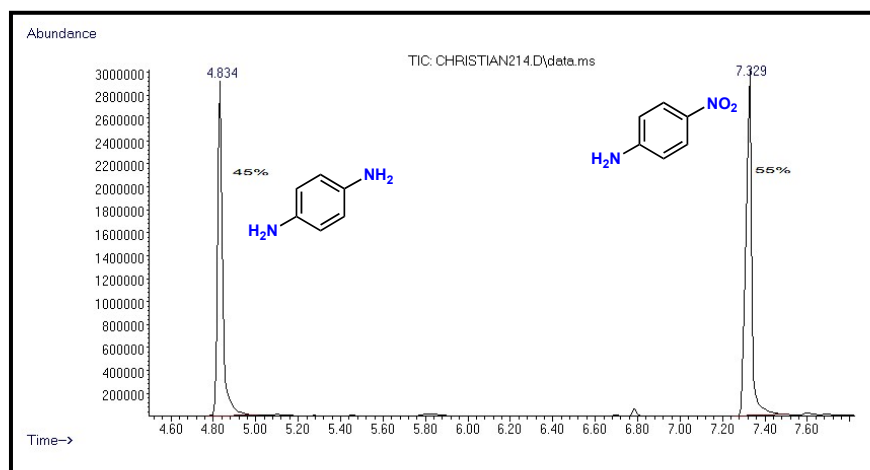


Figure S117. Chromatogram of the reduction of 4-aminonitrobenzene (Table S6, entry 1).

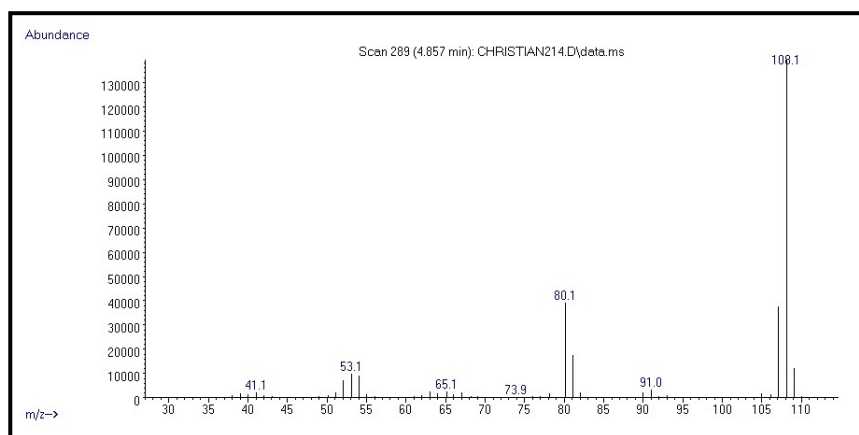


Figure S118. Mass spectrum of the component at 4.85 min identified as 4-aminoaniline.

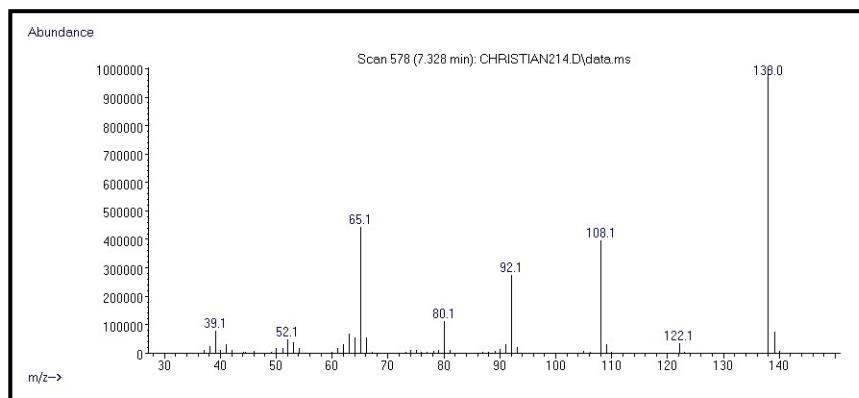
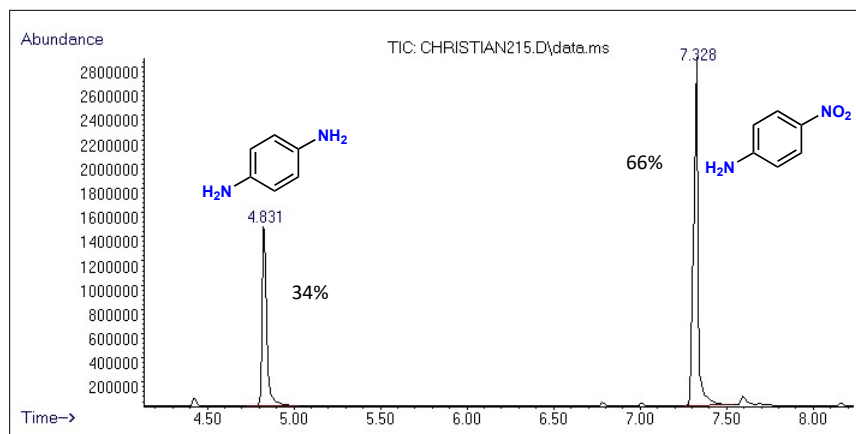
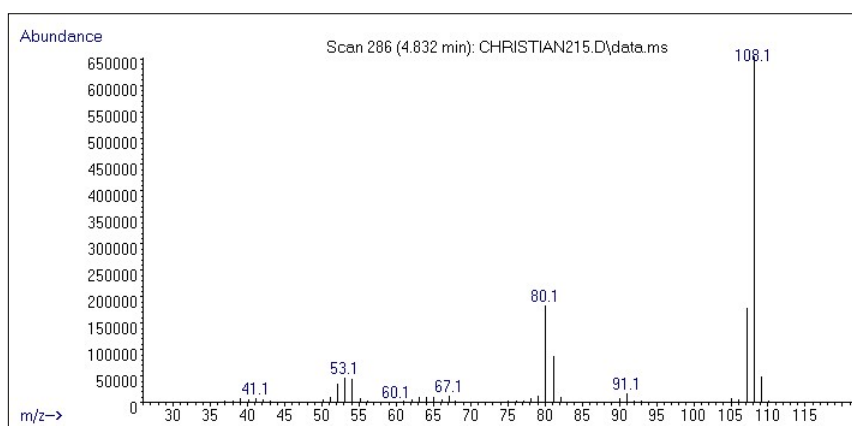


Figure S119. Mass spectrum of the component at 7.32 min identified as 4-aminonitrobenzene.



**Figure S120.** Chromatogram of the reduction of 4-aminonitrobenzene (Table S6, entry 2).



**Figure S121.** Mass spectrum of the component at 4.83 min identified as 4-aminoaniline.

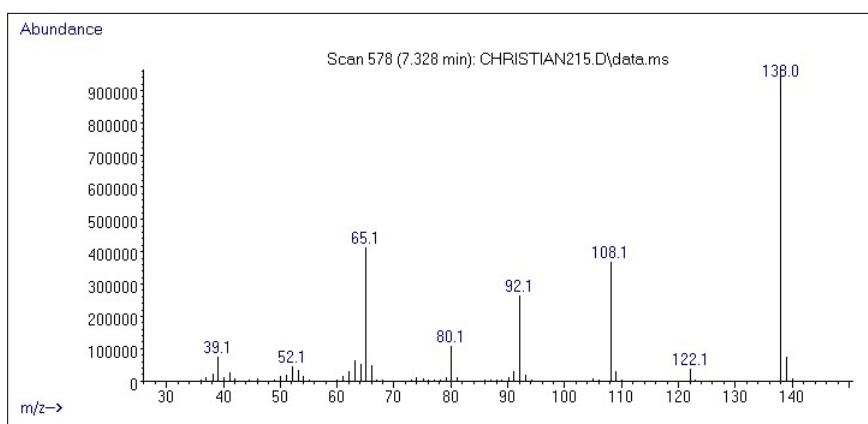


**Figure S122.** Mass spectrum of the component at 7.32 min identified as 4-aminonitrobenzene.

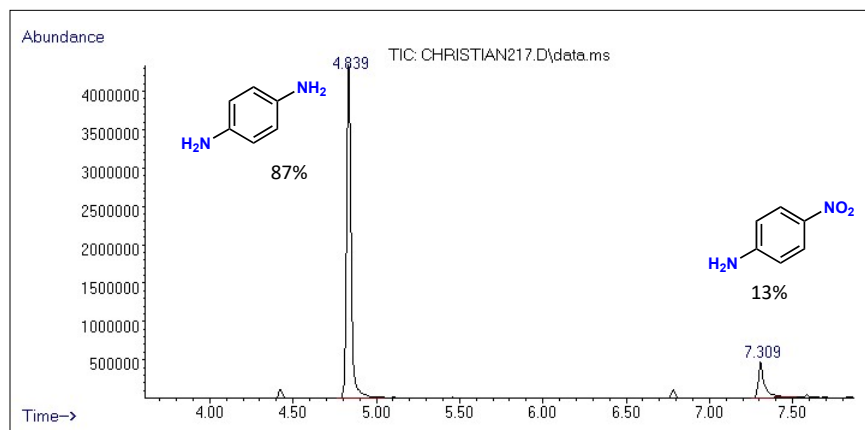


**Figure S123.** Chromatogram of the reduction of 4-aminonitrobenzene (Table S6, entry 7).

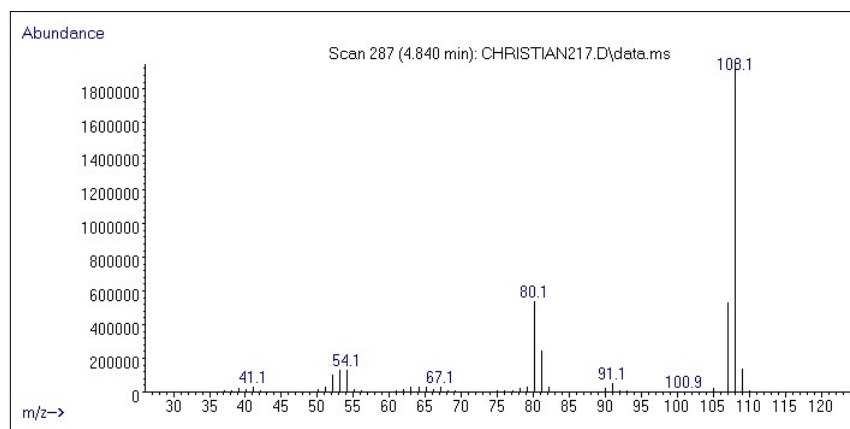


**Figure S124.** Mass spectrum of the component at 4.84 min identified as 4-aminoaniline.

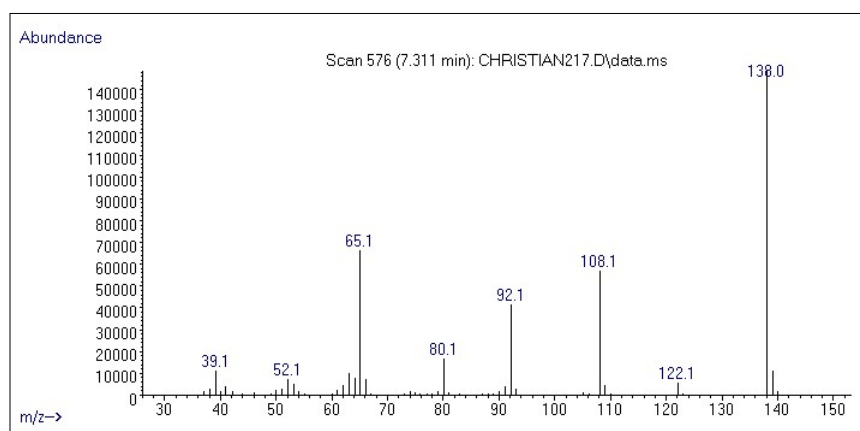


**Figure S125.** Mass spectrum of the component at 7.31 min identified as 4-aminonitrobenzene.

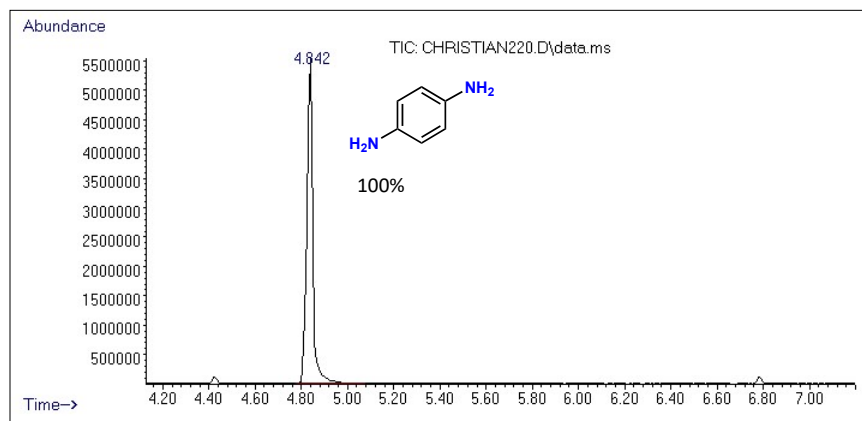


**Figure S126.** Chromatogram of the reduction of 4-aminonitrobenzene (Table S6, entry 13).

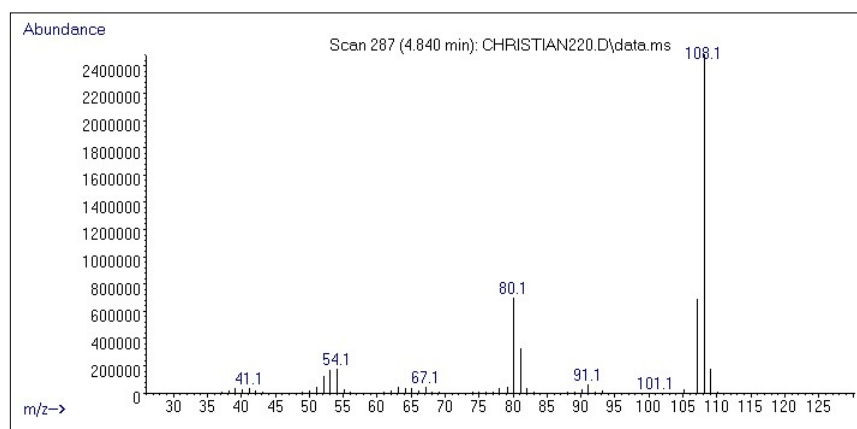


**Figure S127.** Mass spectrum of the component at 4.84 min identified as 4-aminoaniline.

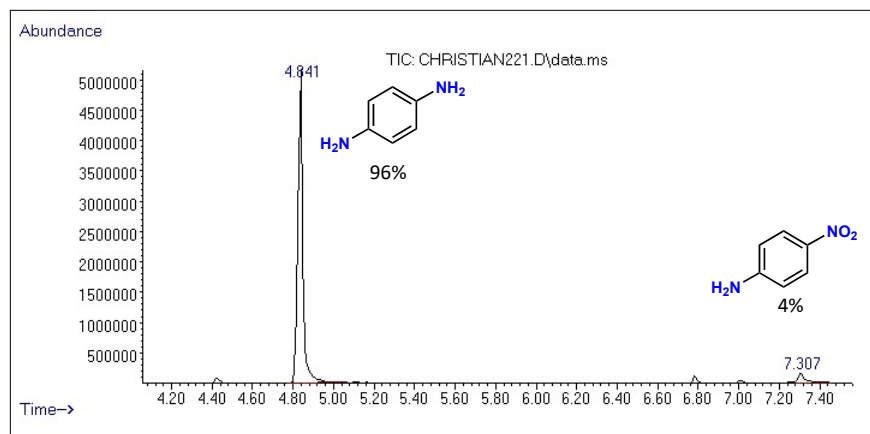


**Figure S128.** Chromatogram of the reduction of 4-aminonitrobenzene (Table S6, entry 14).

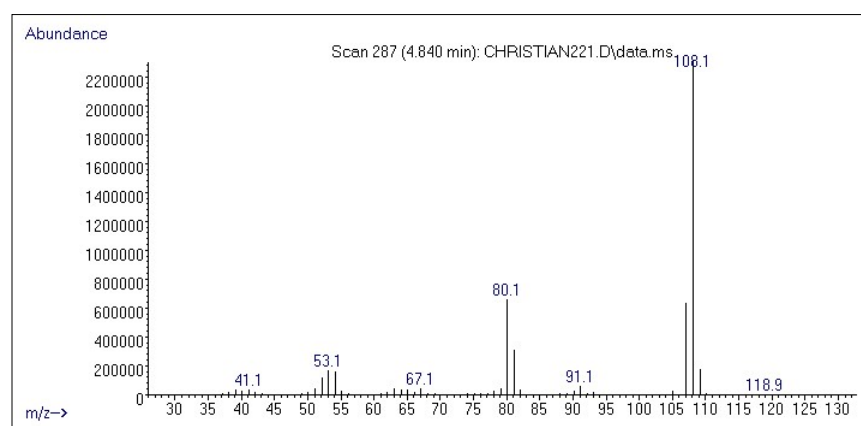


**Figure S129.** Mass spectrum of the component at 4.84 min identified as 4-aminoaniline.

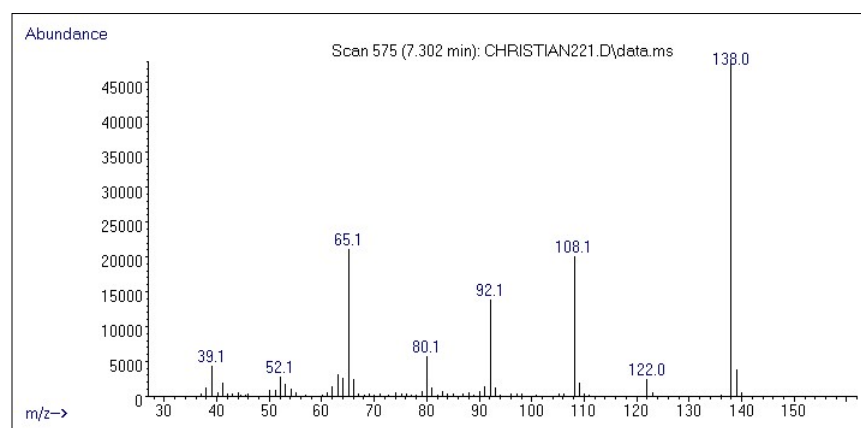


**Figure S130.** Mass spectrum of the component at 7.30 min identified as 4-aminonitrobenzene.



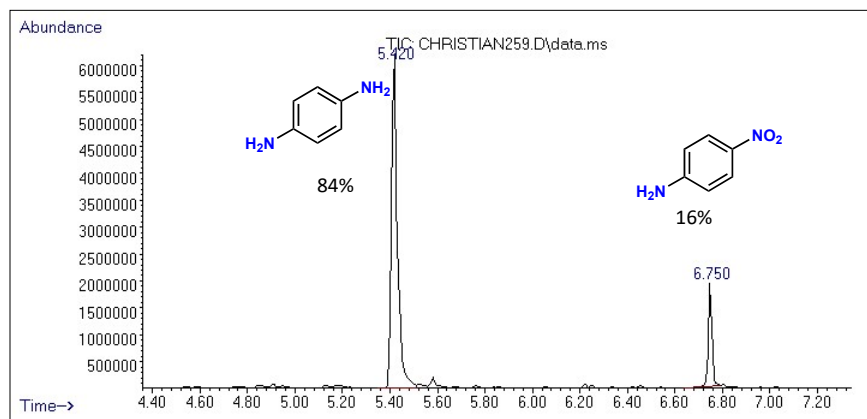


**Figure S131.** Chromatogram of the reduction of 4-aminonitrobenzene (Table S6, entry 17).

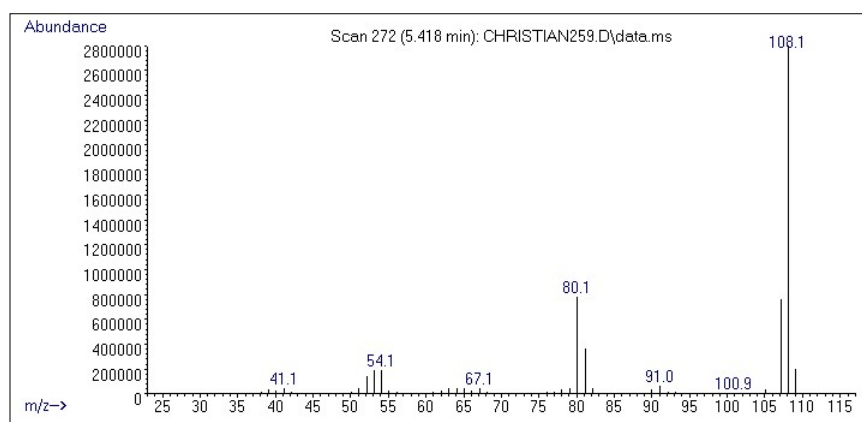


**Figure S132.** Mass spectrum of the component at 5.41 min identified as 4-aminoaniline.

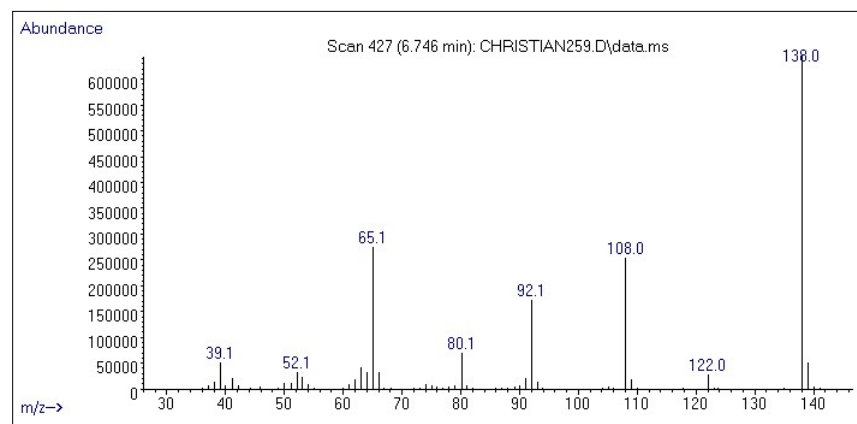


**Figure S133.** Mass spectrum of the component at 6.74 min identified as 4-aminonitrobenzene.

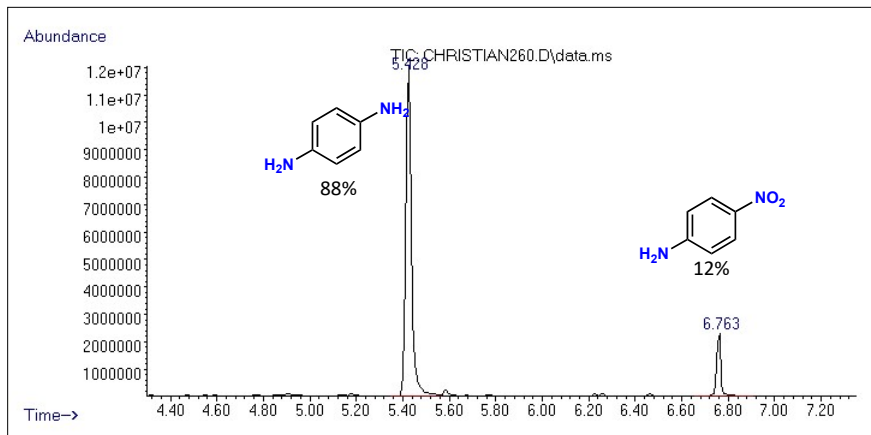


**Figure S134.** Chromatogram of the reduction of 4-aminonitrobenzene (Table S6, entry 18).

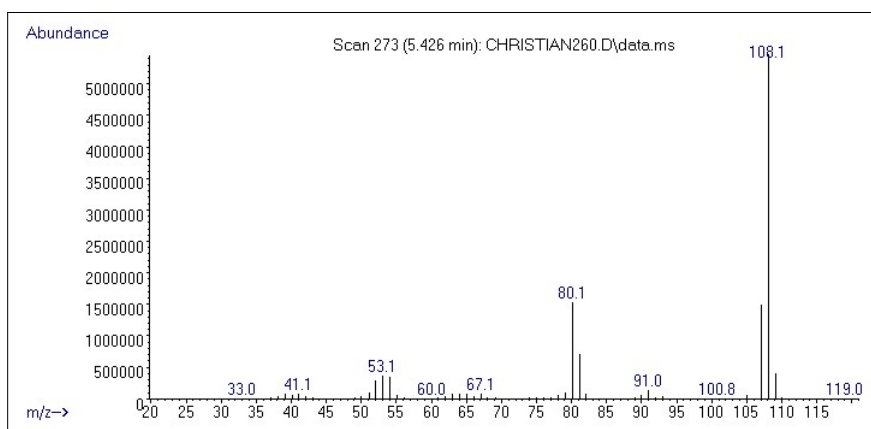


**Figure S135.** Mass spectrum of the component at 5.42 min identified as 4-aminoaniline

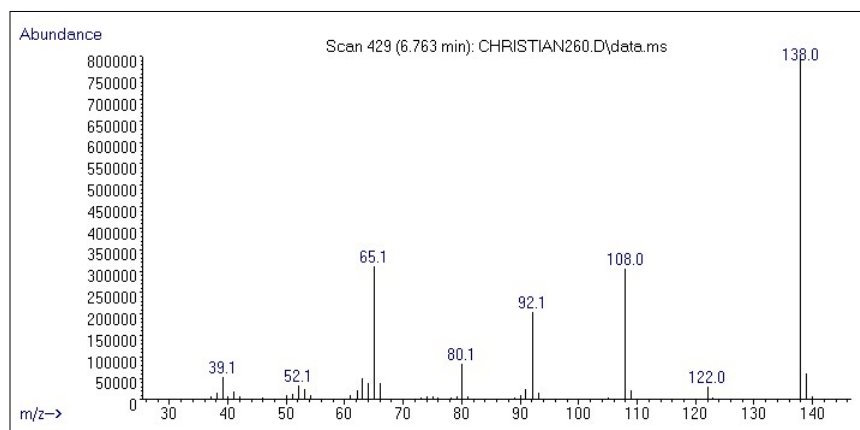


**Figure S136.** Mass spectrum of the component at 6.74 min identified as 4-aminonitrobenzene.

GC-MS data of the catalytic hydrogenation of nitroarenes (Table 2)

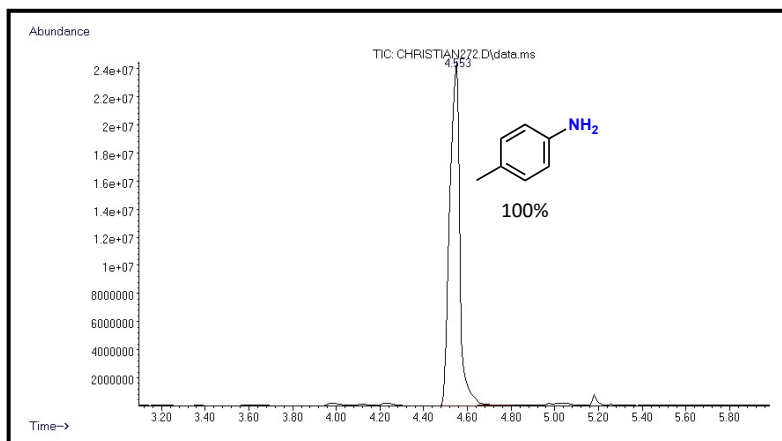


Figure S137. Chromatogram of the reduction of 4-nitrotoluene (Table 2, entry 1).

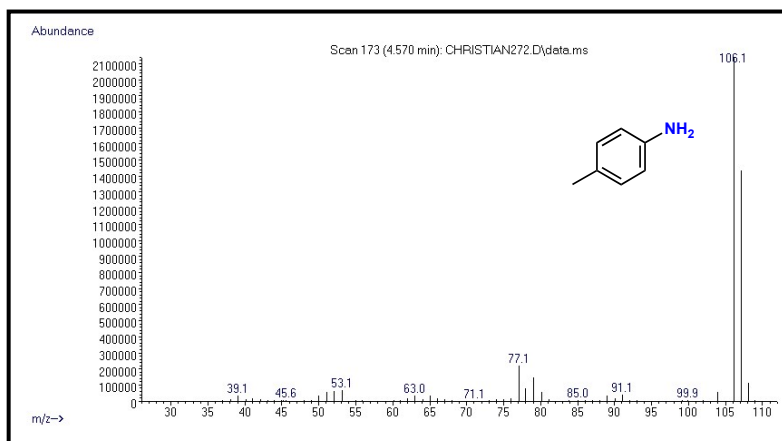
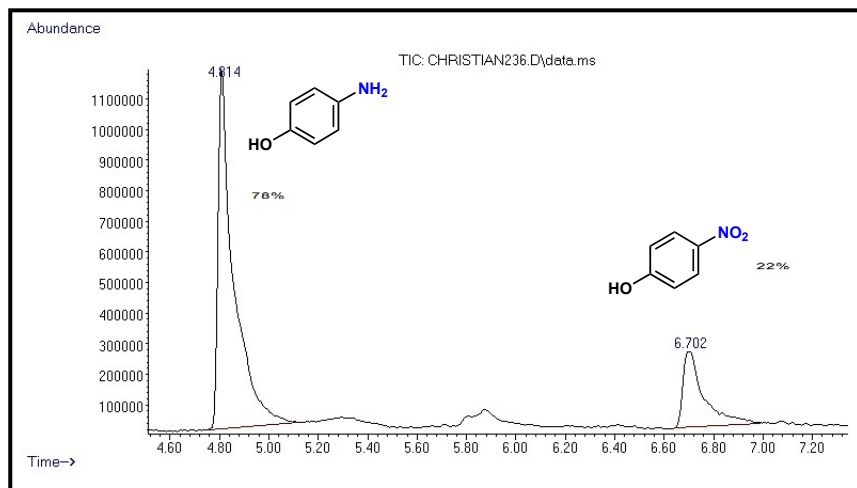
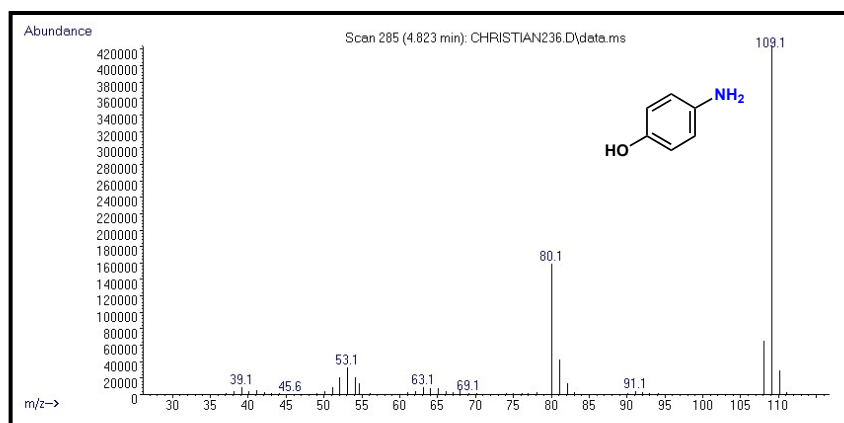


Figure S138. Mass spectrum of the component at 4.57 min identified as 4-aminotoluene.



**Figure S139.** Chromatogram of the reduction of 4-nitrophenol (Table 2, entry 2).



**Figure S140.** Mass spectrum of the component at 4.82 min identified as of 4-aminophenol.

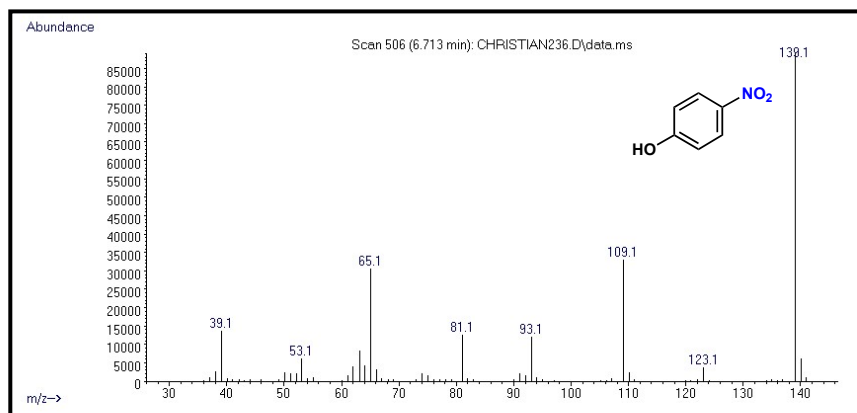


**Figure S141.** Mass spectrum of the component at 6.71 min identified as 4-nitrophenol.

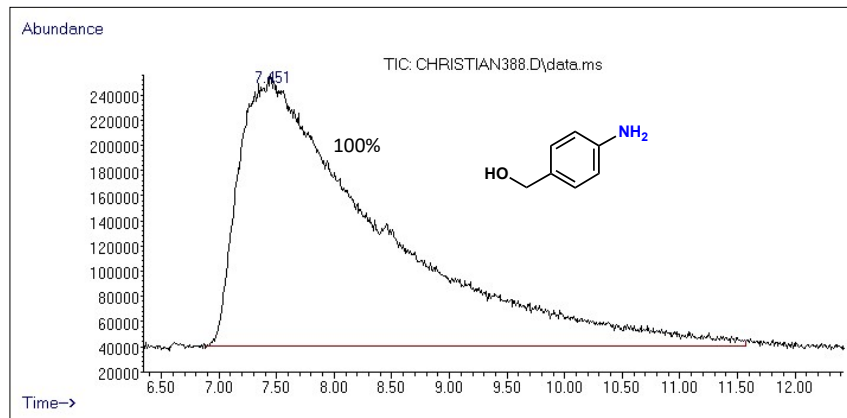


Figure S142. Chromatogram of the reduction of 4-nitrobenzyl alcohol (Table 2, entry 3).

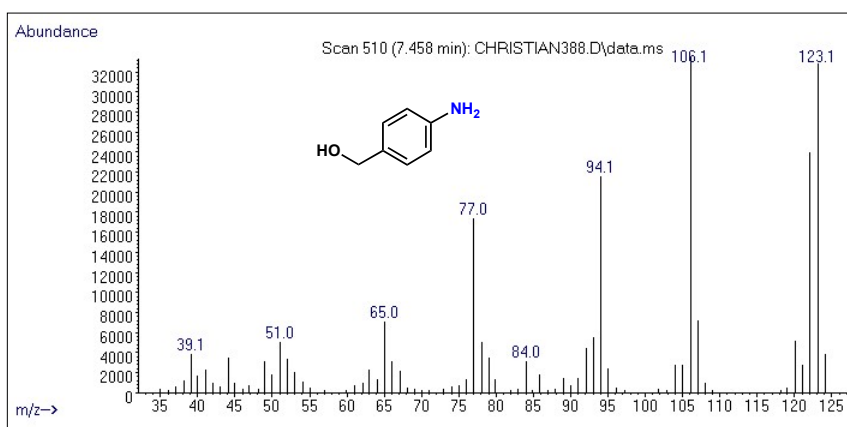


Figure S143. Mass spectrum of the component at 7.45 min identified as of 4-aminobenzyl alcohol.

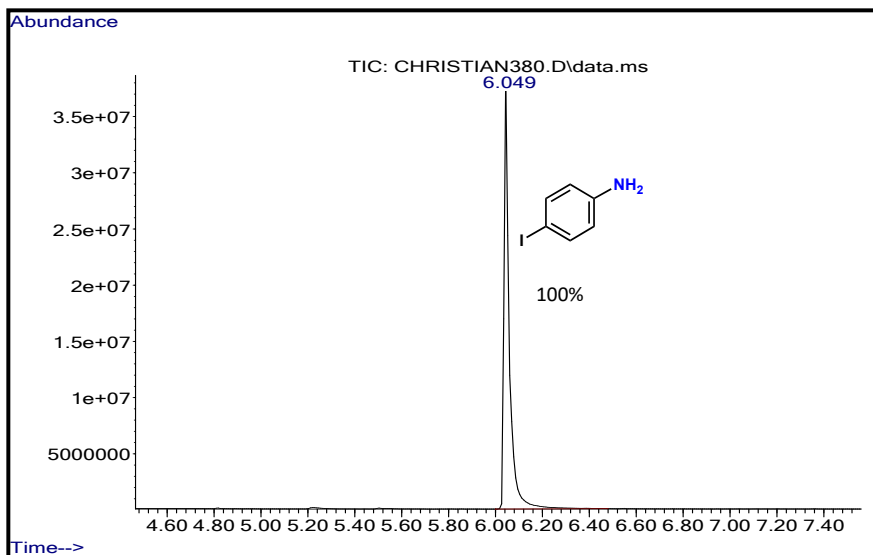


Figure S144. Chromatogram of the reduction of 1-Iodo-4-nitrobenzene (Table 2, entry 4).

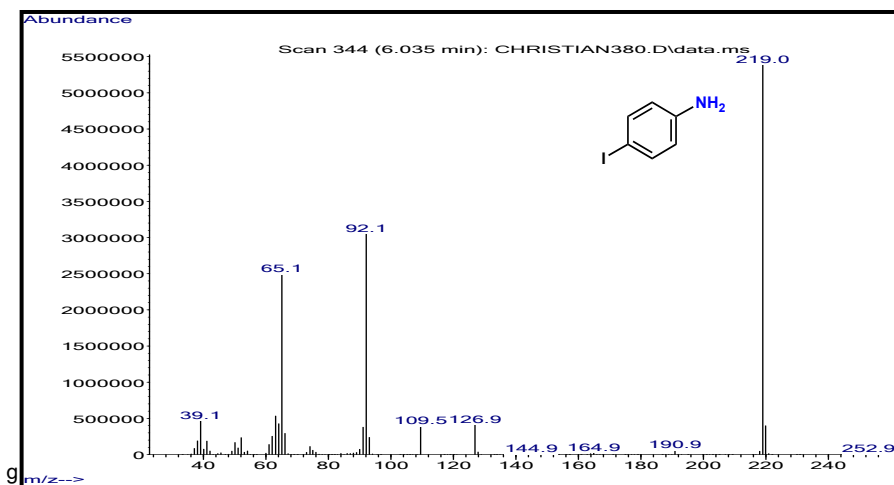
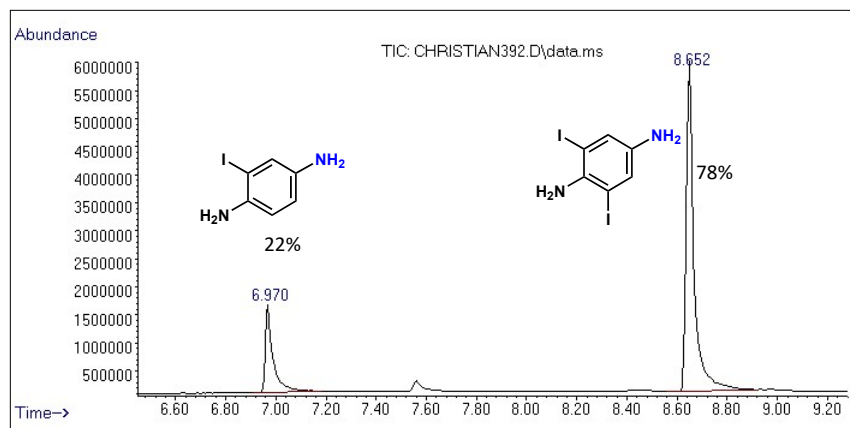
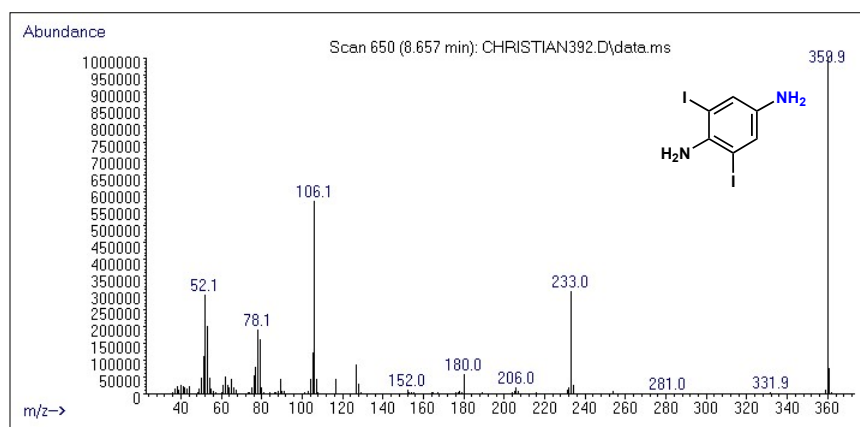


Figure S145. Mass spectrum of the component at 6.03 min identified as of 4-Iodo-aniline.



**Figure S146.** Chromatogram of the reduction of 2,6-diiodo-4-nitroaniline (Table 2, entry 5).



**Figure S147.** Mass spectrum of the component at 8.65 min identified as 2,6-diiodo-4-aminoaniline.

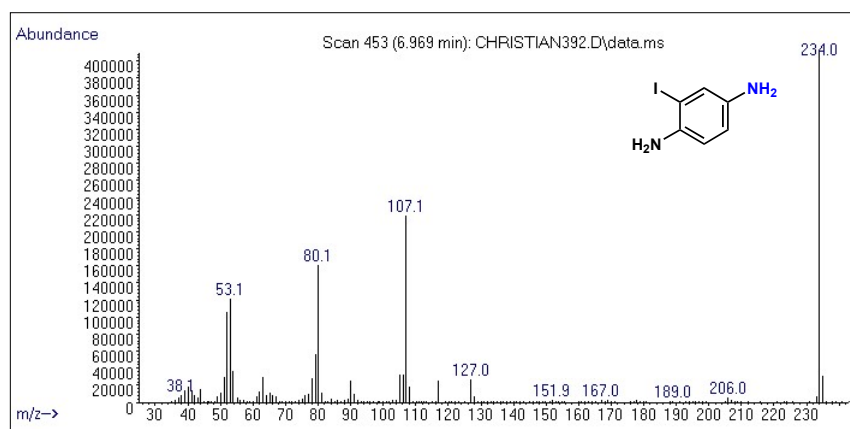


**Figure S148.** Mass spectrum of the component at 6.96 min identified as 2-iodo-4-aminoaniline (dehalogenation product).

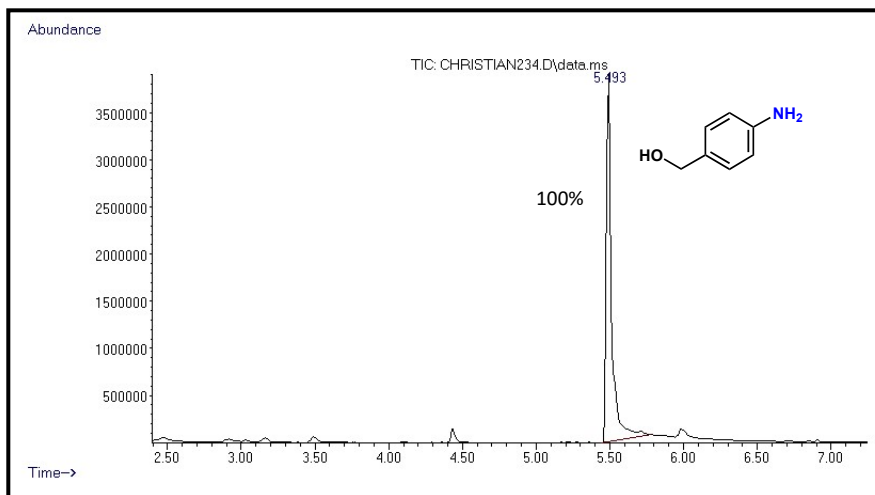


**Figure S149.** Chromatogram of the reduction of 4-nitrobenzaldehyde (Table 2, entry 6).

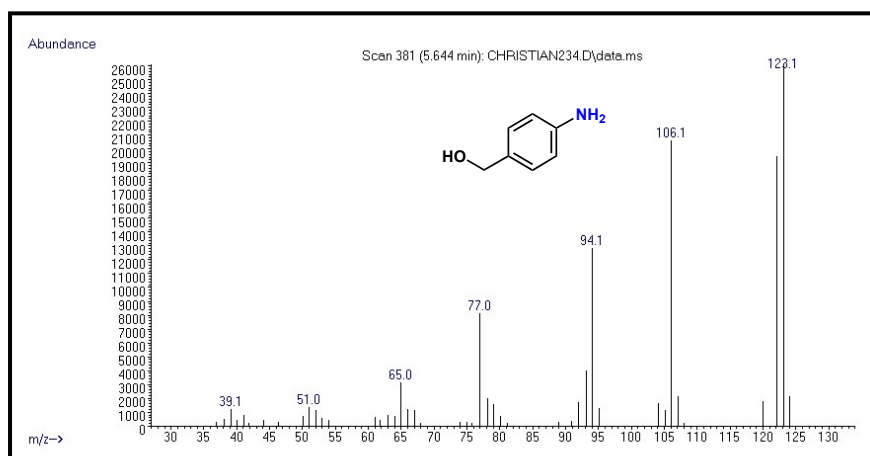


**Figure S150.** Mass spectrum of the component at 5.64 min identified as (4-aminophenyl)methanol.



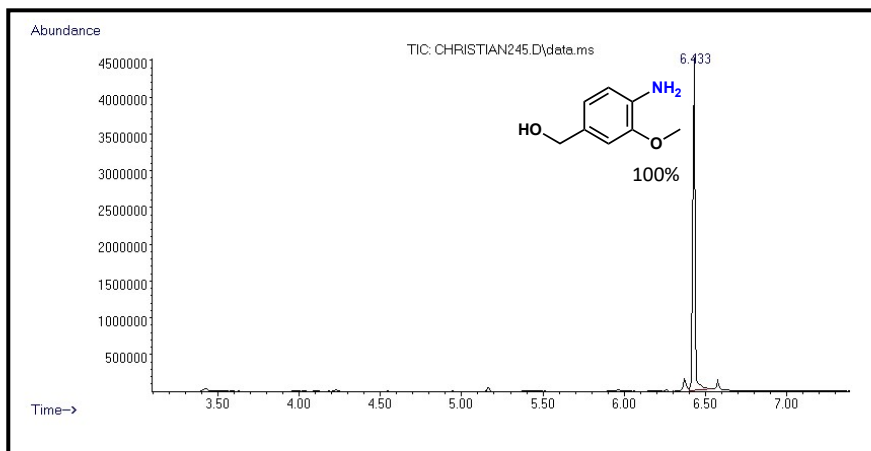


**Figure S151.** Chromatogram of the reduction of 4-nitro-3-methoxybenzaldehyde (Table 2, entry 7).

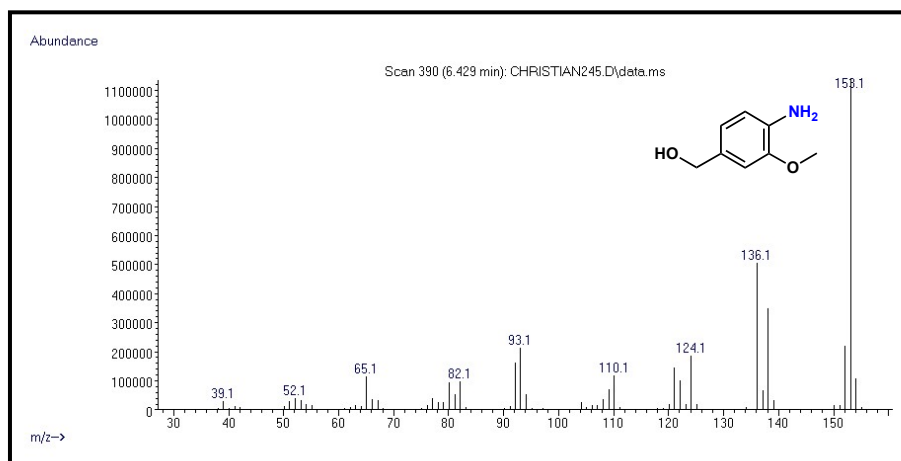


**Figure S152.** Mass spectrum of the component at 6.42 min identified as (4-amino-3-methoxyphenyl)methanol.

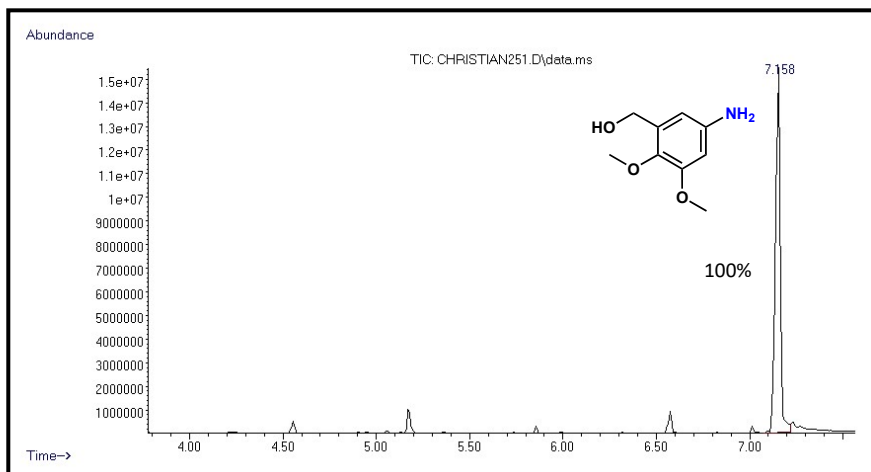


**Figure S153.** Chromatogram of the reduction of 2,3-dimethoxy-5-nitrobenzaldehyde (Table 2, entry 8).

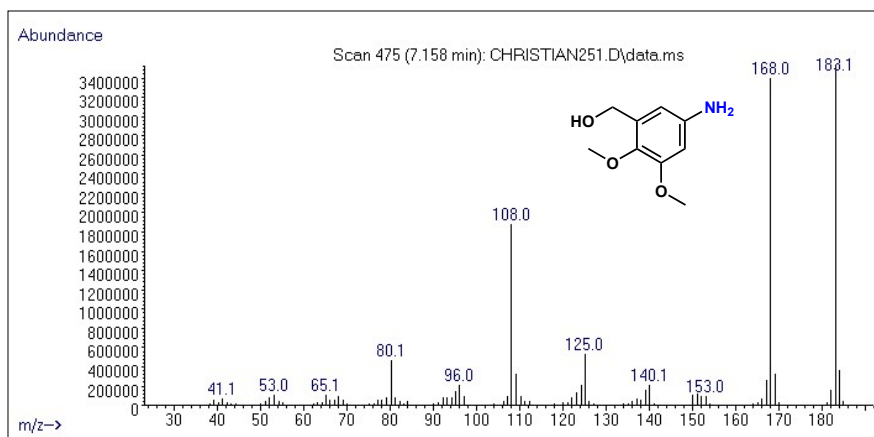


**Figure S154.** Mass spectrum of the component at 7.14 min identified as (5-amino-2,3-dimethoxyphenyl)methanol.

Products of entries 9 and 10 were isolated and identified by NMR.

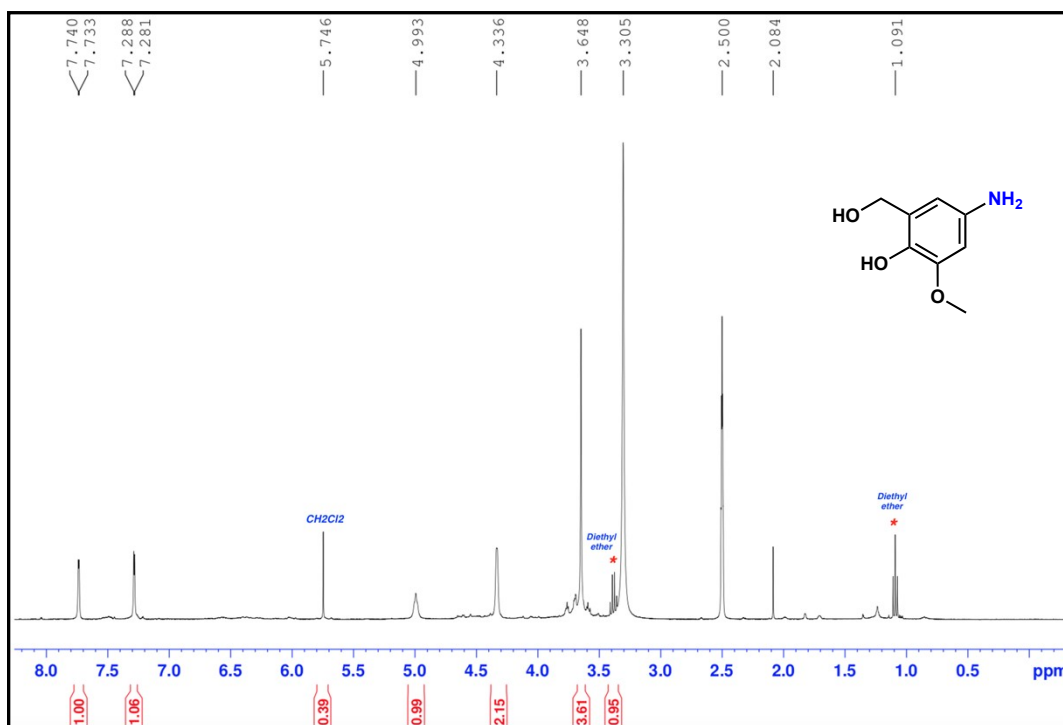


Figure S155.  $^1\text{H}$  NMR data of the hydrogenation product of entry 9, Table 2 in  $\text{DMSO-}d_6$ .

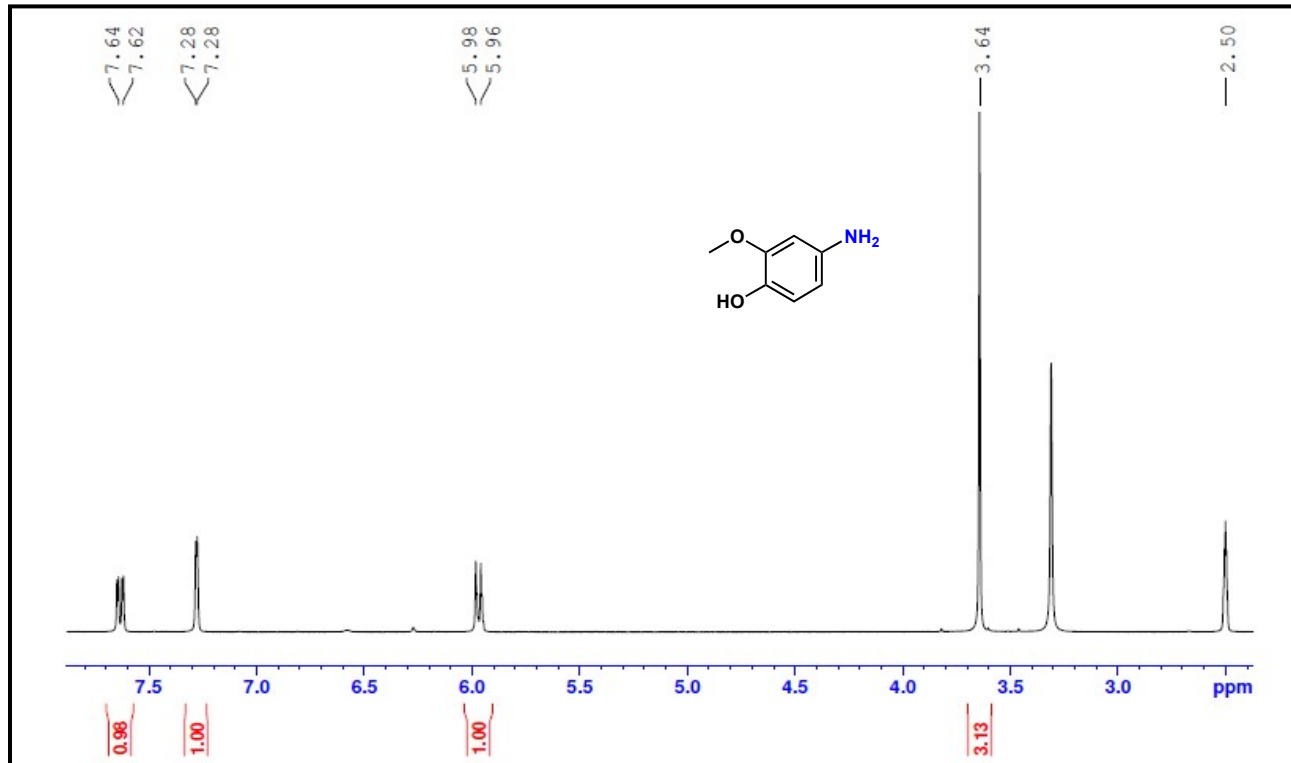
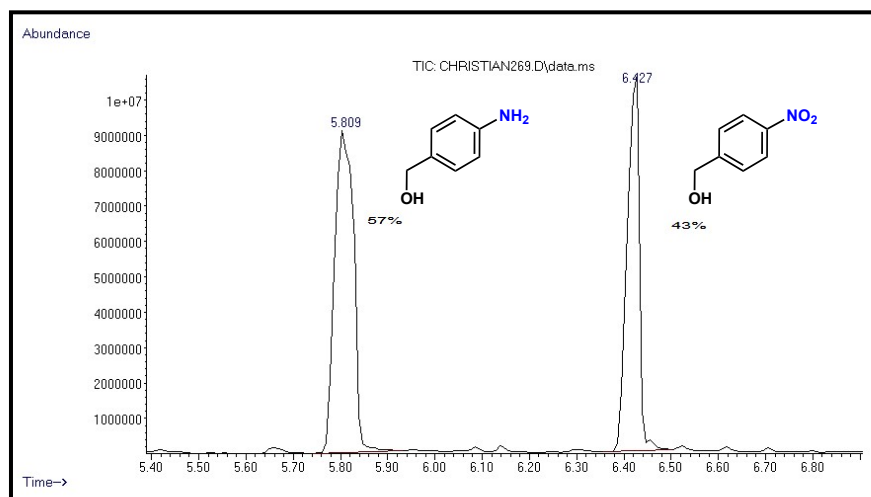
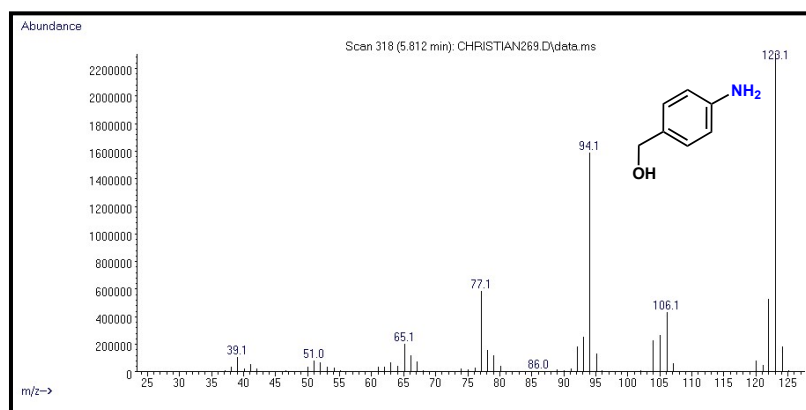


Figure S156.  $^1\text{H}$  NMR data of the hydrogenation product of entry 10, Table 2 in  $\text{DMSO-}d_6$ .



**Figure S157.** Chromatogram of the reduction of ethyl 4-nitrobenzoate (Table 2, entry 11).



**Figure S158.** Mass spectrum of the component at 5.81 min identified as (4-aminophenyl)methanol.

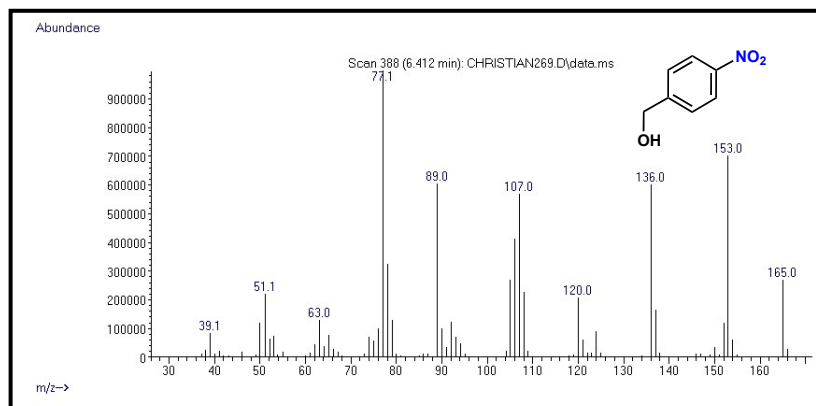


**Figure S159.** Mass spectrum of the component at 6.41 min identified as (4-nitrophenyl)methanol.

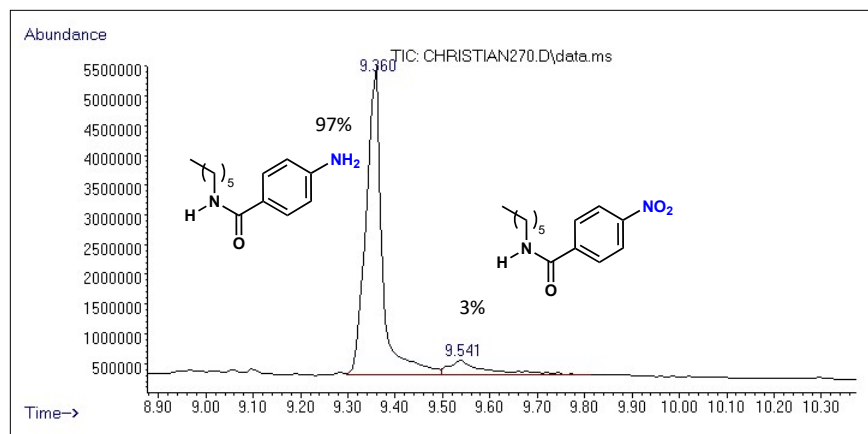


**Figure S160.** Chromatogram of the reduction of *N*-hexyl-4-nitrobenzamide (Table 2, entry 12).

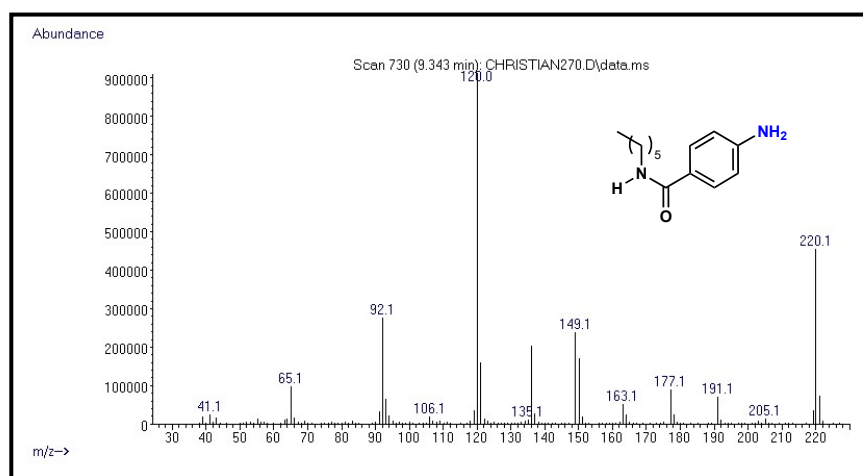


**Figure S161.** Mass spectrum of the component at 9.36 min identified as 4-amino-*N*-hexylbenzamide.

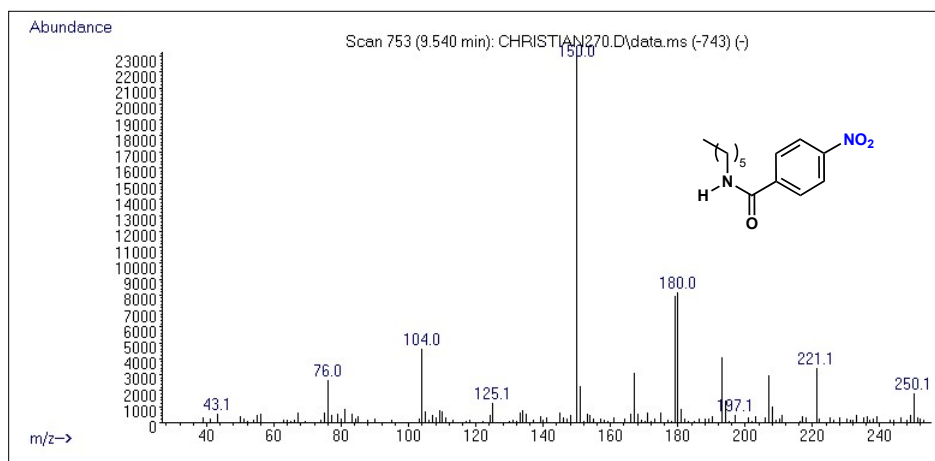


**Figure S162.** Mass spectrum of the component at 9.54 min identified as *N*-hexyl-4-nitrobenzamide.

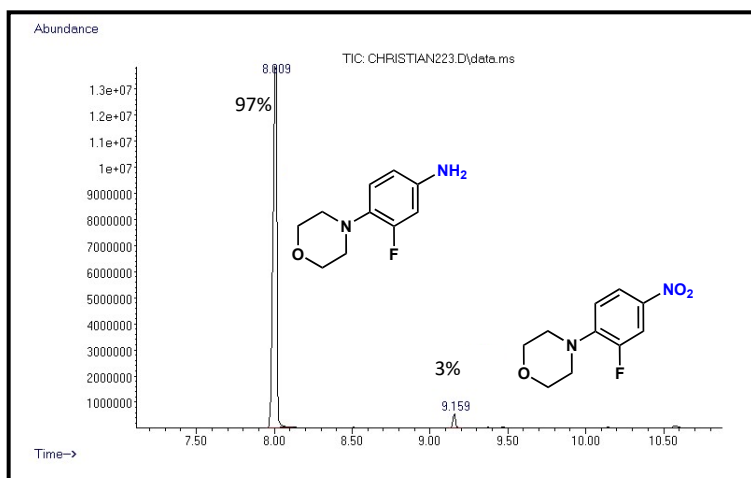


**Figure S163.** Chromatogram of the reduction of 4-(2-fluoro-4-nitrophenyl)morpholine (Table 2, entry 13).

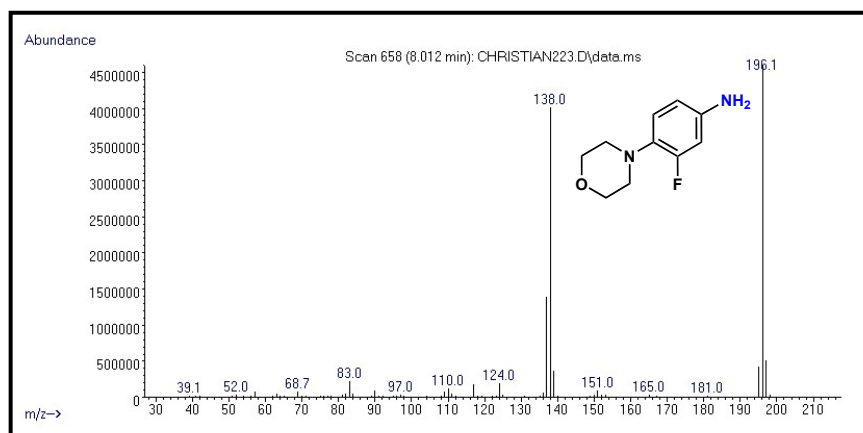


**Figure S164.** Mass spectrum of the component at 8.01 min identified as 3-fluoro-4-morpholinoaniline.

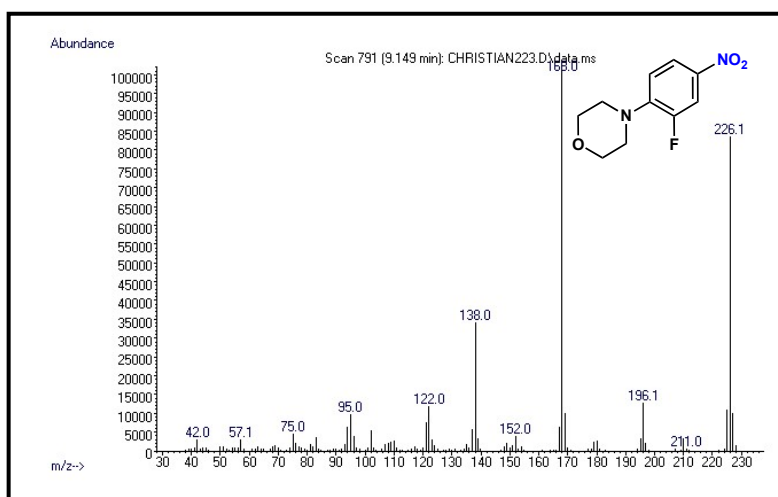


**Figure S165.** Mass spectrum of the component at 9.14 min identified as 4-(2-fluoro-4-nitrophenyl)morpholine.

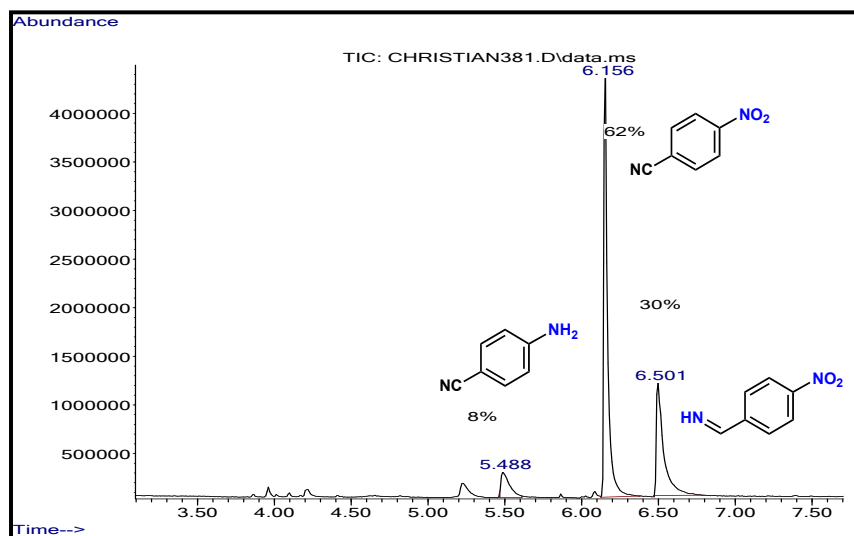


Figure S166. Chromatogram of the reduction of 4-nitrobenzotrile (Table 2, entry 14).

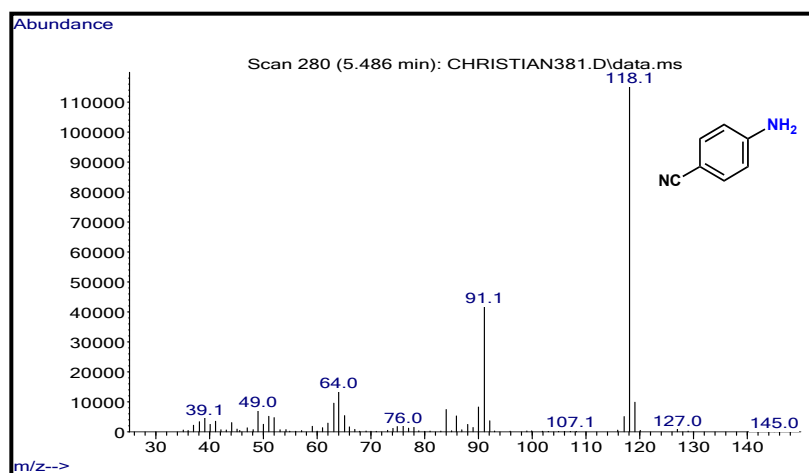


Figure S167. Mass spectrum of the component at 5.48 min identified as 4-aminobenzotrile.

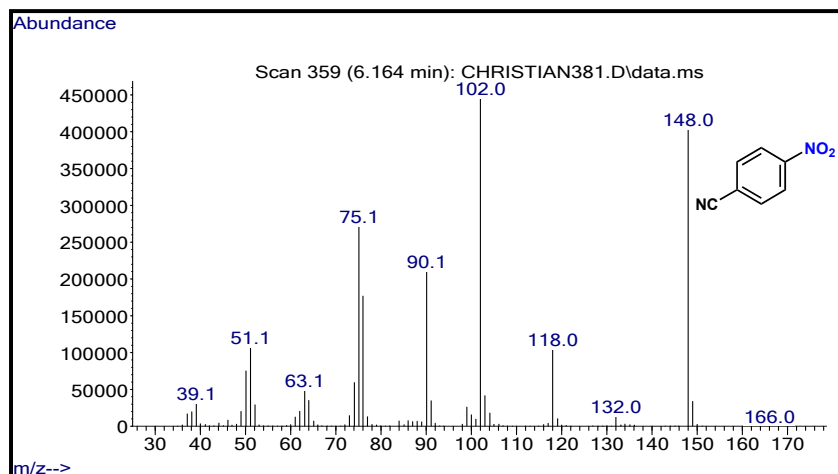


Figure S168. Mass spectrum of the component at 6.16 min identified as 4-nitrobenzotrile.

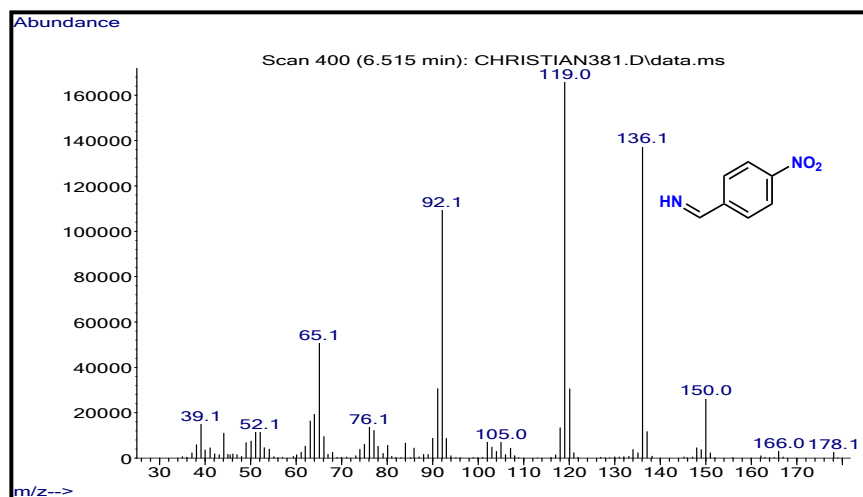


Figure S169. Mass spectrum of the component at 6.51 min identified as (4-nitrophenyl)methanimine.

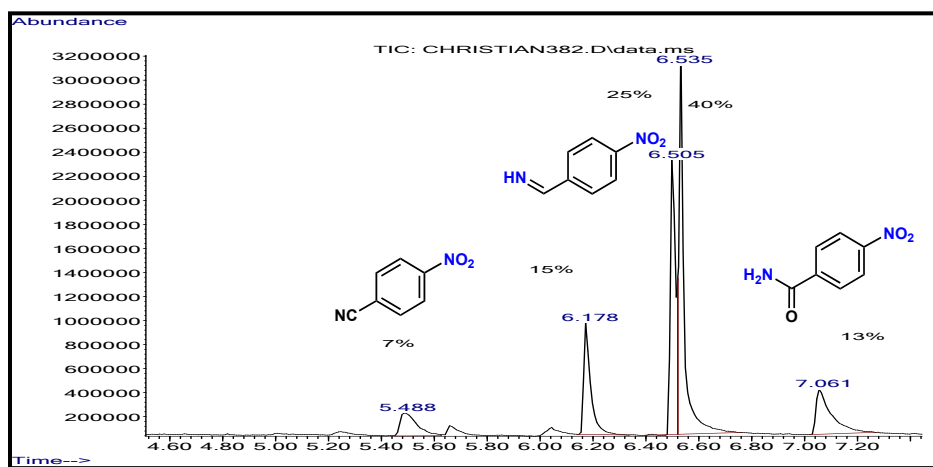


Figure S170. Chromatogram of the reduction of 4-nitrobenzonnitrile after 16 h (Table 2, entry 14).



**Table S7.** Reduction of *p*-nitrotoluene without NaBH<sub>4</sub>.<sup>a</sup>

Entry	Time	Temp °C	Base (10% mol)	% conversion <sup>[a]</sup>
1	2H	50	--	< 1%
2	16H	50	--	< 1%
3	2H	70	--	< 1%
4	16H	70	--	< 1%
5	2H	70	KOH	< 1%
6	16H	70	KOH	< 1%
7	2H	70	KOtBu	< 1%
8	16H	70	KOtBu	< 1%

[a] Reactions were also run in methanol and isopropanol yielding the same results; no reduction of the *p*-nitrotoluene was detected by GC-MS.

**GC-MS Data of the Oxyazo intermediate in the reduction of *p*-nitrotoluene**

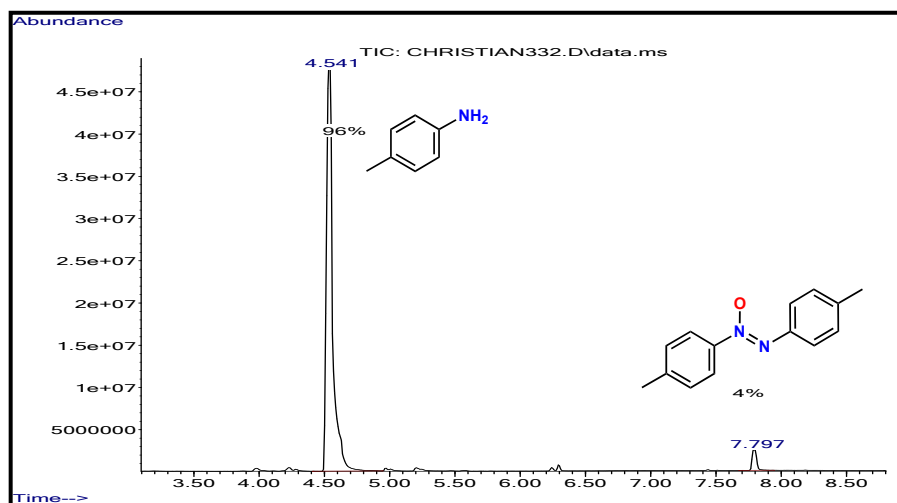
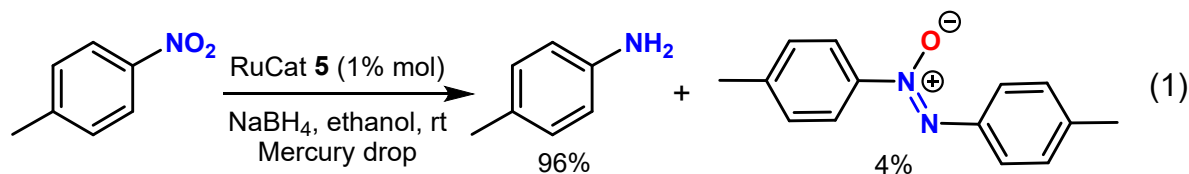


**Figure S171.** Chromatogram of the reduction of *p*-nitrotoluene in presence of a mercury drop (Eq. 1).

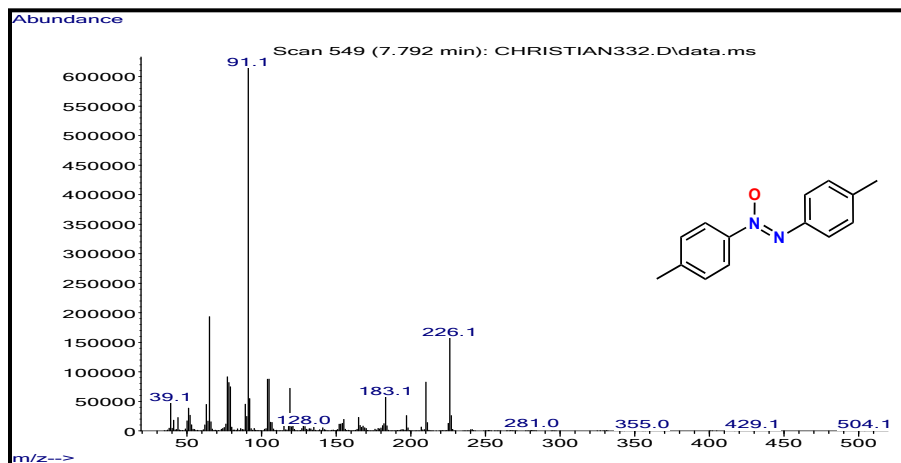


**Figure S172.** Mass spectrum of the component at 7.79 min, which was identified as the oxyazo intermediate.

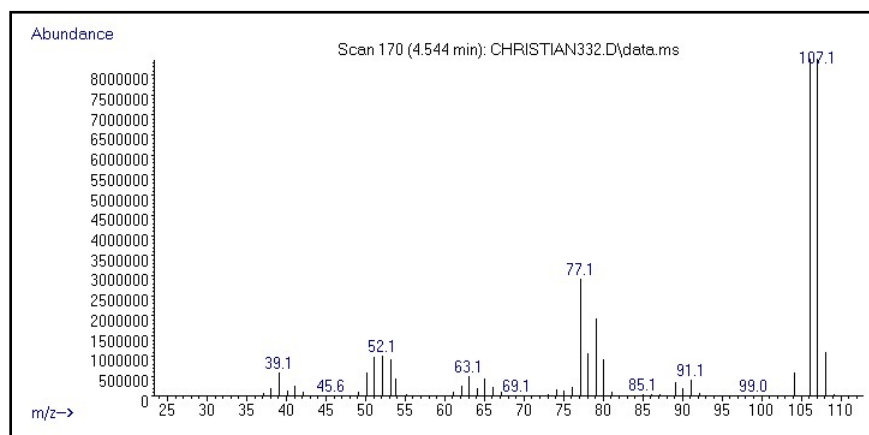


**Figure S173.** Mass spectrum of the component at 4.54 min, which was identified as 4-methylaniline.

GC-MS Data of the Azo intermediate in the reduction of *p*-nitrotoluene

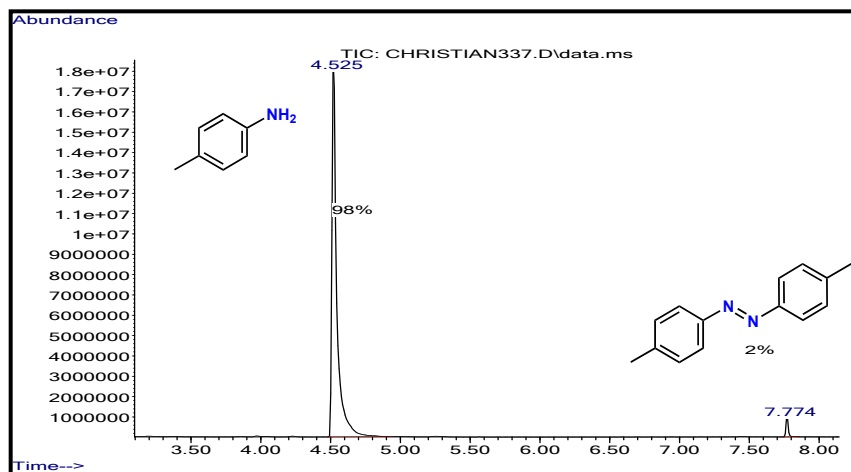
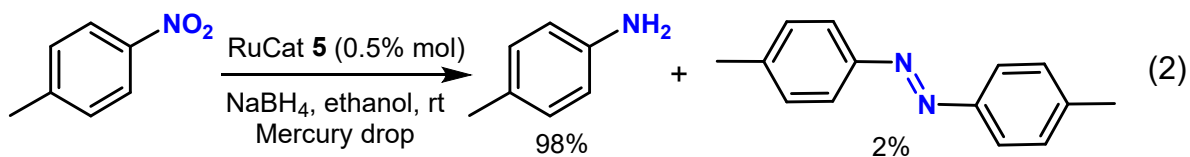


Figure S174. Chromatogram of the reduction of *p*-nitrotoluene in the presence of a mercury drop (Eq. 2).

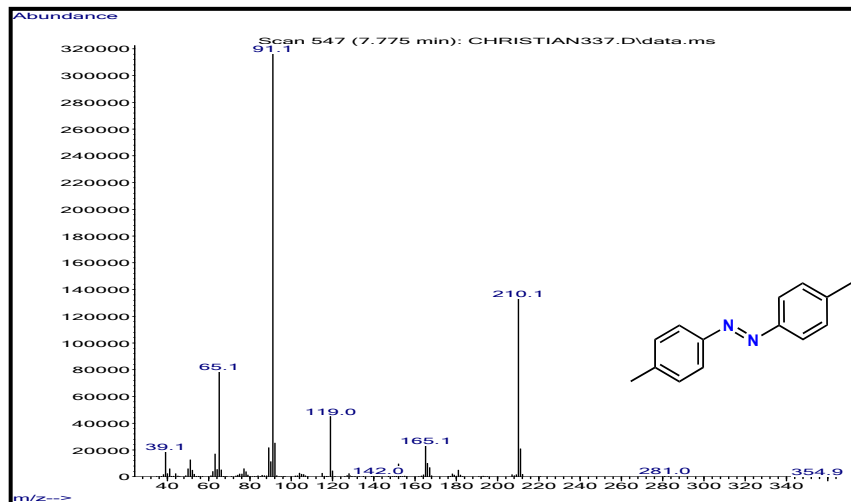
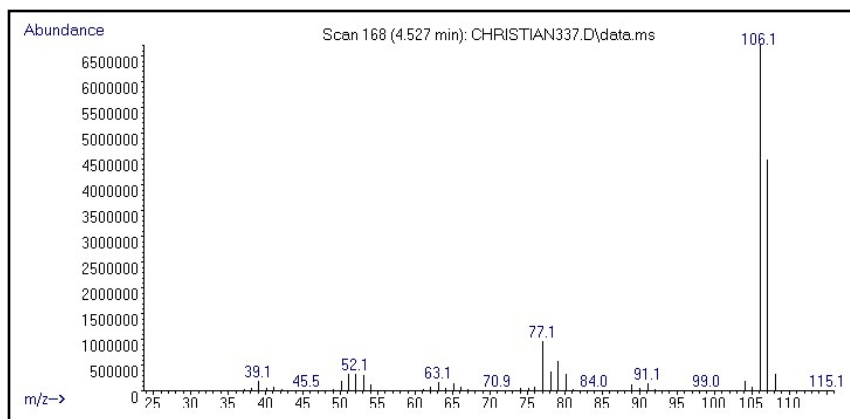
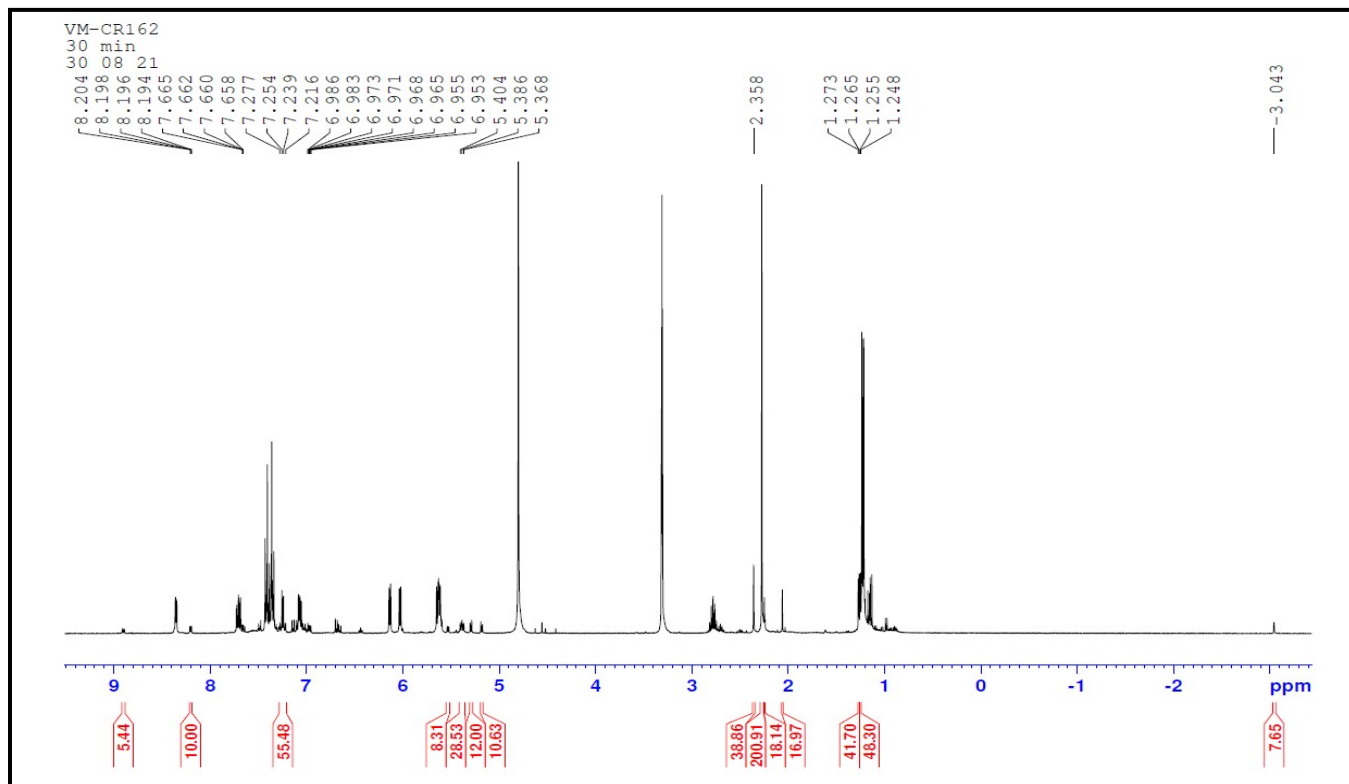


Figure S175. Mass spectrum of the component at 7.77 min, which was identified as the azo intermediate.



**Figure S176.** Mass spectrum of the component at 4.52 min, which was identified as 4-methylaniline.



**Figure S177.**  $^1\text{H}$  NMR spectrum for the equimolar reaction of **5** with  $\text{NaBH}_4$  in  $\text{CD}_3\text{OD}$  (400 MHz).

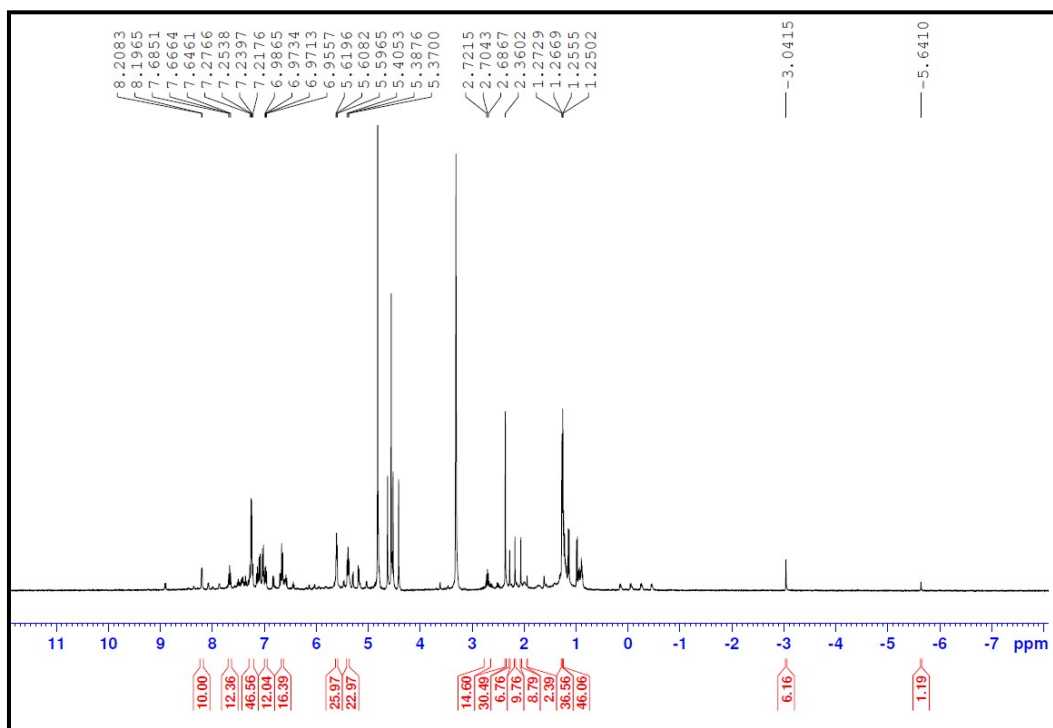


**Figure S178.**  $^1\text{H}$  NMR spectrum for the reaction of **5** with four equivalents of  $\text{NaBH}_4$  in  $\text{CD}_3\text{OD}$  (400 MHz).

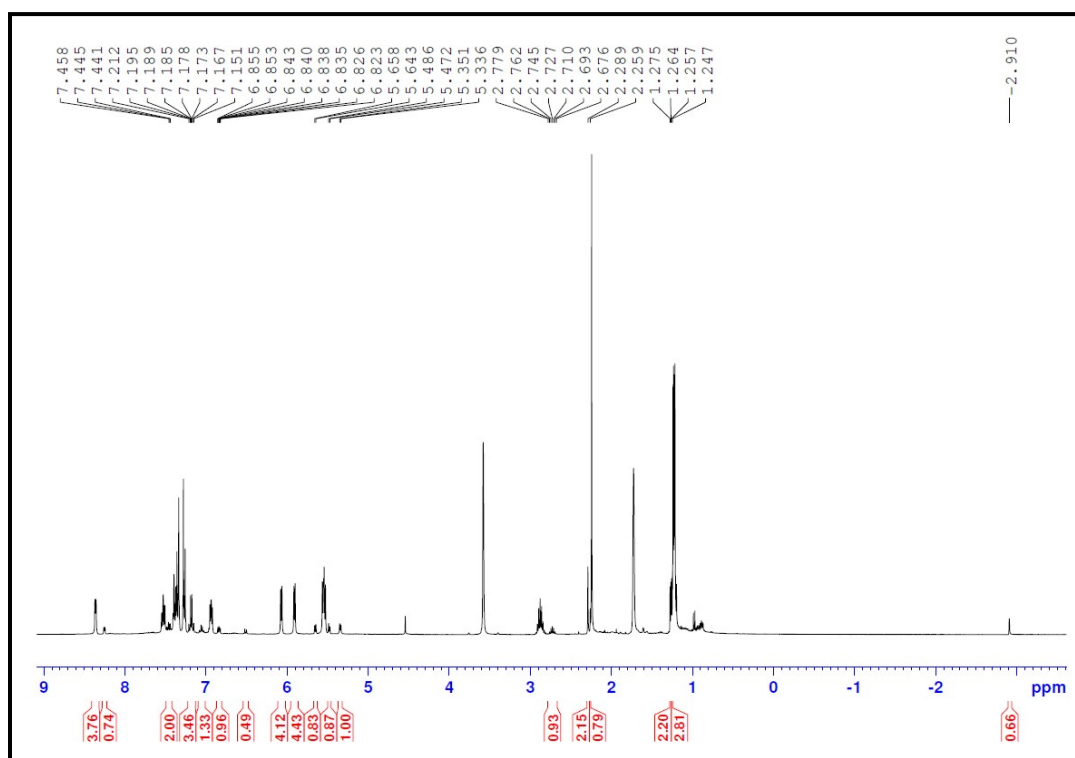


**Figure S179.**  $^1\text{H}$  NMR spectrum for the formation of Ru-hydride for **5** in  $\text{THF-}d_8$  (400 MHz).

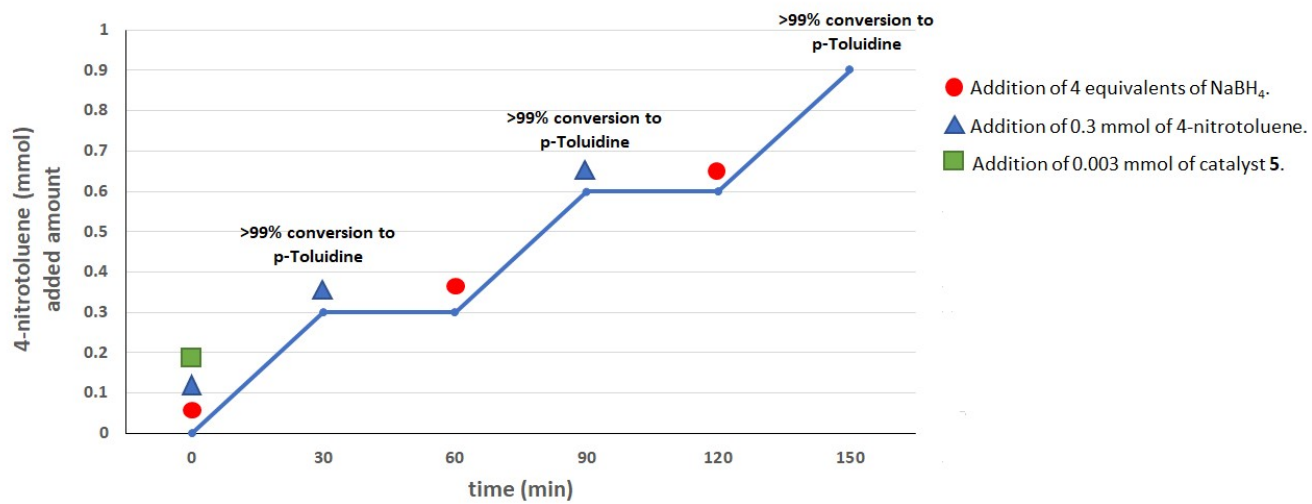


**Chart S1.** Reutilization of the catalytic system.